

Alma Mater Studiorum – Università di Bologna

DOTTORATO DI RICERCA IN

Scienze Veterinarie

Ciclo XXIX

Settore Concorsuale di afferenza: 07/H1

Settore Scientifico disciplinare: VET02

THE PIGLET AS BIOMEDICAL MODEL:

Physiological investigations, new techniques

and future applications

Presentata da: dott. Domenico Ventrella

Coordinatore Dottorato:

Prof. Arcangelo Gentile

Relatore

Prof.ssa Maria Laura Bacci

Esame finale anno 2017

“Il fatto che l'attività svolta in modo così imperfetto sia stata e sia tuttora per me fonte inesauribile di gioia, mi fa ritenere che l'imperfezione nell'eseguire il compito che ci siamo prefissi o ci è stato assegnato, sia più consona alla natura umana così imperfetta che non la perfezione.”

Rita Levi Montalcini,

Elogio dell'imperfezione

Summary

Introduction.....	2
The Piglet.....	3
<i>Taxonomic Classification and Breeds</i>	<i>3</i>
<i>General Biology.....</i>	<i>5</i>
<i>Genetics and Genomics.....</i>	<i>10</i>
Biomedical Models.....	13
<i>History and Applications of Animal Models.....</i>	<i>13</i>
<i>Piglets' Biomedical Models</i>	<i>16</i>
Aims of the Study	21
Experimental Part.....	23
Physiological Investigations	24
<i>First Paper.....</i>	<i>26</i>
<i>Second Paper</i>	<i>40</i>
New Techniques and Future Applications.....	49
<i>First Paper.....</i>	<i>51</i>
<i>Second Paper</i>	<i>64</i>
<i>Third Paper.....</i>	<i>79</i>
Conclusions	102
References	106

Introduction

The Piglet

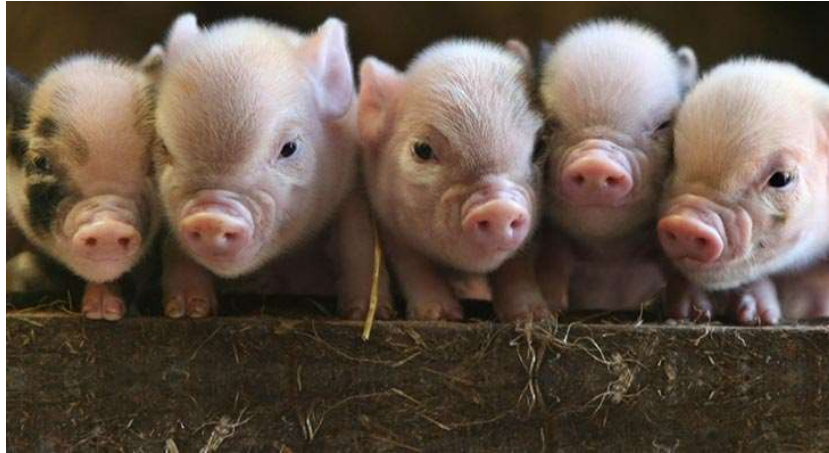


Figure 1 Piglets (<https://www.pennywellfarm.co.uk/perfect-piglets>)

Taxonomic Classification and Breeds

The taxonomic classification of pigs, according to Erxleben¹, is the following:

- Phylum: Chordata
 - Subphylum: Vertebrata
- Class: Mammalia
- Order: Artiodactyla
 - Suborder: Suiforme
- Family: Suidae
- Genus: *Sus*
- Species: *scrofa*
- Subspecies: *domestica*

Pigs are even-toed ungulates mammals². When talking about swine breeds, the two main chapters are the ones represented by standard domesticated pigs and minipigs. The domesticated pig and its variations, including minipigs, have a strong phylogenetic relationship with the Eurasian wild boar (*Sus scrofa scrofa*) and the Asia wild boar (*Sus scrofa vittatis*)^{3,4}. Nowadays, the breeds of both pigs and minipigs are numerous and, to certain extents, uncertain since they depend on how the breed is defined itself. Two important overviews summarizing pigs and minipigs breeds, can be find in two “holy grail” books for biomedical researcher: “Swine in the Laboratory”, edited by M. Michael Swindle⁴, and “The Minipig in Biomedical Research”, edited by Peter A. McAnulty, Anthony D. Dayan, Niels-Christian Ganderup, and Kenneth L. Hastings⁵. Roughly, it is safe to talk about at least 73 pure breeds of pigs, as reported by the Table 1(<http://www.thepigsite.com/info/swinebreeds.php>⁶) and 16 of minipigs.

Table 1 Pig breeds

Pig Breeds			
American Landrace	Danish Landrace	Lacombe	Philippine Native
American Yorkshire	Dermantsi Pied	Large Black	Pietrain
Angeln Saddleback	Duroc	Large Black-white	Poland China
Arapawa Island	Dutch Landrace	Large White	Red Wattle
Ba Xuyen	Fengjing	Lithuanian Native	Saddleback
Bantu	Finnish Landrace	Mangalitsa	Spots
Banza	French Landrace	Meishan	Swabian-Hall Swine
Beijing Black	German Landrace	Middle White	Swedish Landrace
Belarus Black Pied	Gloucestershire Old Spot	Minzhu	SwallowBelied Mangalitza
Belgian Landrace	Guinea Hog	Mong Cai	Tamworth
Bentheim Black Pied	Hampshire	Mukota	Thuoc Nhieu
Berkshire	Hereford	Mora Romagnola	Tibetan
Black Slavonian	Hezuo	Moura	Turopolje
British Landrace	Iberian	Mulefoot	Vietnamese Potbelly
British Lop	Italian Landrace	Neijiang	Welsh
Bulgarian White	Jinhua	Ningxiang	Wuzhishan
Cantonese	Kele	Norwegian Landrace	
Chester White	Krskopolje	Ossabaw Island	
Czech Improved White	Kunekune	Oxford Sandy and Black	

General Biology

Before starting talking about the biology of the piglet, it has to be stated and stressed that the high number and variability between breeds makes for an extreme difficult generalization on some biological and zootechnical patterns. The above-mentioned variability immediately finds an example when discussing one of the main fertility parameter: the litter size, which indicates the number of offspring produced at one birth by an animal. Several studies have been published about it, with numbers going from 7.2 up to 14.3 depending on the sow's breed⁷. In addition, the weights of the piglets at birth can have huge fluctuations not only depending on the breed, but also on the number of born and the nutritional status of the sow². Generally speaking, newborns range from 0.5kg (miniature pigs⁸) to 2kg (domestic pigs⁹).

Piglets do not have brown fat and, during the first days of life, struggle to maintain homeothermy since they are not immediately able to metabolize energetic stores such as lipids and glycogen to thermoregulate¹⁰. It is therefore mandatory to supply them with an external heating source in order to compensate the difference between body temperature (39°C) and the external environment (extremely dependent on breeding conditions) (Fig 2). This situations evolves within the first weeks of life with maturation of the physiological pattern involved in this process¹¹. Behavior is also a pivotal factor in thermoregulation and hypothermia prevention: piglets will indeed move towards the warmest spot of the pen when in need for additional heating¹².



Figure 2 The picture shows a standard delivery pen where the piglets have easily access to the sow and are provided with an infrared heating lamp.

Obviously, piglets solely rely on sow's milk during the first weeks of life. The Council Directive 2008/120/EC of 18 December 2008 dictates that: *"no piglets shall be weaned from the sow at less than 28 days of age unless the welfare or health of the dam or the piglet would otherwise be adversely affected"*¹³. During this period, newborn can develop severe iron deficiency eventually leading to anemia due to the high zootechnical standards and poor maternal storages^{14,15}. This condition occurs regardless of the breed and management system, and is the result of interactions of several factors¹⁶. It is therefore mandatory to administer animals with exogenous iron dextrane (intramuscularly) within the first 48 hours of life to prevent it¹⁷.

Once weaned, piglets are usually fed commercial diets, either in the form of solid pellet or broth. Depending on the kind of chosen diet, water requirement varies, but it is usually 2.5 liters for each kg of feed eaten².

The weaning process is extremely delicate and, unfortunately, often leads to the development of pathologies, either subclinical or clinical, and eventually death¹⁸. It has been proved that colostrum intake actually is the main determinant of neonatal survival by providing energy and immune protection¹⁹. Experiments showed how lack of colostrum negatively influences protection towards those physiological system changes²⁰. The change in diet, from milk to diets rich in complex proteins, carbohydrates and anti-nutritional factors²¹, subsequently determines important changes in gut function, reflecting on the inflammatory and immune status²². It was proved how the majority of piglets, at weaning, have a strong reduction in feed intake, with only approximately the 50% of animals eating within 24h²³. Weaning is also a strong behavioral stress factor since piglets are force to abruptly change their social interaction status with both the sow and the littermates, and immediately need to adapt to new environmental situations²¹.

Among the most feared viral neonatal pathologies, the Post-weaning multisystemic wasting syndrome (PMWS) is probably one of the most important. The disease is caused by the Porcine circovirus type 2 (PCV2) and represents the most important porcine circovirus disease²⁴. Nonetheless, when combined with other pathogens, PCV2 infection leads to a variety of diseases including reproductive alterations²⁵, Porcine respiratory disease complex (PRDC)²⁶, enteritis²⁷ and porcine dermatitis and nephropathy syndrome (PDNS)²⁸.

Viruses aside, the most high incidence pathology, dreaded by any breeding facility either commercial or experimental, is the post weaning diarrhea (PWD) This pathology is almost always associated with over-proliferation of one or more strains

of enterotoxigenic *Escherichia Coli* (ETEC)^{29,30}. It is characterized by frequent discharge of watery feces and can last up to fifteen days post weaning³¹, and is the primary cause of mortality in young piglets. The pathology is probably the first reason why swine starter diets are implemented with antibiotics, that unfortunately leads to the development of antibiotic resistance³². Nowadays, in the light of the prospective of in-feed antibiotics ban, the search for valid alternatives to antibiotics is still open.

After weaning, growth rate can be tricky to be analyze since, again, depends on too many variables. In domestic pigs, the daily weight gain can go from 0.2 to 1kg². Recent studies have been carried out in order to try and find any association between genomic patterns and food intake, weight gain and feed efficiency^{33,34}. This topic is extremely important for both biomedical and zootechnical use of this mammal. As expected, the growth rates are highly different between domestic and minipigs. Figure 2 shows a standard growth rate curve for domestic pigs³⁵, while figure 3 the one of Göttingen minipigs³⁶.

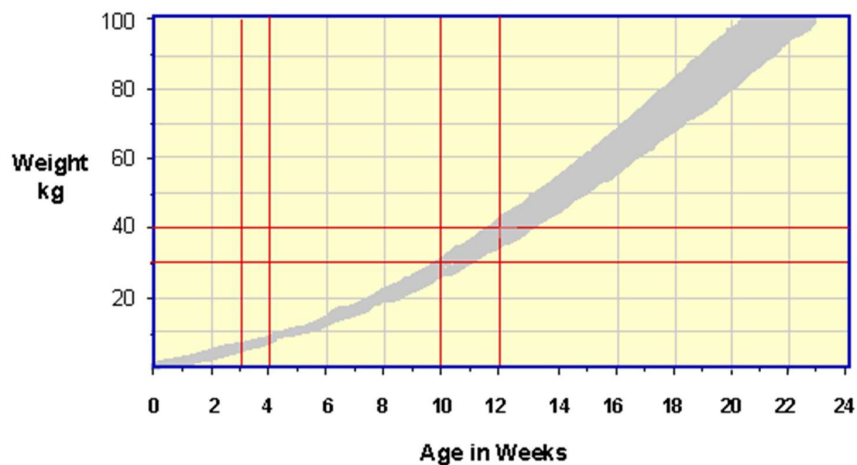


Figure 3 Growth rate curve. (<http://www.thepigsite.com/stockstds/17/growth-rate>)

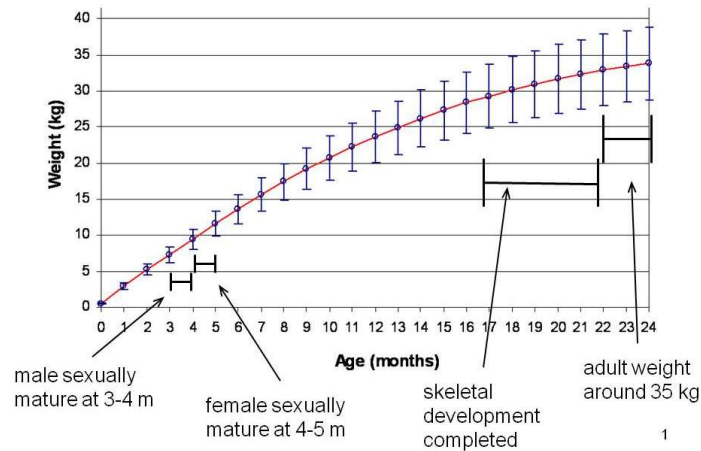


Figure 4 Göttingen minipig growth rate
http://en.wikipedia.org/wiki/G%C3%B6ttingen_minipig

Still today, it is extremely hard to summarize the life cycle of pigs and to define when they can actually be considered as adults. Usually, adult life overlaps with puberty and sexual maturation. Table 2 approximately shows the key life cycle point of domestic pigs. This important steps are also highly variable when taking into account different breeds: minipigs and Asian domestic pigs seem to reach puberty quite earlier than North American and European domestic pigs³⁷.

Table 2 Life Cycle of domestic pigs³⁷

Prenatal period	114 ± 4 days
Suckling period	28 days
Growing-finishing period (90kg)	90 - 200 days
Age at puberty	150 – 200 days
Reproductive longevity	4 – 8 years
Longevity	12 – 15 years

Genetics and Genomics

During the last twenty year, huge progresses have been made in the characterization of the swine genome. The pig, indeed, has always been one of the most widely studied farm animals when it comes to cytogenetics and genetics in general. This may be due to the fact that, compared to other mammalian domestic species, the pig has fewer chromosomes ($2n=38$)³⁸. In addition to that, pigs chromosomes are easy to distinguish between each other, and can mostly be identified without the need for special stainings³⁸. Molecular hybridization-based methods have rapidly become an important tool for cytogenetics, leaning toward the integration of cytogenetics itself and molecular biology. This overlap of methods and capabilities probably represents the pivotal point for the new era of cytogenomics³⁹, and the pig is no exception.

The first porcine karyotype dates back to 1972 and was based on the banding method known as Q-banding (quinacrine fluorescence banding)⁴⁰. Several advances have been made since then, including the development and improvement of the RBG-banding technique (reverse (R)-banding with Giemsa staining), eventually leading to the standardized schematic karyotype of the pig⁴¹ represented in Figure 5. It actually represented the first nomenclature of chromosomes for domestic animals and enabled the analysis of normal karyotypes and their aberrant patterns acting as foundation for physical chromosome mapping³⁸.

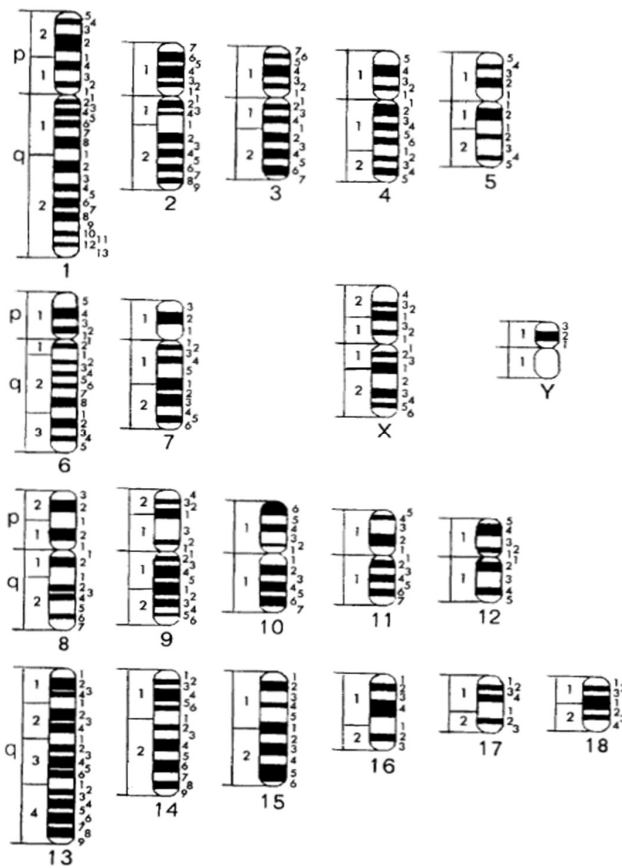


Figure 5 Schematic drawings of G-banded porcine chromosomes⁴¹

On a different scale, also porcine gene mapping studies have witnessed huge improvements starting from the 90s. In this decade, the quantity, but most importantly the quality of the pre-existent maps were improved thanks to radiation hybrid panels and in situ hybridization (ISH). Eventually, the construction of radiation hybrid⁴² and high-resolution BAC contiguous maps⁴³ was incredibly facilitated by novel tool such as cDNA and BAC genomic libraries⁴⁴. Nowadays, the number of mapped loci within the pig genome is higher than 10000 and provide vital information for both pigs themselves and humans³⁸.

In the light of the successful generation of the porcine genetic map, studies for genome sequencing started to take over with the foundation of the Swine Genome Sequencing Consortium (SGSC) in 2003⁴⁵. Almost nine years after, the first draft reference genome sequence of the *Sus scrofa*, derived from a female Duroc pig, was published³. It was the result of the implementation of hierarchical shotgun Sanger sequencing of BAC (bacterial artificial chromosome) clones and Illumina next-generation sequencing data^{46,47}. This first step was then rapidly followed by the publication of genomes of the Chinese Wuzhishan minipig⁴⁸, the Göttingen minipig⁴⁹ and the Tibetan wild boar⁵⁰. To this date, the number of completely sequenced porcine genomes has grown up to 350⁵¹, allowing researches from the scientific community to study their variations, evolution and selection.

Despite the incredible amount of advances in this field, further genomics studies are still needed before being able to talk about a complete and standardized knowledge. Indeed, the current draft status of the genome of reference somehow hampers the analysis at a considerably high number of loci within the porcine genome⁵². Moreover, the analyses showed selective sweeps at regions lacking annotated genes that might hold regulatory sequences form contiguous genes⁵¹. Finally, a recent publication about the assembly of X and Y chromosomes⁵³ further highlighted the need for improved reference genome⁵⁴ and annotation for all pig chromosomes⁵¹.

Biomedical Models

History and Applications of Animal Models



Figure 6 Image from the bottom panel of the title page to the 1541 Junta edition of Galen's Works. Depicts Galen demonstrating that the recurrent laryngeal nerves render an animal voiceless when cut (<http://commons.wikimedia.org/wiki/File:Galen-Pig-Vivisection.jpg>)

The use of animal models can be traced back to the Second Century Common Era (CME)^{55,56} and plays a pivotal role in the biomedical research field due to two main reasons: not only they can provide key information regarding the pathogenesis of the diseases, but they can also help in developing and analyzing new therapeutic approaches⁵⁷. In 1865⁵⁸, a French physiologist named Claude Bernard, father of what is considered to be the modern experimental medicine, stated that: “I not only conclude that experiments made on animals from the physiological, pathological and therapeutic points of view have results that are applicable to theoretic medicine, but I think that without such comparative study of animals, practical medicine can never acquire a scientific character”⁵⁹. Always with Bernard, the idea of creating induced

model of diseases using both chemicals and physical methods came along⁵⁶, thus allowing for a much more extensive use of animals in research.

Another important turning point in experimental medicine came in the 20th century with the “germ theory of disease” and the use of animal models of infectious diseases⁵⁶. Nowadays preclinical studies performed on animals are still extremely necessary, if not mandatory, when it comes to this research field and provide pivotal information regarding both pathogenic mechanisms and therapeutic approaches. This statement is indeed validated by the large use of animal models for study of two important infectious pathogens like HIV⁶⁰ and Influenza Virus⁶¹ among other.

One of the most important chapter in the history of animal models is probably represented by the one about genetic diseases. Indeed, in the second half of the 20th century, veterinarians started describing the presence of spontaneous genetic diseases in several animal species, perfectly mimicking the analogue ones in the human species, and spontaneous mutants in mice perfectly suitable for experimental studies^{62,63}. Nonetheless, the search was still open for all of the diseases that did not seem to naturally occur in animals. The biggest answer to this question was represented by genetic engineering, allowing to potentially customize and tailor any model for genetic diseases.

The first genetically modified mice was created by Rudolf Jaenisch in 1974, who microinjected explanted blastocysts with simian virus 40 (SV40) viral DNA in the blastocoel cavity⁶⁴. The injection proved to be safe and effective since the technique did not interfere with the physiological development of the mice, and the animals showed the presence of the virus-specific DNA sequences. In 1988, Robert

P. Erickson wrote and published one of the first reviews regarding the creation of murine animal models of genetic diseases⁶³, discussing mutations and direct screening, transgenic mice and genetic alterations of embryonic cells. One of the first report, if not the first one, of transgenic livestock animals came in 1985⁶⁵. Aim of the study was to introduce relatively new techniques, such as the microinjection of genes into the pronuclei or nuclei, to larger animals including rabbits, sheep and pigs. Twelve years later, in 1997, Patters (*et al.*) successfully created a large animal model of a human disease, the retinitis pigmentosa, using pigs⁶⁶.

Nowadays, the number of genetically engineered animals for biomedical research, whether small or large, has incredibly grown, and they probably represent one the key factor for scientific progress. This phenomenon has to be imputed to new transgenesis techniques such as Somatic Cell Nuclear Transfer (SCNT)⁶⁷, Sperm Mediated Gene Transfer (SMGT)⁶⁸ and, ultimately, CRISPR/Cas9⁶⁹. In the last 10 years, more than 35000 papers were published regarding transgenic animal models, proving their vital importance and constant growth (data collected from NCBI – Pubmed, <https://www.ncbi.nlm.nih.gov/pubmed>).

Piglets' Biomedical Models

As previously stated, swine are extremely similar to humans in different fields including genetics, physiology, and anatomy making it a highly relevant model for biomedical research⁷⁰. Therefore, if compared to mice and rats, they actually share several patterns with humans with respect to the cardiovascular, respiratory, hepatic metabolism, gastrointestinal, renal, reproductive, endocrine, immune, central nervous, optical, dermal, and musculoskeletal systems^{71,70}. As a consequence, pigs are deservedly one of the most important large animal models for preclinical studies including tests of drugs and other therapeutic interventions⁷², toxicity testing⁷³, studies of disease pathogenesis⁷⁴, and functional genomics⁷⁵.

In this chapter, as in this entire thesis, the focus will be only directed to the use of newborn and neonatal piglets in the biomedical research world. Over the last two decades, the piglet has strongly emerged as the most complete and accurate model for pediatric nutrition, metabolism and toxicology^{76,77}. In addition to that, the piglets also acts as a “perfect” preterm model, as long as any model can be perfect. It is indeed clear how pigs are born at a stage of organ maturation that still needs maternal care⁷⁸. Moreover, quite a considerable number of piglets is born few days before or even earlier for either maternal problems or mistakes in the labor induction, with an important increase of mortality⁷⁹, thus proving to be a sensitive model to study the mechanisms behind near-term mortality⁷⁸.

Gastrointestinal System

When discussing about the piglet model, it is very hard to summarize its application fields, since it is almost possible to find at least one publication for every apparatus and metabolic/physiological process. Most certainly, amongst the most relevant biomedical applications, the gastrointestinal one is the most representative and important. An important example is the use of piglets to study and analyze the Necrotizing Enterocolitis (NEC), a potentially lethal disease of preterm neonates⁸⁰. This pathology is unfortunately highly common, with an incidence that goes from 3 to 10 %⁸¹. The piglet is an attractive model because of its similarities with the infant when it comes to gastrointestinal (GI) system. The majority of the GI development and maturation, in the porcine species, happens within the first few weeks of life, while in humans it is mainly in-utero⁸⁰. This delay provides a good advantage in using a near term piglet to reflect a definitely more premature infant. It is indeed ascertained how a preterm pig at 90% gestation accurately mimics an infant at 75% gestation⁸². Moreover, the preterm pig shows other characteristics that make it a good model for NEC such as its weight and the ease of handling and surgical approaches⁸³ and the fact that both symptoms and pathological finding resemble those seen in humans^{84,85}. Finally, when compared to other models, the pig also shows the ability to be easily administered with Total Parenteral Nutrition (TPN), which again, is a condition often recurring in infants with GI issues⁸⁶.

Another important GI pathology often studied on the piglet model is the Short Bowel Syndrome (SBS). Different animals have been used in order to create translational animal of SBS, but even in this case, the similarities between the human

and the porcine species make the pig a better model⁸⁷. For this kind of pathology, piglets ranging from 1-12 days⁸⁸ old up to 4-5 weeks^{89,90} old have been used. It has to be acknowledged though that while juvenile pigs can approximate the physiology in young children, piglets within this age range are probably too old for adaptation studies⁹¹. As a consequence of this gap, preterm piglet models of SBS have recently been developed⁹².

When discussing the GI system, it is important to notice that models of pathology only represent a small fraction of the piglet biomedical capabilities. Neonatal and juvenile pigs in physiological conditions can indeed be enrolled in nutritional studies providing important data regarding the absorption and overall effects of novel products of the food industry⁹³. Generally speaking, it is safe to say that piglets, both wild type and transgenic, are providing vital information regarding the GI system and its pathologies.

Cardiopulmonary System

Pigs share important characteristics with humans in anatomy and physiology patterns even when it comes to the cardiovascular and pulmonary system⁹⁴. Alongside with morphometric characteristics, similarities can be found as well in coronary blood flow, growth of the cardiovascular system and pulmonary development in the neonatal stages⁹⁴. Differently from other mammals such as dogs, the circulation to the conduction system, in pigs, is mainly right-side dominant from the posterior septal artery, therefore porcine models accurately mimic humans with acute myocardial infarction (MI)⁹⁴⁻⁹⁶. Several studies have used ameroid constriction

as a way to determine initial high-grade coronary stenosis followed by occlusion⁹⁵. Despite the fact that progressive occlusion of a coronary artery can lead to left ventricle (LV) dysfunction, the heart failure (HF) phenotype is better produced by total coronary artery occlusion. Acute coronary occlusion depresses LV function and prompts neurohormonal activation, therefore satisfying most criteria characteristic of the HF phenotype⁹⁷. Moreover, pig models of MI can also be useful to study infarct expansion and LV remodeling in the post-MI setting⁹⁸.

Even in this research area, the use of piglets has rapidly increased in the last decade. For instance, the piglet is becoming the most important animal model for hypoxia and most importantly resuscitation studies^{99,100}. In this latter field there is a paucity of good-quality evidence mainly due to difficulties in obtaining informed consent to conduct clinical trials. Furthermore, restricting resuscitation or applying methods of uncertain benefit in human neonates is not ethically acceptable¹⁰¹. Moreover, it is unethical to use novel techniques in humans unless they have already been applied effectively to animal models. Therefore animal and extrapolated adult data have been used, in order to revise the neonatal resuscitation guideline¹⁰².

It is important to mention one of the latest “trend” in the field which is therapeutic hypothermia, again well studied in the piglet neonatal models of perinatal asphyxia¹⁰³. This kind of approach aims to lower body temperature in order to minimize brain injuries, and is considered to be one of the safest and most effective treatment for moderate and severe neonatal encephalopathy¹⁰⁴.

Nervous System

When it comes to neuroscience, the porcine brain resembles the human brain in terms of weight, volume, cortical surface area, myelination, composition and electrical activity, and its development, just like in humans, extends from prenatal to early postnatal life^{105,106}. Those similarities not only apply to the brain, but to the rest of the entire nervous system¹⁰⁷. Moreover, the fact that the life span of pigs better resembles humans' when compared to smaller laboratory animals¹⁰⁸, makes it a better model to study congenital and genetic neurodegenerative diseases⁷⁶.

As previously stated for the other mentioned apparatuses, even in this case the piglet, finds a variety of different applications and it is pretty hard to summarize them. Standard wild type healthy piglets, for example, are often used for preclinical studies to be later on applied to transgenic or naturally occurring models of pathologies.

The number of swine model of neurological diseases is constantly increasing^{105,109}, including Huntington disease¹¹⁰, Amyotrophic Lateral Sclerosis¹¹¹, Spinal Muscular Atrophy(SMA)¹¹² and Parkinson disease¹¹³.

In this application area, it is mandatory to mention the huge amount of gene therapy studies performed on the porcine species. Gene therapy, nowadays, probably represents the most promising and effective therapeutic approach to a variety of neurological disorders¹¹⁴, and again pigs proved to be a vital model for preclinical protocols¹¹⁵.

Aims of the Study

By the analysis of the literature and in the light of the introduction hereby elaborated, it looks like the strive for new piglets' models of disease have prevaricated the necessity for a deeper knowledge of the physiology of the animal to be modified.

As researchers, we all know how difficult it can be to interpret obtained data when poor to none reference standards are provided and how hard it is to apply techniques and methods borrowed from other models, no matter how similar they can look.

The key for successful translational medicine lies within the capability to overlay the model and the final recipient as accurately as possible, and this require deep knowledge.

The aim of the present work was to collect knowledge and information regarding the piglets, its physiology and its pivotal utility in translational medicine. It is indeed clear how different piglets are when compared to adult pigs, thus the need for age-specific knowledge.

Experimental Part

Physiological Investigations

This section shows two experiments aimed to expand the knowledge regarding physiological and metabolic patterns of the piglet by analyzing, in both a qualitative and quantitative manner, two important body fluids such as blood and cerebrospinal fluid.

Blood is a relatively easy to sample body fluid that can provide vital information regarding both the health of the animal used as a model and the success of the experimental treatment. As previously stated in the introduction of the present work, the biology of the piglet, just like any mammalian, can be quite different from the adults', thus requiring age-related reference intervals.

Cerebrospinal fluid, on the other hand, requires an experienced staff and advanced equipment to be performed safely as it involves general anesthesia. Nonetheless, its importance has largely been proved for any experimental protocol involving the Central Nervous System (CNS) or toxicity in general. For this specimen, we decided to use an innovative metabolic approach, tailored for this kind of analyses, capable of high sensitivity and reliability.

As expected, a large population is a mandatory requirement when trying to set standard reference intervals in order to obtain strong and reliable data. This is why we enrolled a total number of 130 piglets for the blood experiment and 44 for the Cerebrospinal Fluid one. Animals used for this two physiological investigations were actually enrolled in other experimental protocols, approved by the Italian

Ministry of Health, as untreated controls or in occasion of the pre-treatment samplings. It is indeed extremely important to try and gain as much information from every animal that takes part in an experimental protocol in accordance to the principles of the Refinement and Reduction of the 3Rs¹¹⁶. Refining the knowledge about a model helps reducing the number of animals needed, thus making any research more ethical and sustainable.

First Paper

Age-Related ^1H NMR Characterization of Cerebrospinal Fluid in
Newborn and Young Healthy Piglets

RESEARCH ARTICLE

Age-Related ¹H NMR Characterization of Cerebrospinal Fluid in Newborn and Young Healthy Piglets

Domenico Ventrella¹*, Luca Laghi²*, Francesca Barone¹, Alberto Elmi¹, Noemi Romagnoli¹, Maria Laura Bacci¹

1 Department of Veterinary Medical Sciences, University of Bologna, Bologna, Italy, **2** Centre of Foodomics, Department of Agro-Food Science and Technology, University of Bologna, Bologna, Italy

✉ These authors contributed equally to this work.

* domenico.ventrella2@unibo.it



Abstract

When it comes to neuroscience, pigs represent an important animal model due to their resemblance with humans' brains for several patterns including anatomy and developmental stages. Cerebrospinal fluid (CSF) is a relatively easy-to-collect specimen that can provide important information about neurological health and function, proving its importance as both a diagnostic and biomedical monitoring tool. Consequently, it would be of high scientific interest and value to obtain more standard physiological information regarding its composition and dynamics for both swine pathology and the refinement of experimental protocols. Recently, proton nuclear magnetic resonance (¹H NMR) spectroscopy has been applied in order to analyze the metabolomic profile of this biological fluid, and results showed the technique to be highly reproducible and reliable. The aim of the present study was to investigate in both qualitative and quantitative manner the composition of Cerebrospinal Fluid harvested from healthy newborn (5 days old-P5) and young (30-P30 and 50-P50 days old) piglets using ¹H NMR Spectroscopy, and to analyze any possible difference in metabolites concentration between age groups, related to age and Blood-Brain-Barrier maturation. On each of the analyzed samples, 30 molecules could be observed above their limit of quantification, accounting for 95–98% of the total area of the spectra. The concentrations of adenine, tyrosine, leucine, valine, 3-hydroxyvalerate, 3-methyl-2-oxovalerate were found to decrease between P05 and P50, while the concentrations of glutamine, creatinine, methanol, trimethylamine and myo-inositol were found to increase. The P05-P30 comparison was also significant for glutamine, creatinine, adenine, tyrosine, leucine, valine, 3-hydroxyisovalerate, 3-methyl-2-oxovalerate, while for the P30-P50 comparison we found significant differences for glutamine, myo-inositol, leucine and trimethylamine. None of these molecules showed at P30 concentrations outside the P05–P50 range.

OPEN ACCESS

Citation: Ventrella D, Laghi L, Barone F, Elmi A, Romagnoli N, Bacci ML (2016) Age-Related ¹H NMR Characterization of Cerebrospinal Fluid in Newborn and Young Healthy Piglets. *PLoS ONE* 11(7): e0157623. doi:10.1371/journal.pone.0157623

Editor: Richard H Barton, Imperial College London, UNITED KINGDOM

Received: February 11, 2016

Accepted: June 2, 2016

Published: July 8, 2016

Copyright: © 2016 Ventrella et al. This is an open access article distributed under the terms of the [Creative Commons Attribution License](https://creativecommons.org/licenses/by/4.0/), which permits unrestricted use, distribution, and reproduction in any medium, provided the original author and source are credited.

Data Availability Statement: All relevant data are within the paper and its Supporting Information files.

Funding: This study was supported by RFO 60%, Ateneo di Bologna.

Competing Interests: The authors have declared that no competing interests exist.

Introduction

Pigs represent an important animal model, being phylogenetically similar to primates [1], therefore extremely similar to humans, especially when compared to other models such as the murine one [2]. It is therefore necessary and mandatory to acquire as much knowledge as possible regarding porcine genetics and physiology in order to create specific models for each pathology and understand its correlation to its human analogue. When it comes to neuroscience, the porcine brain resembles the human brain in terms of weight, volume, cortical surface area, myelination, composition and electrical activity, and its development, just like in humans, extends from prenatal to early postnatal life [3]. Throughout the years, several porcine models carrying gene variants that cause neurological pathologies in men have been created [3] validating and proving the importance of this species in the laboratory and translational medicine.

Due to its position and fragility, Central Nervous System (CNS) samples can be hard to collect and the procedure may lead to severe damage, but Cerebrospinal fluid (CSF) represents a relatively easy to collect specimens that can provide important information about neurological health and function [4]. CSF functions include regulation of the intracranial pressure (ICP), regulation of the chemical environment of the CNS and intracerebral transport [5]. CSF is the product of plasma ultrafiltration and membrane secretion, usually clear and colorless [5]. It is nearly acellular, and does not contain erythrocytes in physiological conditions [6]. On average, dogs and cats have from 0 to 2 cells/ μ l, with specific normal nucleated cell count ranges for different species [7]. Protein concentration is usually very low: canine CSF samples usually show 10–40mg/dl of proteins compared to 5–7 g/dl in serum, the majority of which is represented by albumin (50–70%) [5]. Its production and absorption are the result of the interaction of several interfaces such as the Blood-Brain-Barrier (BBB) and the blood-CSF barrier [8], therefore it can vary depending on the age and the maturation of the above-mentioned barriers.

Recently, canine CSF small organic molecules profile, referred to as metabolome [9], was investigated using proton nuclear magnetic resonance (¹H NMR) spectroscopy [10], in order to outline a fingerprint of healthy status useful for designing and interpreting clinical trials. ¹H NMR is indeed ideally tailored for metabolomics investigations on biofluids, due to its high reproducibility, its intrinsic quantitative nature and the minimum sample preparation required [11]. Investigations of this kind have been, in the recent past, precious for characterizing diseases [12–13] and inflammation conditions [14]. In addition, focusing on rats, it was proven that CSF metabolomics can reveal changes in CNS metabolism in key conditions, strongly suggesting that interesting insights of CNS metabolism can be obtained also during animal growth [15]. In order for these investigations to be effective, a key role is covered by the exploration of the widest possible portions of the metabolome space [11], given by the number of quantified molecules and the by the knowledge about the connection between the metabolome profile and natural fluctuations of the physiological status, such as those connected to ageing.

Regarding the swine metabolome, the characterization of urine, serum, liver and kidney metabolome was recently performed, using both one and two-dimensional ¹H and ¹³C nuclear magnetic resonance spectroscopy (NMR) and high-resolution magic angle spinning (HR-MAS) NMR [16]. The study provided valuable information for translational medicine, validating once again the importance of metabolomics.

The aim of the present study was to investigate in both qualitative and quantitative manner the composition of Cerebrospinal Fluid harvested from healthy newborn (5 days old) and young (30 and 50 days old) piglets using ¹H NMR Spectroscopy, and to analyze any possible difference in metabolites concentration between age groups, related to age and Blood-Brain-Barrier maturation.

Material and Methods

Animals

Animals used in this study were Large White x Landrace x Duroc commercial hybrids. The total amount of animals sampled for this study was 44: 17 5-days old piglets (P05), 18 30-days old piglets (P30) and 9 50-days old piglets (P50). None of the animals was sampled at two different time points. Pregnant sows (for P05 animals) and weaned piglets (for P30 and P50 animals) were delivered to our facility from the same farm (Societa' Agricola Pasotti S.s, Imola 40026, Italy) in order to obtain a population as consistent and coherent as possible. P05 animals were housed with the sow in the farrowing crate with a heating lamp, while P30 and P50 in multiple pens according to their age. Weaned animals (P30-P50) were fed an age-appropriate commercial diet twice a day. All animals were enrolled as negative controls or as pre-treatment individuals in different protocols approved by the Italian Ministry of Health (art.7, D.Lgs 116/92), and were monitored at least once a day by the veterinarian. The sampling procedure was performed under general anaesthesia in order to avoid stress and guarantee the welfare of the animals. All pigs were constantly monitored during and after the procedure to rule out any possible complication. According to the individuals' protocols, all animals were eventually euthanized upon intravenous administration of Tanax (embutramide, mebenzonium iodide and tetracaine hydrochloride; 0.3 ml/kg; MSD Animal health, Milano, Italy) after general anesthesia.

Sampling procedure

Animals were considered to be healthy on the basis of clinical examination and blood tests, including a Complete Blood Count (CBC) and Chemistry Profile. Sampling procedures were performed as previously described by Romagnoli et al. [17]. Briefly, animals were anesthetized using inhalational induction with 8% Sevoflurane (SevoFlo; Abbott Laboratories, Chicago, IL, USA) in a oxygen and air mixture (1:1). After endotracheal intubation, piglets were positioned in lateral recumbency, and the dorsal area of the neck was clipped and surgically prepared. Cisterna Magna was punctured using a 75mm 22gauge spinal needle, and 1 ml of clear, non-hemorrhagic Cerebrospinal Fluid was collected into a sterile cryogenic tube and immediately frozen in liquid nitrogen, then stored in a -80°C freezer until analysis.

NMR spectra acquisition and treatment

The samples constituting each of the three groups were collected in two batches of similar size. The samples from each batch were prepared for ¹H-NMR analysis simultaneously, to minimize possible variability due to preparation conditions. To meet the sample volume specifications of the NMR probe, 300 µl of CSF were added to 300 µl of distilled water. The samples were centrifuged for 15 minutes at 15,000 rpm at 4°C. 500 µl of supernatant were added to 100 µl of a D₂O 1M phosphate buffer at pH 7.00 solution of 3-(trimethylsilyl)-propionic-2,2,3,3-d₄ acid sodium salt (TSP) 6.25 mM, added as reference compound, and of 2 mM sodium azide, to avoid bacteria proliferation [18]. To minimize time at room temperature between sample preparation and spectra acquisition, the samples were stored at -20°C prior to analysis for a time varying between 12 and 24 hours. Immediately before spectra acquisition the samples were thawed and centrifuged again. The samples underwent analysis in random order, requiring a maximum of 6 hours. ¹H-NMR spectra were recorded in 5 mm NMR tubes at 298 K with an AVANCE III spectrometer (Bruker, Milan, Italy) operating at 600.13 MHz.

Following Öhman et al. [19], the signals from broad resonances originating from large molecules were suppressed by a CPMG-filter composed by 400 echoes with a τ of 400 µs and a

180° pulse of 24 μs, for a total filter of 330 ms. The HOD residual signal was suppressed by means of presaturation. This was done by employing the `cpmgpr1d` sequence, part of the standard pulse sequence library. Each spectrum was acquired by summing up 256 transients using 32 K data points over a 7184 Hz spectral window, with an acquisition time of 2.28s. In order to apply NMR as a quantitative technique [20], the recycle delay was set to 5s, keeping into consideration the relaxation time of the protons under investigation. Pre-analytical sample management protocol and NMR experiments are conveniently summarized in [S1 File](#), according to Rubtsov et al. guidelines [21]. The signals were assigned by comparing their chemical shift and multiplicity with Chenomx software (Chenomx Inc., Canada, ver 8.1) standard (ver. 10) and HMDB (ver. 2) data banks, as described in detail in [S1A and S1B Fig](#). In case of ambiguity, proton-proton 2D experiments were performed, as shown in [S1C Fig](#).

Data analysis

Spectra were manually phase adjusted by means of Tospin (ver 3 –Bruker, Milan, Italy) and then transferred to Mestrenova (ver 10.0.2—Mestrelab Research S.L., Spain). Here a line broadening of 0.3 Hz was applied and an alignment towards TSP signal, set to 0 ppm, was applied. The baseline was adjusted by means of the Whittaker smoother algorithm [22], by applying a filter of 100 and a smoothing factor of 16384. Finally, the irregularities of the magnetic field leading to imperfections of the signals shape were compensated by reference deconvolution, by considering TSP singlet and a target linewidth of 1.2 Hz. No manual alignment of the signals was necessary, different to other body fluids [23]. Differences in water content among samples were taken into consideration by probabilistic quotient normalization [24], applied to the entire spectra array.

Data analyses were performed on R environment (version 3.2.2; the R Foundation for Statistical Computing, Vienna, Austria). Molecules showing different concentrations between time points were analyzed using a non-parametric Mann-Whitney U test. A probability lower than 0.05 was considered as significant, adjusted for multiple comparisons through Bonferroni correction.

Models of discriminant analysis based on projection on latent structures (PLS-DA) were built and graphically represented by means of the package `mixOmics`, formerly known as `integrOmics` [25]. For the purpose 75% of the samples from each group were randomly employed as a training set, while the remaining samples were used to test the model's performance. The optimal number of new space components was found by 10 fold cross-validation. The trends in the individuals distribution were highlighted by representing them in the XY-variate subspace described by PLS-DA model. For each component, the importance of the molecules in the samples distribution was highlighted by calculating the correlation between each metabolite and the selected latent variable, thus obtaining the so called correlation circle plot. To rank the overall importance of each molecule in the model, we calculated its variable importance over projection (VIP) [26]. As an alternative criterion, PLS-DA models were built in their sparse version (sPLS-DA) [27]. Briefly, sPLS-DA algorithm does not build DA models on the entire set of molecules, but pre-selects only those with the highest discriminative power, thus indirectly acting as a molecules ranking procedure. In our case, for each iteration models of increasing complexity were built by adding one new molecule at each iteration to a starting number of two.

The concentrations of the molecules observed in the present work spanned four orders of magnitude. The most concentrated molecules, with no biological reasons, would have dominated any multivariate model if employed as is. This forced us to scale each concentration to unit variance. This choice reduced the possibility for the reader to visually rank the molecules

according to their importance in the models. Such drawback was solved by setting up a cascade analysis protocol, where each multivariate algorithm refined the information granted by the previous.

Results

The sampling procedure proved to be strong and reliable, allowing the operator to collect blood-contamination free samples, suitable for analysis. Moreover, none of the animals showed alterations related to the procedure.

All the raw data are showed in [S1 Table](#).

A 1D-NMR spectrum of CSF from a 30d pig, representative of all the spectra registered in the present work, is depicted in [Fig 1](#). On each of the analyzed samples, 29 molecules could be observed above their limit of quantification, accounting for 95–98% of the total area of the spectra. Their concentration was obtained by integrating each spectrum over the ranges listed in [Table 1](#), comprising complete multiplets, as in the case of lactate, or portions, as in the case of glucose. The concentration of the molecules quantified by NMR in CSF are reported in [Table 2](#).

To gain an overall first impression of how the samples spread in the 29 dimensions space, for each P05 sample we calculated the median euclidean distances from the other P05 samples and from the samples collected at P50. The so obtained intergroup/intragroup distance ratio resulted statistically higher than 1 ($P < 7.63 \times 10^{-6}$). The same significant difference was found for the P05–P30 and the P30–P50 comparisons. In the same 29 dimension space, we found that P30 samples were equally distant from those collected at P05 and to those collected at P50. These observations show that the metabolome of each of three groups of samples was different from the others and that the characteristics of the samples at P30 were intermediate. To have a pictorial representation of this status, we calculated a PCA model on the centered and scaled concentrations of the molecules ([Fig 2](#)). The first principal component, even if representing the 22.7% of the total samples variance only, allowed a clear view of the samples metabolome overall evolution over time.

To focus on the molecules that mostly contributed to such overall trend along swine growth, we performed comparisons between P05 and P50 sample on a molecular basis. The concentration of adenine, tyrosine, leucine, valine, 3-hydroxyvalerate and 3-methyl-2-oxovalerate was found to decrease between P05 and P50, while the concentration of glutamine, creatinine, methanol, trimethylamine and myo-inositol was found to increase. The P05–P30 comparison

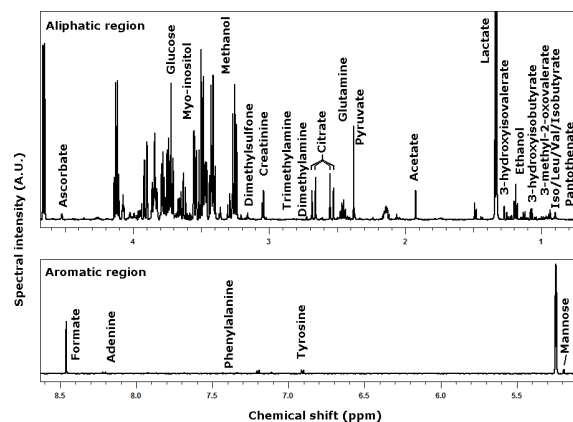


Fig 1. A 1D-NMR spectrum of CSF from a 30d pig, representative of all the registered spectra.

doi:10.1371/journal.pone.0157623.g001

Table 1. Location of the NMR signals employed for molecules quantification, identified in CSF of pigs in the 5–50 days range

Molecule	Range*	Protons**	Molecule	Range*	Protons**
Glucose	3.698–3.711	0.25	3-hydroxyisobutyrate	1.075–1.085	1.5
Lactate	1.298–1.356	3	Adenine	8.193–8.226	1
Formate	8.444–8.473	1	Acetate	1.914–1.933	3
Glutamine	2.433–2.484	2	Tyrosine	6.891–6.923	2
Citrate	2.521–2.563	2	Leucine	0.951–0.98	3
myo-inositol	3.608–3.636	1.5	Pantothenate	0.877–0.882	3
Pyruvate	2.373–2.385	3	Phenylalanine	7.416–7.452	2
Ascorbate	4.515–4.527	1	Valine	1.035–1.056	3
Ethanol	1.171–1.206	3	3-hydroxyisovalerate	1.267–1.277	6
Mannose	5.185–5.197	0.5	Dimethylamine	2.728–2.718	6
Creatinine	3.046–3.056	3	Isoleucine	1.004–1.023	3
Alanine	1.472–1.497	3	Isobutyrate	1.057–1.065	3
Creatine	3.036–3.045	3	Trimethylamine	2.879–2.894	9
Dimethyl sulfone	3.154–3.161	6	3-methyl-2-oxovalerate	1.117–1.136	3
Methanol	3.362–3.37	3			

* Portion of spectrum (expressed in ppm) where the multiplet employed for quantification were identified

** Number of protons giving rise to the multiplet. A fractional number indicates that a multiplet was not considered in its entirety.

doi:10.1371/journal.pone.0157623.t001

was also significant for glutamine, creatinine, adenine, tyrosine, leucine, valine, 3-hydroxyisovalerate, 3-methyl-2-oxovalerate, while for the P30-P50 comparison we found significant differences for glutamine, myo-inositol, leucine and trimethylamine. None of these molecules showed at P30 concentrations outside the P05–P50 range.

Focusing on the molecules that were found to differ between P05 and P50 samples, we desired to robustly rank them according to their importance in discriminating the three groups of samples. For the purpose, we followed a double procedure based on PLS-DA with VIP calculation on one side, and on sPLS-DA models on the other side. In detail, the concentrations of the molecules were employed to build 100 PLS-DA models, one of which presented in Fig 3. The discriminant models were preferred to the regression counterparts because we did not have any a-priori information about linearity of metabolome evolution along swine growth. Over the 100 built models, the average variance of the original samples explained by the first component was $83.1\% \pm 1.7\%$. No error was made in the assignment of the samples constituting the test set. The average number of latent components required by the models for such correct classification was 2.25 ± 1.67 , with a median of 1. Over the 100 models, tyrosine, 3-hydroxyisovalerate and trimethylamine were the only variables with average VIP above 1, which is typically considered as a safe threshold of importance for variables in PLS [26].

For each PLS-DA model, we created also a sPLS-DA counterpart, to take advantage of its pre-screening procedure of the molecules with the highest discriminating power. Over the 100 sPLS-DA models, the system selected as most important 3-hydroxyisovalerate and tyrosine 100 times, and creatinine, leucine and trimethylamine, 68, 61 and 57 times respectively.

Discussion

In the present work, we wanted to characterize the metabolome of cerebrospinal fluid of healthy newborn piglets, and to observe its modifications over the very first stages of life. The metabolome characterization was conveniently performed by means of ¹H-NMR, one of the leading techniques in the field due to its high reproducibility. The modifications along swine

Table 2. Concentration of the molecules quantified by NMR in CSF (mM).

	P05*	P30	P50	P05—P50 P-values
Lactate	2.42E+00 ± 3.68E-01	2.11E+00 ± 2.69E-01	2.84E+00 ± 3.99E-01	2.14E-02
Glucose	2.01E+00 ± 1.89E-01	1.72E+00 ± 2.89E-01	1.92E+00 ± 3.89E-01	8.33E-01
myo-inositol	3.87E-01 ± 7.38E-02	3.86E-01 ± 1.18E-01	6.03E-01 ± 1.49E-01	1.23E-03**
Ethanol	3.76E-01 ± 4.85E-01	8.42E-01 ± 1.51E+00	1.45E-01 ± 1.53E-01	2.87E-01
Glutamine	2.78E-01 ± 1.81E-02	3.56E-01 ± 9.99E-02	5.14E-01 ± 1.19E-01	6.40E-07**
Formate	2.27E-01 ± 2.82E-02	1.78E-01 ± 5.03E-02	2.56E-01 ± 4.71E-02	1.20E-01
Citrate	1.99E-01 ± 3.10E-02	1.27E-01 ± 2.19E-02	2.30E-01 ± 4.85E-02	1.33E-01
Pyruvate	1.52E-01 ± 3.26E-02	1.46E-01 ± 2.47E-02	1.13E-01 ± 2.02E-02	2.86E-03
Ascorbate	1.06E-01 ± 5.17E-02	1.11E-01 ± 6.94E-02	7.30E-02 ± 1.00E-02	3.96E-01
Mannose	9.16E-02 ± 1.09E-02	9.05E-02 ± 2.13E-02	7.79E-02 ± 1.51E-02	5.10E-02
Alanine	7.53E-02 ± 1.47E-02	9.52E-02 ± 1.61E-02	5.74E-02 ± 1.31E-02	1.10E-02
Acetate	6.72E-02 ± 2.30E-02	4.93E-02 ± 3.56E-02	6.96E-02 ± 1.88E-02	7.11E-01
Creatine	5.28E-02 ± 1.09E-02	4.38E-02 ± 7.42E-03	5.54E-02 ± 1.44E-02	7.11E-01
Creatinine	3.54E-02 ± 3.40E-03	4.39E-02 ± 6.01E-03	4.99E-02 ± 7.82E-03	2.56E-06**
3-hydroxyisobutyrate	3.04E-02 ± 7.63E-03	1.63E-02 ± 9.46E-03	2.22E-02 ± 4.03E-03	5.27E-03
Leucine	2.88E-02 ± 4.40E-03	2.11E-02 ± 3.87E-03	1.61E-02 ± 3.02E-03	6.40E-07**
Adenine	2.73E-02 ± 8.21E-03	1.47E-02 ± 7.44E-03	1.60E-02 ± 6.74E-03	4.09E-04**
Tyrosine	2.71E-02 ± 7.18E-03	1.19E-02 ± 3.75E-03	8.58E-03 ± 1.53E-03	6.40E-07**
3-methyl-2-oxovalerate	2.21E-02 ± 4.52E-03	1.36E-02 ± 5.88E-03	1.40E-02 ± 3.79E-03	2.30E-04**
Methanol	1.44E-02 ± 1.89E-03	2.74E-02 ± 1.45E-02	4.08E-02 ± 1.77E-02	6.40E-07**
3-hydroxyisovalerate	1.22E-02 ± 3.35E-03	4.22E-03 ± 2.10E-03	3.90E-03 ± 9.29E-04	6.40E-07**
Valine	1.13E-02 ± 2.47E-03	8.10E-03 ± 3.37E-03	5.52E-03 ± 1.85E-03	6.40E-07**
Phenylalanine	8.71E-03 ± 2.58E-03	7.56E-03 ± 2.38E-03	6.23E-03 ± 2.00E-03	2.50E-02
Dimethyl sulfone	8.45E-03 ± 2.09E-03	1.05E-02 ± 4.88E-03	5.35E-03 ± 2.08E-03	2.86E-03
Isoleucine	5.48E-03 ± 1.54E-03	6.53E-03 ± 4.49E-03	3.97E-03 ± 1.46E-03	1.31E-02
Pantothenate	3.91E-03 ± 2.76E-03	4.94E-03 ± 4.16E-03	2.58E-03 ± 8.16E-04	3.39E-01
Dimethylamine	2.71E-03 ± 5.03E-04	2.79E-03 ± 5.84E-04	2.27E-03 ± 6.14E-04	9.52E-02
Isobutyrate	2.53E-03 ± 7.23E-04	2.06E-03 ± 1.46E-03	3.06E-03 ± 1.24E-03	3.12E-01
Trimethylamine	7.57E-04 ± 3.49E-04	4.56E-04 ± 4.29E-04	4.97E-03 ± 3.82E-03	9.02E-04**

*The concentrations are expressed as mean ± standard deviation. The molecules are sorted according to their concentration at P05.

** Molecules showing statistical differences between P05 and P30.

doi:10.1371/journal.pone.0157623.t002

development were looked for through a multistep protocol, based on uni- and multivariate algorithms, able to put in progressive evidence the molecules mainly evolving over time.

The time points used in this paper were 5, 30 and 50 days of life. As previously stated, all the animals analyzed in this study were enrolled in different experimental protocols held in our facility, therefore samplings occurred according to the previously chosen times. One of the few attempts to compare swine and human ages suggests that our time points might approximately mimic 1, 6 and 12 months of age in humans. [28]. Due to the lack of specific data, every time point can provide important insights, and the 30 days old model has recently been used to describe new techniques [17, 29] and characterize new gene therapy patterns [30].

Before discussing the most representative molecules and the ones showing statistical differences, it is important to acknowledge the presence of ethanol within all of the samples. Its role in the CSF has recently been thoroughly analyzed by van der Sar et al. [31]: its presence has been interpreted as either a contaminant or a disease process-related molecule, but the same work also proved its capability to diffuse into ex vivo CSF samples via air transmission,

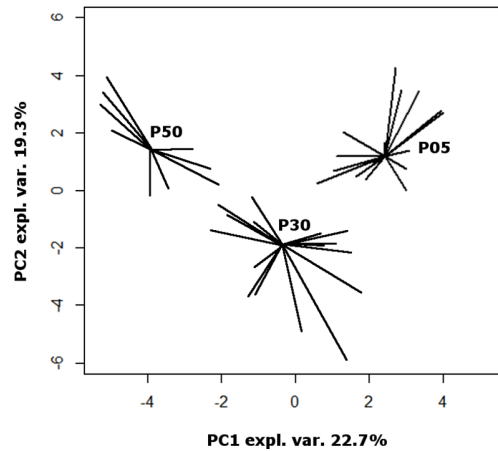


Fig 2. Scoreplot of a PCA model built on the concentrations of 29 molecules listed in Table 1. For each group, segments are drawn from each sample position to the median of the group. “Expl.Var.” stands for explained variance of the original data.

doi:10.1371/journal.pone.0157623.g002

therefore altering the metabolome post sample collection [31]. In addition, it is important to mention that the area of the neck used for puncture was prepped by means of a chlorhexidine gluconate/ethanol surgical scrub. Therefore, considering this potential contaminative source and the fact that our animals showed no signs of disease, its presence is most likely to be due to contamination.

The most representative molecules, consistently throughout the analyzed groups, are glucose and lactate, related to energy metabolism. This finding is coherent with the data already available for dogs [10] and humans [32]. Glucose represents the most important energy supply, and, within the CNS, plays an important role in the synthesis of pivotal neurotransmitters as glutamate, GABA and aspartate [33], so that high concentrations are highly common. Regarding the neonatal brain, the specific glucose metabolism has been recently described, showing that, compared to adult brains, more of this compound is prioritized to the pentose phosphate

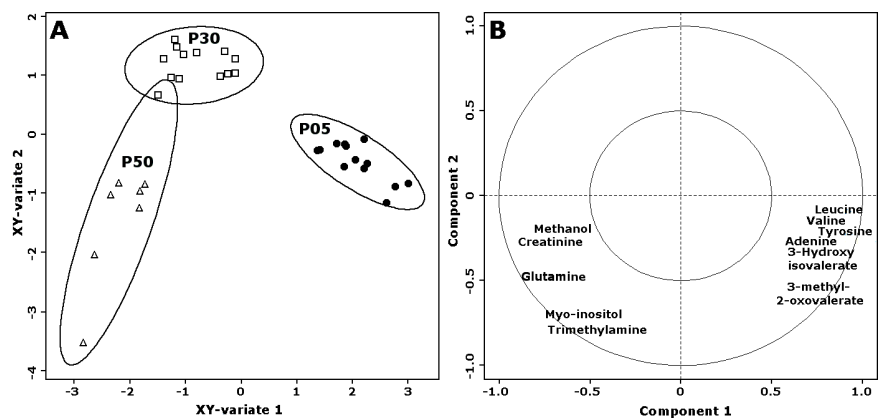


Fig 3. Scoreplot (A) and correlation plot (B) of one of the PLS-DA models built. The base of data was represented by the centered and scaled concentrations of the 11 molecules showing statistically significant differences between P05 and P50. The inner and outer circles of the correlation plots represent correlations of 0.5 and 1 respectively. P05, P30 and P50 samples are represented with filled circles, empty squares and empty triangles respectively.

doi:10.1371/journal.pone.0157623.g003

pathway (PPP). The latter is pivotal for the synthesis of DNA/RNA and the regeneration of NADPH [34]. Alongside, lactate represents the major product of anaerobic glycolysis, so that its high concentration is consistent with CSF composition of any animal species. As a diagnostic marker, high concentrations of lactate are reported to be related with both hypoxia and bacterial infections, particularly meningitis [35]. The characterization of glycolysis through the CSF metabolome might have extreme diagnostic capabilities. Indeed it seems that the shift from aerobic to anaerobic glycolysis is related with improvements of cognitive status in HIV affected patients [36].

Out of the 29 identified molecules, only 11 showed significant differences between the three groups, with P30 animals leaning more towards P5 or P50 depending on the specific compound. It has already been demonstrated that the concentration of the metabolites within CSF is influenced by several factors such as genetics, breeding, diet, and environment [37]. The impact of age on the CNS metabolome is nowadays an object of study, with one the most recent aiming to describe the brain metabolome of rats throughout their lifespan. The analyses proved that compared with regional differences, age contributed more substantially to the detected differences [38]. Differences in metabolites concentrations may be due to a number of factors related to both cerebral and systemic processes, including the maturation of the Blood-Brain-Barrier (BBB), age-related differences in brain metabolic rates and blood composition. It is therefore very likely to detect both increasing and decreasing trends when analyzing these molecules. Obviously, molecules fluctuating between individuals may be due as well to underlying pathologies. CSF metabolomics is indeed one of the most innovative and promising technique for the diagnosis of CNS diseases such as glioma [39] and leptomeningeal carcinomatosis [40]. Our animals were proved to be healthy on the bases on clinicopathological evaluations, and no individual differences were noticed. It is therefore safe to say the differences between homogeneous groups are to be imputed to the progression of the developmental stages.

Glutamine (glutamatergic system), myo-inositol (second messenger pathways), creatinine (energy metabolism), methanol (diet/systemic metabolism), and trimethylamine (diet/systemic metabolism) were found to significantly increase in concentration over time. The first three molecules, while ubiquitous, are involved in brain metabolism processes [10]; their increasing trend might reflect higher cerebral activity rates alongside with higher blood concentrations and BBB permeability. It is important to discuss the trend of glutamine, since it has been proven that it can act as an important biomarker in human medicine: an increase in its CSF concentration can be related to pathological processes such as depression [41]. On the other hand, concentrations lower than normal were detected in patients affected by multiple sclerosis [42]. We suggest that its increase in our animals may be reported to a higher rate in glucose metabolism and the proliferation of astrocytes within the neonatal brain. Astrocytes are the only cells containing Glutamine Synthetase, the only enzyme capable of converting glutamate and ammonia to glutamine in the mammalian brain [43]. The number of astrocytes at birth is sensibly lower when compared to adults, but the majority of gliogenesis occurs during the first weeks of life, making them the most present cells of CNS [44]. These cells play a pivotal role in the function and maintenance of the BBB [45], therefore, if we relate high concentrations of glutamine to an increasing number of astrocytes, we might use this finding as an indirect index of BBB maturation. Methanol and Trimethylamine, on the other hand, are considered to be waste products of food and/or systemic metabolism. In particular, metabolic methanol may occur as a result of fermentation by gut bacteria and metabolic processes involving S-adenosyl methionine [46]. Food probably represents the most important source of exogenous methanol and trimethylamine, and it is important to state that animals enrolled in the three groups, received different feed. P05 did not receive any solid feed in addition to the milk produced by the sows. P30 animals were freshly weaned (28th day of life) piglets that had just started eating

solid feed, and P50 had eaten solid feed for the previous 20 days. This feeding difference may be related to higher methanol and trimethylamine blood concentrations reflecting in increasing CSF concentrations. Unfortunately, due to the complexity of the metabolic pathways, partly still unknown, it is not possible to rule out any other hypothesis regarding these molecules. However it is important to stress this important correlation between metabolomics and food. The reflection of ingested molecules and their metabolites in the CSF metabolome profile might open new doors for more in depth analyses. This statement is true especially when it comes to orally administered integrators expressing their beneficial effects on the CNS such as quercetin [47] or to potential toxic agents introduced with food such as mercury [48].

Molecules showing significant decrease were adenine (protein synthesis/cellular respiration), tyrosine, leucine, valine (amino acids), and 3-hydroxyisovalerate and 3-methyl-2-oxovalerate (amino acid metabolism). It is very well acquainted that amino acids take part in a variety of biological processes, regulating in general the proteome. Free amino acids are pivotal for protein synthesis, acting as substrate for the growth and maintenance of tissues. They have impact on several events such as gene expression or transcription, immune response and autophagy. Moreover, as signaling molecules, they might have regulatory functions on protein turnover [49]. The influx of amino acids from the blood to the brain, and the regulatory role of the BBB has been extensively reviewed by Saunders et al [50], stating that essential amino acids are transported into the brain to a greater extent than non-essential ones; the correlation with BBB developmental state was not investigated. 3-Hydroxyisovalerate is derived from isovaleryl-CoA, a catabolic intermediate of leucine, and its concentration in adults' CSF was analyzed in the human metabolome database [32]. It was suggested that a decrease of 3-hydroxyisovalerate level in the human serum may be related to the development of neoplastic disease and in particular pancreatic cancer [51], but its role in the CSF has not been investigated. 3-methyl-2-oxovalerate, just like the previously mentioned compound, is involved in amino acid metabolism, representing the first degradation product of isoleucine [52]. In authors' opinion, the decrease of nucleobases and amino-acids, and of their metabolism products, might be related with the maturation and the increase in selectivity of the blood-brain barrier, but it is not possible to exclude an increase in their utilization within the CNS, thus making free concentrations lower. The concentrations of amino-acids in infant and newborn CSF were analyzed due to their possible role as diagnostic biomarkers for inborn errors of metabolism [53], therefore standard reference for piglets can be of extreme interest, especially considering transgenic models for this class of diseases.

Alongside the physiological analysis of CSF, a secondary aim of the present paper was to evaluate the evolution and the dynamics of the blood brain barrier in the swine model. Our data doesn't allow us to hypothesize a physiological age range for complete maturation of the blood brain barrier as suggested by differences between 30 and 50 days old piglets. Further studies on older animals are needed in order to be able to set a possible mark on complete maturation when no differences will be noticed between two age groups.

In conclusion, the present paper seems to supply with robust and valuable data regarding the physiological description of the swine CSF, providing new knowledge about such an important animal model. The extensive statistical analyses proved the 3 groups to be well assorted and homogeneous, providing more relevance and impact to the results and interesting hints for further studies about the BBB physiology. Diagnostic procedures involving CSF analyses for the swine medicine itself are very unlikely to be performed on a routine basis, but the situation is completely different regarding pigs enrolled in translational medicine protocols. This approach towards the quali-quantitative analysis of CSF and the maturation of the BBB is indeed an important step for the refinement and the standardization of the swine model.

Supporting Information

S1 Fig. Molecules assignment.

(DOCX)

S1 File. NMR additional info.

(DOCX)

S1 Table. Raw data.

(XLSX)

Acknowledgments

This study was supported by RFO 60%, Ateneo di Bologna.

Author Contributions

Conceived and designed the experiments: MLB DV AE FB. Performed the experiments: DV FB AE NR. Analyzed the data: LL DV AE. Contributed reagents/materials/analysis tools: MLB LL. Wrote the paper: DV LL.

References

1. Chen K, Baxter T, Muir WM, Groenen MA, Schook LB. Genetic resources, genome mapping and evolutionary genomics of the pig (*Sus scrofa*). *Int J Biol Sci*. 2007; 3:153–65. PMID: [17384734](#)
2. Wernersson R, Schierup MH, Jorgensen FG, Gorodkin J, Panitz F, Staerfeldt HH, et al. Pigs in sequence space: a 0.66X coverage pig genome survey based on shotgun sequencing. *BMC genomics*. 2005; 6:70. PMID: [15885146](#)
3. Bassols A, Costa C, Eckersall PD, Osada J, Sabria J, Tibau J. The pig as an animal model for human pathologies: A proteomics perspective. *Proteomics Clin Appl*. 2014; 8:715–31. doi: [10.1002/prca.201300099](#) PMID: [25092613](#)
4. Di Terlizzi R, Platt SR. The function, composition and analysis of cerebrospinal fluid in companion animals: part II—analysis. *Vet J (London, England: 1997)*. 2009; 180:15–32.
5. Di Terlizzi R, Platt S. The function, composition and analysis of cerebrospinal fluid in companion animals: part I—function and composition. *Vet J (London, England: 1997)*. 2006; 172:422–31.
6. Bailey CS, Higgins RJ. Comparison of total white blood cell count and total protein content of lumbar and cisternal cerebrospinal fluid of healthy dogs. *Am J Vet Res*. 1985; 46:1162–5. PMID: [4003891](#)
7. Desnoyers MBC, Meinkoth JH, Crystal MA. Cerebrospinal fluid analysis. In: Cowell RL TR, Meinkoth JH, DeNicola DB, editor. *Diagnostic cytology and hematology of the dog and the cat*. 3rd ed. ST. Louis: Mosby Elsevier; 2008. p. 215–33.
8. Andrews FM. Cerebrospinal fluid analysis and blood-brain barrier function. *Compendium on Continuing Education for the Practising Veterinarian*. 1998; 20:376.
9. Trimigno A, Marincola FC, Dellarosa N, Picone G, Laghi L. Definition of food quality by NMR-based foodomics. *Curr Opin Food Sci*. 2015; 4:99–104.
10. Musteata M, Nicolescu A, Solcan G, Deleanu C. The ¹H NMR profile of healthy dog cerebrospinal fluid. *PLOS One*. 2013; 8:e81192. doi: [10.1371/journal.pone.0081192](#) PMID: [24376499](#)
11. Laghi L, Picone G, Cruciani F, Brigidi P, Calani F, Donders G, et al. Rifaximin modulates microbiome and metabolome in women affected by bacterial vaginosis. *Antimicrob Agents Chemother*. 2014; 58:3411–3420. doi: [10.1128/AAC.02469-14](#) PMID: [24709255](#)
12. Di Cagno R, De Angelis M, De Pasquale I, Ndagijimana M, Vernocchi P, Ricciuti P, et al. Duodenal and faecal microbiota of celiac children: molecular, phenotype and metabolome characterization. *BMC microbiology*. 2011; 11:219. doi: [10.1186/1471-2180-11-219](#) PMID: [21970810](#)
13. Francavilla R, Calasso M, Calace L, Siragusa S, Ndagijimana M, Vernocchi P, et al. Effect of lactose on gut microbiota and metabolome of infants with cow's milk allergy. *Pediatr Allergy Immunol*. 2012; 23:420–427. doi: [10.1111/j.1399-3038.2012.01286.x](#) PMID: [22435727](#)
14. Carnevali A, Gianotti A, Benedetti S, Tagliamonte MC, Primiterra M, Laghi L, et al. Role of Kamut® brand khorasan wheat in the counteraction of non-celiac wheat sensitivity and oxidative damage. *Food Res Int*. 2014; 63:218–226.

15. Noga MJ, Dane A, Shi S, Attali A, van Aken H, Suidgeest E, et al. Metabolomics of cerebrospinal fluid reveals changes in the central nervous system metabolism in a rat model of multiple sclerosis. *Metabolomics*. 2012; 8:253–263. PMID: [22448154](#)
16. Merrifield CA, Lewis M, Claus SP, Beckonert OP, Dumas ME, Duncker S, et al. A metabolic system-wide characterisation of the pig: a model for human physiology. *Mol Biosyst*. 2011; 7:2577–2588. doi: [10.1039/c1mb05023k](#) PMID: [21761043](#)
17. Romagnoli N, Ventrella D, Giunti M, Dondi F, Sorrentino NC, et al. Access to cerebrospinal fluid in piglets via the cisterna magna: optimization and description of the technique. *Lab Anim*. 2014; 48:345–348. doi: [10.1177/0023677214540881](#) PMID: [24968696](#)
18. Beckonert O, Keun HC, Ebbels TM, Bundy J, Holmes E, et al. Metabolic profiling, metabolomic and metabolomic procedures for NMR spectroscopy of urine, plasma, serum and tissue extracts. *Nat Protoc*. 2007; 2:2692–2703. PMID: [18007604](#)
19. Ohman A, Forsgren L. NMR metabolomics of cerebrospinal fluid distinguishes between Parkinson's disease and controls. *Neurosci Lett*. 2015; 594:36–9. doi: [10.1016/j.neulet.2015.03.051](#) PMID: [25817365](#)
20. Simmler C, Napolitano JG, McAlpine JB, Chen SN, Pauli GF. Universal quantitative NMR analysis of complex natural samples. *Curr Opin Biotechnol*. 2014; 25: 51–59. doi: [10.1016/j.copbio.2013.08.004](#) PMID: [24484881](#)
21. Rubtsov DV, Jenkins H, Ludwig C, Easton J, Viant MR, Gunther U, et al. Proposed reporting requirements for the description of NMR-based metabolomics experiments. *Metabolomics*. 2007; 3:223–299.
22. Cobas JC, Bernstein MA, Martín-Pastor M, Tahoces PG. A new general-purpose fully automatic baseline-correction procedure for 1D and 2D NMR data. *J Magn Reson*. 2006; 183:145–151. PMID: [16891135](#)
23. De Filippis F, Pellegrini N, Vannini L, Jeffery IB, La Storia A, Laghi L, et al. High-level adherence to a Mediterranean diet beneficially impacts the gut microbiota and associated metabolome. *Gut*. 2015; pii: [gutjnl-2015-309957](#).
24. Dieterle F, Ross A, Schlotterbeck G, Senn H. Probabilistic quotient normalization as robust method to account for dilution of complex biological mixtures. Application in ¹H NMR metabolomics. *Anal Chem*. 2006; 78:4281–4290. PMID: [16808434](#)
25. Lê Cao KA, Gonzalez I, Dejean S. *integrOmics*: an R package to unravel relationships between two omics datasets. *Bioinformatics (Oxford, England)*. 2009; 25:2855–6.
26. Eriksson L, Johansson E, Kettaneh-Wold N, Wold S. (2001). *Multi- and megavariable data analysis: principles and applications*. 1st edition. Umeå: Umetrics Academy; 2001.
27. Lê Cao KA, Boitard S, Besse P. Sparse PLS discriminant analysis: biologically relevant feature selection and graphical displays for multiclass problems. *BMC bioinformatics*. 2011; 12:253 doi: [10.1186/1471-2105-12-253](#) PMID: [21693065](#)
28. Niblock MM, Luce CJ, Belliveau RA, Paterson DS, Kelly ML, Sleeper LA, et al. Comparative anatomical assessment of the piglet as a model for the developing human medullary serotonergic system. *Brain Res Brain Res Rev*. 2005; 50:169–83. PMID: [16043226](#)
29. Lambertini C, Ventrella D, Barone F, Sorrentino NC, Dondi F, Fraldi A, et al. Transdermal spinal catheter placement in piglets: Description and validation of the technique. *J Neurosci Methods*. 2015; 255:17–21. doi: [10.1016/j.jneumeth.2015.07.021](#) PMID: [26238729](#)
30. Sorrentino NC, Maffia V, Strollo S, Cacace V, Romagnoli N, Manfredi A, et al. A Comprehensive Map of CNS Transduction by Eight Recombinant Adeno-associated Virus Serotypes Upon Cerebrospinal Fluid Administration in Pigs. *Mol Ther*. 2016; 24:276–286. doi: [10.1038/mt.2015.212](#) PMID: [26639405](#)
31. van der Sar SA, Zielman R, Terwindt GM, van den Maagdenberg AM, Deelder AM, Mayboroda OA, et al. Ethanol contamination of cerebrospinal fluid during standardized sampling and its effect on (1)H-NMR metabolomics. *Anal Bioanal Chem*. 2015; 407:4835–4839. doi: [10.1007/s00216-015-8663-9](#) PMID: [25935669](#)
32. Wishart DS, Lewis MJ, Morrissey JA, Flegel MD, Jeroncik K, Xiong Y, et al. The human cerebrospinal fluid metabolome. *J Chromatogr B Analyt Technol Biomed Life Sci*. 2008; 871:164–73. doi: [10.1016/j.jchromb.2008.05.001](#) PMID: [18502700](#)
33. Amaral AI, Hadera MG, Tavares JM, Kotter MR, Sonnewald U. Characterization of glucose-related metabolic pathways in differentiated rat oligodendrocyte lineage cells. *Glia*. 2016; 64:21–34. doi: [10.1002/glia.22900](#) PMID: [26352325](#)
34. Brekke E, Morken TS, Sonnewald U. Glucose metabolism and astrocyte-neuron interactions in the neonatal brain. *Neurochem Int*. 2015; 82:33–41. doi: [10.1016/j.neuint.2015.02.002](#) PMID: [25684072](#)

35. Giulieri S, Chapuis-Taillard C, Jatou K, Cometta A, Chuard C, Hugli O, et al. CSF lactate for accurate diagnosis of community-acquired bacterial meningitis. *European journal of clinical microbiology & infectious diseases: official publication of the European Society of Clinical Microbiology*. 2015; 34:2049–55.
36. Dickens AM, Anthony DC, Deutsch R, Mielke MM, Claridge TD, Grant I, et al. Cerebrospinal fluid metabolomics implicate bioenergetics adaptation as a neural mechanism regulating shifts in cognitive states of HIV-infected patients. *AIDS*. 2015; 29:559–69. doi: [10.1097/QAD.0000000000000580](https://doi.org/10.1097/QAD.0000000000000580) PMID: [25611149](https://pubmed.ncbi.nlm.nih.gov/25611149/)
37. Crews B, Wikoff WR, Patti GJ, Woo HK, Kalisiak E, Heideker J, et al. Variability analysis of human plasma and cerebral spinal fluid reveals statistical significance of changes in mass spectrometry-based metabolomics data. *Anal Chem*. 2009; 81:8538–8544. doi: [10.1021/ac9014947](https://doi.org/10.1021/ac9014947) PMID: [19764780](https://pubmed.ncbi.nlm.nih.gov/19764780/)
38. Zheng X, Chen T, Zhao A, Wang X, Xie G, Huang F, et al. The Brain Metabolome of Male Rats across the Lifespan. *Scientific Reports*. 2016; 11; 6:24125. doi: [10.1038/srep24125](https://doi.org/10.1038/srep24125) PMID: [27063670](https://pubmed.ncbi.nlm.nih.gov/27063670/)
39. Nakamizo S, Sasayama T, Shinohara M, Irino Y, Nishiumi S, Nishihara M, et al. GC/MS-based metabolomic analysis of cerebrospinal fluid (CSF) from glioma patients. *J Neurooncol*. 2013; 113:65–74. doi: [10.1007/s11060-013-1090-x](https://doi.org/10.1007/s11060-013-1090-x) PMID: [23456655](https://pubmed.ncbi.nlm.nih.gov/23456655/)
40. Jeon JP, Kim JE. NMR-based metabolomics analysis of leptomeningeal carcinomatosis. *Neurosurgery*. 2014; 75:N12–3.
41. Levine J, Panchalingam K, Rapoport A, Gershon S, McClure RJ, Pettegrew JW. Increased cerebrospinal fluid glutamine levels in depressed patients. *Biol Psychiatry*. 2000; 47:586–593. PMID: [10745050](https://pubmed.ncbi.nlm.nih.gov/10745050/)
42. Aasly J, Gårseth M, Sonnewald U, Zwart JA, White LR, Unsgård G. Cerebrospinal fluid lactate and glutamine are reduced in multiple sclerosis. *Acta Neurol Scand*. 1997; 95:9–12. PMID: [9048978](https://pubmed.ncbi.nlm.nih.gov/9048978/)
43. Eid T, Tu N, Lee TS, Lai JC. Regulation of astrocyte glutamine synthetase in epilepsy. *Neurochem Int*. 2013; 63:670–681. doi: [10.1016/j.neuint.2013.06.008](https://doi.org/10.1016/j.neuint.2013.06.008) PMID: [23791709](https://pubmed.ncbi.nlm.nih.gov/23791709/)
44. Bandeira F, Lent R, Herculano-Houzel S. Changing numbers of neuronal and non-neuronal cells underlie postnatal brain growth in the rat. *Proc Natl Acad Sci USA*. 2009; 106:14108–13. doi: [10.1073/pnas.0804650106](https://doi.org/10.1073/pnas.0804650106) PMID: [19666520](https://pubmed.ncbi.nlm.nih.gov/19666520/)
45. Alvarez JI, Katayama T, Prat A. Glial influence on the blood brain barrier. *Glia*. 2013; 61:1939–58. doi: [10.1002/glia.22575](https://doi.org/10.1002/glia.22575) PMID: [24123158](https://pubmed.ncbi.nlm.nih.gov/24123158/)
46. Dorokhov YL, Shindyapina AV, Sheshukova EV, Komarova TV. Metabolic methanol: molecular pathways and physiological roles. *Physiol Rev*. 2015; 95:603–44. doi: [10.1152/physrev.00034.2014](https://doi.org/10.1152/physrev.00034.2014) PMID: [25834233](https://pubmed.ncbi.nlm.nih.gov/25834233/)
47. Wiczowski W, Skipor J, Misztal T, Szawara-Nowak D, Topolska J, Piskula MK. Quercetin and isorhamnetin aglycones are the main metabolites of dietary quercetin in cerebrospinal fluid. *Mol Nutr Food Res*. 2015; 59:1088–94 doi: [10.1002/mnfr.201400567](https://doi.org/10.1002/mnfr.201400567) PMID: [25727325](https://pubmed.ncbi.nlm.nih.gov/25727325/)
48. Lohren H, Bornhorst J, Galla HJ, Schwerdtle T. The blood-cerebrospinal fluid barrier—first evidence for an active transport of organic mercury compounds out of the brain. *Metallomics*. 2015; 7:1420–30. doi: [10.1039/c5mt00171d](https://doi.org/10.1039/c5mt00171d) PMID: [26267314](https://pubmed.ncbi.nlm.nih.gov/26267314/)
49. Bourgoin-Voillard S, Goron A, Seve M, Moinard C. Regulation of the proteome by amino acids. *Proteomics*. 2016; 16:831–846. doi: [10.1002/pmic.201500347](https://doi.org/10.1002/pmic.201500347) PMID: [26786846](https://pubmed.ncbi.nlm.nih.gov/26786846/)
50. Saunders NR, Habgood MD, Møllgård K, Dziegielewska KM. The biological significance of brain barrier mechanisms: help or hindrance in drug delivery to the central nervous system? *F1000Res*. 2016; 5. pii: F1000 Faculty Rev-313.
51. OuYang D, Xu J, Huang H, Chen Z. Metabolomic profiling of serum from human pancreatic cancer patients using ¹H NMR spectroscopy and principal component analysis. *Appl Biochem Biotechnol*. 2011; 165:148–54. doi: [10.1007/s12010-011-9240-0](https://doi.org/10.1007/s12010-011-9240-0) PMID: [21505807](https://pubmed.ncbi.nlm.nih.gov/21505807/)
52. Schicho R, Shaykhtudinov R, Ngo J, Nazyrova A, Schneider C, Panaccione R, et al. Quantitative metabolomic profiling of serum, plasma, and urine by (1)H NMR spectroscopy discriminates between patients with inflammatory bowel disease and healthy individuals. *J Proteome Res*. 2012; 11:3344–3357. doi: [10.1021/pr300139q](https://doi.org/10.1021/pr300139q) PMID: [22574726](https://pubmed.ncbi.nlm.nih.gov/22574726/)
53. Jones CM, Smith M, Henderson MJ. Reference data for cerebrospinal fluid and the utility of amino acid measurement for the diagnosis of inborn errors of metabolism. *Ann Clin Biochem*. 2006; 43(Pt 1):63–6. PMID: [16390611](https://pubmed.ncbi.nlm.nih.gov/16390611/)

Second Paper

The biomedical piglet: establishing reference intervals for
haematology and clinical chemistry parameters of two age groups
with and without iron supplementation

RESEARCH ARTICLE

Open Access



The biomedical piglet: establishing reference intervals for haematology and clinical chemistry parameters of two age groups with and without iron supplementation

Domenico Ventrella, Francesco Dondi*, Francesca Barone, Federica Serafini, Alberto Elmi, Massimo Giunti, Noemi Romagnoli, Monica Forni and Maria L. Bacci

Abstract

Background: The similarities between swine and humans in physiological and genomic patterns, and the great correlation in size and anatomy, make pigs extremely useful in preclinical studies. New-born piglets can represent a model for congenital and genetic diseases in new-born children. It is known that piglets may have significant differences in clinicopathological results compared to adult pigs. Therefore, adult laboratory reference intervals cannot be applied to piglets. The aim of this study was to compare haematological and chemical variables in piglets of two ages and determinate age-related reference intervals for commercial hybrid young pigs.

Blood samples were collected under general anaesthesia from 130 animals divided into five- (P5) and 30- (P30) day-old piglets. Only P30 animals were treated with parenteral iron after birth. Samples were analysed using automated haematology (ADVIA 2120) and chemistry analysers, and age-related reference intervals were calculated.

Results: Significant higher values of RBC, Hb and HCT were observed in P30 animals when compared to P5, with an opposite trend for MCV. These results were associated with a reduction of the RBC regeneration process and the thrombopoietic response. The TSAT and TIBC were significantly higher in P30 compared to P5; however, piglets remained iron deficient compared to adult reference intervals reported previously.

Conclusions: In conclusion, this paper emphasises the high variability occurring in clinicopathological variables between new-born and 30-day-old pigs, and between piglets and adult pigs. This study provides valuable reference data for piglets at precise ages and could be used in the future as historical control improving the Reduction in animal experiments, as suggested by the 3Rs principle.

Keywords: ADVIA 2120, Clinical chemistry, Haematology, Reference intervals, Swine

* Correspondence: f.dondi@unibo.it

Department of Veterinary Medical Sciences, Alma Mater Studiorum, University of Bologna, Via Tolara di Sopra 50, 40064 Ozzano dell'Emilia, BO, Italy



Background

The interest in the pig as an animal model for experimental medicine can be traced back to Galen, in 1586 [1]. One reason for this interest is the strong similarities between the pig and the human in both physiological [2] and genomic [3] patterns. In addition, size and anatomy can be easily related to the development stages of people, making the pig the perfect preclinical model for human diseases [4, 5], surgical techniques and, more recently, for transplantation research [6–8]. When compared to other models such as mice or rats, the pig has a longer lifespan of 10–15 years [9], so disease progression is more similar to that seen in humans [1]. Furthermore, in the neonatal period, pigs represent an accurate model for studying congenital and genetic diseases in humans [10]. Piglets can even represent a good model for the preterm neonate, as they show similar anthropometric and physiological characteristics [11].

However, age differences, even within the same species, significantly affect the comparison of some developmental patterns, especially in extremely young subjects. Therefore, these processes need to be thoroughly investigated in order to create an accurate and standardised preclinical model and to help reduce and refine experimental protocols. As an important example, iron deficiency, which is one of the most common nutritional defects during the neonatal period in mammals [12, 13], is extremely common in swine, due to the high reproductive performance required of these animals. Unless given iron supplements, piglets may develop iron-deficiency a few days after birth [14, 15]. This condition occurs regardless of the breed and management system, and is the result of interactions of several factors including low levels of iron stores, increased requirements, poor exogenous supply and immaturity of absorption mechanisms [15, 16]. Similarly, iron requirements cannot be completely fulfilled by hepatic reserves and milk consumption due to the constant request for larger litter sizes, higher birth weights and faster growth that result in a greater blood volume and red blood cell (RBC) count [17]. It is therefore mandatory to supplement piglets with exogenous iron to prevent dangerous deficiency [18]. This procedure may interfere with several clinical chemistry parameters [19] and is the reason why it is very inaccurate to evaluate piglets based on the clinicopathological findings of older pigs. Therefore, it is extremely important to have specific age-related reference intervals for both haematological and chemical variables for piglets. Some values have been described in a single litter of Duroc x Jersey piglets [20], but the small number of animals and the lack of information about iron supplementation make them hard to rely on.

The aim of this study was to evaluate haematological and chemical variables in two groups of healthy hybrid

piglets of different ages. Secondary objectives were to establish age-related reference intervals (RI) for both haematology and clinical chemistry variables and to evaluate the iron profile in new-born piglets without exogenous supplementation (5 days old) and young pigs administered with exogenous iron within 3 days after birth (30 days old).

Methods

Animals

All of the animals were Italian Large White x Duroc x Landrace commercial hybrids used in our facility. We only selected control and/or pre-treated animals previously enrolled in other experimental protocols and approved by the local ethical committee to be part of this study. The above mentioned protocols included blood tests to evaluate the animals, and we decided to work on the obtained data set of blood values.

We analysed piglets at two different time points: P5 were five-day-old piglets born in our facility that had not received any iron supplementation before blood sampling and were not neutered; P30 were 30-day-old pigs that were transferred to our piggery on the day of weaning (28th day of life) and were administered a single iron injection (100 mg IM; Endofer, FATRO, Italy) within the first 72 h after birth, and males were neutered. None of the animals was included in both age groups. In order to rule out any possible variation in genetic line and management, both pregnant sows and pigs were born and raised in the same farm. All of the animals were housed in multiple stalls and fed with a standard swine diet; P5 were housed in the farrowing crate with the sow until weaning. Body weight (kg) was measured in P5 and P30 and recorded.

A total of one hundred-thirty animals were included in the study; 74/130 (57%) were females, while 56/130 (43%) were males. Body weight was 2.3 (1.2–3.8) kg in P5 and 8.0 (5.3–11.2) kg in P30. For haematological analyses, samples from 130 animals were available: 66 P5 and 64 P30. For chemistry evaluations, samples from 119 animals were available: 56 P5 and 63 P30.

Blood sample collection and analyses

Blood samplings were performed on day 5 (P5) or 30 (P30) under general anaesthesia, using an advanced anaesthesia delivery unit (Datex-Ohmeda ADU S/5, GE Healthcare, USA), achieved by inhalation induction with sevoflurane (Sevoflo, Abbott Laboratories, Chicago, USA). No premedication was performed in order to avoid blood alterations due to injected drug adsorption. After oro-tracheal intubation, anaesthesia was maintained with $4 \pm 0.5\%$ sevoflurane in a 1:1 oxygen/air mixture. Samples were obtained from the femoral artery using a 21 G butterfly needle and a vacuum system;

tubes with K₃EDTA anticoagulant, citrate and clot activator were used. The total volume of withdrawn blood was approximately 10 ml, which was considered completely safe and negligible for these animals.

Blood samples (K₃EDTA tubes) were analysed within 30 min from collection; serum (clot activator tubes) and citrate plasma (citrate tubes) were obtained by centrifugation (10 min at 3000 × g) within 1 h and analysed or stored at -80 °C until analysis.

Complete blood count (CBC) was performed with a new automated haematology analyser (ADVIA 2120, Siemens Healthcare Diagnostics, Tarrytown NY, USA) that combines classic haematological variables with individual cell indices. The variables evaluated in our study were haematocrit value (HCT), haemoglobin concentration (Hb), cellular haemoglobin content (CH), cellular haemoglobin content of mature red blood cells (CHm), red blood cells count (RBC), mean corpuscular volume (MCV), mean corpuscular volume of mature RBCs (MCVm), mean corpuscular haemoglobin concentration (MCHC), mean corpuscular haemoglobin (MCH), corpuscular haemoglobin concentration mean (CHCM), corpuscular haemoglobin concentration mean of mature RBCs (CHCMm), haemoglobin concentration distribution width (HDW), haemoglobin concentration distribution width of mature RBC (HDWm), RBC distribution width (RDW) and mature RBC distribution width (RDWm). Total white blood cell (WBC) count and differential WBC count were also performed. Platelet indices were analysed and included platelet count (PLT), mean platelet volume (MPV), PLT volume distribution width (PDW), plateletcrit (PCT), mean PLT component (MPC), platelet component distribution width (PCDW), mean PLT mass (MPM) and platelet mass distribution width (PMDW).

In addition to the above mentioned variables, we evaluated the following reticulocyte indices: absolute reticulocyte count (Retic), percentage of reticulocytes (%Retic), average size of reticulocytes (MCVr), average cell haemoglobin concentration (CHCMr), average haemoglobin content (CHr), distribution width of reticulocyte cell size (RDWr), distribution width of CHCMr (HDWr), percentage of microcytic reticulocytes (%Micro-r), percentage of macrocytic reticulocytes (%Macro-r), percentage of hypochromic reticulocytes (%Hypo-r), percentage of hyperchromic reticulocytes (%Hyper-r), percentage of reticulocytes with a low CH (%LowCHR), percentage of reticulocytes with a high CH (%HighCHR), CHr-CHm (CH delta), CHCMr-CHCMm (CHCM delta), CHDWr-CHDWr (CHDWr delta), HDWr-HDWr (HDWr delta), MCVr-MCVm (MCV delta), and RDWr-RDWr (RDW delta). The haematological evaluation was completed by a blood smear microscopic examination using Romanovsky staining.

All chemistry analyses were carried out on an automated chemistry analyser (Olympus AU 400, Beckman Coulter/Olympus) and included aspartate transaminase (AST), alanine transaminase (ALT), alkaline phosphatase (ALP), creatinine, urea, glucose, total proteins (TP), albumin, albumin to globulin ratio (A/G), sodium, potassium, total iron (TI), unsaturated iron binding capacity (UIBC), total iron binding capacity (TIBC) and TIBC saturation (TSAT). Total iron and UIBC were measured using colorimetric methods (Iron Ferene, KAL 002, Olympus/Sentinel Diagnostics, Milan, Italy; UIBC OSR61205, Olympus/Beckman Coulter, O'Callaghan's Mills, Ireland). Total iron binding capacity and TSAT were calculated as follows: $TIBC = TI + UIBC$; $TSAT = (TI \times 100)/TIBC$.

ADVIA 2120 erythrocytes, reticulocytes and platelet indices, and other variables evaluated in the study are reported in the Additional file 1, including their abbreviations.

Statistical analyses

Statistical analyses were performed using MedCalc statistical software (version 15.6; MedCalc Software, Ostend, Belgium). The D'Agostino-Pearson test was used to assess normal distribution of data. Data were reported as mean ± SD or median (minimum-maximum) based on their distribution. Comparisons between the two age groups were performed using the Mann-Whitney *U* test due to the non-Gaussian distribution of the majority of the data. Reference intervals were obtained using the 2.5th – 97.5th percentiles method following the Clinical and Laboratory Standards Institute (CLSI) guidelines for estimating percentiles and their 90% confidence intervals [21]. Outliers were identified with the Tukey test. Differences were considered to be statistically significant with $P < 0.05$.

Results and discussion

For the haematological and chemical analyses, the number of samples available for each analyses, descriptive statistics, differences between groups and estimated RI in P5 and P30 are reported in Tables 1, 2 and 3. A significant increase in the circulating erythrocyte mass was detected in P30 compared to P5 as demonstrated by the higher values of Hb, HCT and RBC count. This finding was associated with a significant reduction in volume (MCV, MCVm) and a significant increase in anisocytosis (RDW, RDWm). Erythrocyte haemoglobin content indices (CH, CHm, MCH) were significantly lower in P30 compared to P5 with the exception of CHCM which was significantly higher in P30, while MCHC and CHCMm were not significantly different between groups (Table 1). Absolute reticulocyte count and percentage of reticulocytes were significantly lower in P30 compared to P5.

Table 1 Descriptive statistics, differences between groups and estimated reference intervals for haematological variables. Data are expressed as mean \pm SD or median (minimum-maximum)

Variable	P5		P5 <i>n</i>	P30		P30 <i>n</i>	<i>P</i> -value
	Descriptive data	Reference Interval		Descriptive data	Reference Interval		
Hb (g/dL)	6.03 \pm 1.02	3.56-7.74	61	8.84 \pm 2.0	4.32-13.31	64	<0.0001
HCT (%)	20 \pm 3	13-25	61	29 \pm 6	16-41	64	<0.0001
CH (pg)	16.85 (14.10-22.30)	14.30-21.82	66	14.0 (9.0-19.0)	9.3-18.9	64	<0.0001
CHm (pg)	18.3 (16.1-22.4)	16.27-22.01	50	15.4 \pm 1.5	12.7-18.8	33	<0.0001
CHDW (pg)	3.72 (2.90-5.84)	3.01-5.71	66	3.99 \pm 0.66	2.66-5.33	64	0.3541
CHDWm (pg)	3.36 (2.82-5.47)	2.83-5.34	50	4.78 (2.61-5.55)	2.61-5.50	33	<0.0001
RBC ($10^6/\mu\text{L}$)	3.26 \pm 0.52	1.88-4.11	61	6.08 \pm 0.93	4.08-8.17	64	<0.0001
MCV (fL)	61.97 \pm 5.39	51.41-73.65	61	48.5 (32.4-61.5)	34.2-61.3	64	<0.0001
MCVm (fL)	65.9 \pm 4.5	56.4-74.9	50	52.9 \pm 3.9	45.3-60.5	33	<0.0001
MCHC (g/dL)	30.0 \pm 1.6	26.1-32.7	61	29.9 \pm 1.59	26.5-33.6	63	0.9606
MCH (pg)	18.50 \pm 1.36	15.45-21.54	61	14.8 (9.1-20.2)	9.4-19.8	64	<0.0001
CHCM (g/dL)	27.35 \pm 1.11	24.84-29.13	66	28.35 \pm 1.60	25.13-31.62	64	0.0003
CHCMm (g/dL)	28.2 (26.7-30.8)	26.8-30.8	50	28.6 (26.8-30.9)	26.8-30.9	33	0.5389
RDW (%)	18.8 (15.8-25.7)	15.9-25.7	56	26.5 (13.5-38.5)	13.5-38.0	64	<0.0001
RDWm (%)	15.9 (14.2-25.7)	14.2-25.1	50	25.5 (12.7-32.2)	12.7-32.0	33	<0.0001
HDW (g/dL)	2.89 (2.28-4.13)	2.29-3.93	66	2.63 \pm 0.40	2.02-3.50	64	<0.0001
HDWm (g/dL)	2.60 (2.14-3.68)	2.16-3.63	50	2.73 \pm 1.99-3.28	1.99-3.28	33	0.1685
WBC ($10^3/\mu\text{L}$)	7.47 (4.39-12.58)	4.50-12.55	58	11.6 \pm 3.2	5.6-18.5	58	<0.0001
neutrophil (%)	44.71 \pm 9.66	22.77-61.33	60	35.3 \pm 15.0	10.8-70.6	63	0.0001
lymphocyte (%)	49.30 \pm 9.49	33.45-70.86	60	57.9 \pm 14.5	26.2-82.9	64	0.0005
monocyte (%)	3.11 \pm 1.13	1.10-5.85	59	4.4 \pm 1.5	1.4-8.3	64	<0.0001
eosinophil (%)	0.5 (0.1-3.1)	0-2.3	57	0.6 (0.1-7.6)	0-1.9	64	0.5699
basophil (%)	0.41 \pm 0.16	0-0.79	60	0.4 (0.2-1.2)	0-0.9	63	0.1183
neutrophil ($10^3/\mu\text{L}$)	3.17 \pm 0.98	1.15-5.43	54	3.5 (0.8-9.9)	0.8-9.7	61	0.1472
lymphocyte ($10^3/\mu\text{L}$)	3.85 \pm 1.11	1.91-6.45	58	6.6 \pm 2.4	2.7-12.8	60	<0.0001
monocyte ($10^3/\mu\text{L}$)	0.23 (0.07-0.7)	0.075-0.68	59	0.4 (0.1-1.1)	0.1-1.1	59	<0.0001
eosinophil ($10^3/\mu\text{L}$)	0.04 (0.01-0.48)	0-0.28	60	0.07 (0.01-0.38)	0.00-0.20	63	0.0014
basophil ($10^3/\mu\text{L}$)	0.03 (0.01-0.2)	0-0.08	60	0.05 (0.02-0.33)	0.00-0.13	63	<0.0001
PLT ($10^3/\mu\text{L}$)	594 (219-1142)	253-1286	61	503 \pm 141	192-832	63	<0.0001
MPV (fL)	17.84 \pm 3.78	9.99-25.32	61	8.5 (6.2-13.0)	6.5-12.7	63	<0.0001
PDW (%)	84.22 \pm 8.32	69.17-100.30	61	60.40 (17.90-106.60)	18.59-101.98	64	<0.0001
PCT (%)	1.20 \pm 0.50	0.29-2.52	61	0.40 (0.12-0.94)	0.18-0.91	62	<0.0001
MPC (g/dL)	24.5 (17.2-26.3)	17.81-26.30	61	24.09 \pm 0.96	21.69-26.50	64	0.0182
MPM (pg)	2.84 \pm 0.34	2.10-3.44	61	1.96 \pm 0.22	1.58-2.45	63	<0.0001
PCDW (g/dL)	4.6 (4.0-5.7)	4.0-5.6	66	4.6 (3.8-5.9)	3.9-5.9	64	0.4354
PMDW (pg)	1.45 (0.99-1.62)	0.99-1.61	66	0.87 (0.61-1.55)	0.62-1.54	64	<0.0001

Many other reticulocyte indices were significantly different between age groups (Table 2).

Circulating platelet number (PLT, PCT) was significantly decreased in P30 compared to P5; these results were associated with a significant reduction in platelet volume and mass (MPV, MPM) in P30 animals.

In the chemistry analysis, P5 subjects had significantly lower values of creatinine, urea, ALT, albumin and A/G and significantly higher ALP and potassium compared to P30 animals. Total iron concentration and TSAT % were significantly higher in P30 piglets compared to P5 (Table 3).

Table 2 Descriptive statistics, differences between groups and estimated reference intervals for reticulocyte indices. Data are expressed as mean \pm SD or median (minimum-maximum)

Variable	P5	P5	P5 <i>n</i>	P30	P30	P30 <i>n</i>	<i>P</i> -value
	Descriptive data	Reference Interval		Descriptive data	Reference Interval		
Retic (10^9 cell/L)	369.3 \pm 101.1	152.2–547.9	45	148.2 (53.4–554.5)	53.4–554.5	33	<0.000001
%Retic (%)	11.8 \pm 3.8	4.6–20.7	49	2.5 (0.8–9.2)	0.8–9.2	33	<0.000001
MCVr (fL)	74.5 \pm 7.3	60.7–89.4	48	56.5 \pm 6.8	43.0–71.1	33	<0.000001
CHCMr (g/dL)	24.9 \pm 0.9	23.4–27.0	48	26.1 \pm 1.0	24.2–28.0	33	0.000008
CHr (pg)	18.1 (16.0–24.3)	16.2–23.8	48	14.6 \pm 1.4	12.1–18.0	33	<0.000001
CHDWr (pg)	3.7 \pm 0.3	3.1–4.4	48	3.5 (2.4–4.6)	2.4–4.6	33	0.166288
RDW _r (%)	17.6 \pm 2.1	14.2–20.7	48	19.5 (13.0–33.0)	13.0–33.0	33	0.055130
HDW _r (g/dL)	3.36 \pm 0.36	2.66–3.84	48	3.9 \pm 0.62	2.7–5.1	33	0.000003
%Micro-r (%)	0.05 (0–0.8)	0.0–0.45	48	0.7 (0.0–15.5)	0.0–15.5	33	0.000005
%Macro-r (%)	26.5 (4.8–71.9)	6.7–70.7	48	2.6 (1.0–17.4)	1.0–17.4	33	<0.000001
%Hypo-r (%)	83.0 (62.8–94.3)	62.2–92.2	48	76.4 (57.2–85.8)	57.2–85.8	33	0.000036
%Hyper-r (%)	0.1 (0.0–0.3)	0.0–0.3	48	0.3 (0.0–2.7)	0.0–2.7	33	<0.000001
%LowCHr (%)	10.9 (0.5–35.4)	0.5–32.1	48	57.3 (6.0–76.8)	6.0–76.8	33	<0.000001
%HighCHr (%)	22.6 (9.2–76.3)	10.1–74.9	48	7.1 \pm 2.5	3.3–13.0	33	<0.000001
CH delta (pg)	–0.1 \pm 1.6	–3.3–2.1	48	–0.7 \pm 0.7	–2.4–0.7	33	0.012741
CHCM delta (g/dL)	–3.4 \pm 0.9	–5.2–(–1.8)	48	–2.6 \pm 1.7	–5.3–0.8	33	0.075
CHDW delta (pg)	0.38 (–0.54–0.86)	–0.33–0.67	48	–1.0 \pm 0.6	–2.19–(–0.05)	33	<0.000001
HDW delta (g/dL)	0.66 \pm 0.27	0.12–1.07	48	1.26 \pm 0.46	0.18–2.06	33	<0.000001
MCV delta (fL)	8.9 \pm 6.6	–3.4–18.3	48	3.6 \pm 4.4	–3.8–12.5	33	0.000255
RDW delta (%)	1.4 (–7.4–5.2)	–6.3–4.2	48	–3.8 \pm 4.3	–12.6–3.0	33	<0.000001

Table 3 Descriptive statistics, differences between groups and estimated reference intervals for clinical chemistry. Data are expressed as mean \pm SD or median (minimum-maximum)

Variable	P5	P5	P5 <i>n</i>	P30	P30	P30 <i>n</i>	<i>P</i> -value
	Descriptive data	Reference Interval		Descriptive data	Reference Interval		
Glucose (mg/dL)	124 (69–200)	71–196	49	111 \pm 26	34–159	62	0.0016
Urea (mg/dL)	12.4 (4.9–31.7)	5.0–30.8	55	17 (4–40)	4–39	59	0.0002
Creatinine (mg/dL)	0.65 (0.30–0.88)	0.38–0.85	56	1.09 (0.31–1.41)	0.51–1.39	62	<0.0001
AST (U/L)	29 \pm 7	10–47	56	31 (11–68)	13–65	62	0.9915
ALT (U/L)	23 \pm 6	5–38	56	30 (11–58)	14–54	60	<0.0001
ALP (U/L)	3773 \pm 1017	1324–6031	56	770 \pm 270	110–1292	61	<0.0001
TP (g/dL)	5.0 \pm 0.5	3.7–6.2	54	4.8 (1.2–6.7)	2.5–6.6	59	0.4464
Albumin (g/dL)	1.8 \pm 0.3	1.0–2.6	55	3.0 (1.8–4.0)	1.9–4.0	59	<0.0001
A/G	0.56 (0.36–0.99)	0.37–0.98	53	1.5 \pm 0.3	0.7–2.2	60	<0.0001
TI (μ g/dL)	15 (9–31)	9–30	49	34 (7–157)	7–151	60	<0.0001
UIBC (μ g/dL)	338 \pm 72	218–524	44	326 (40–1058)	63–980	62	0.2031
TIBC (μ g/dL)	354 \pm 72	230–542	44	397 (128–882)	142–877	60	0.0031
TSAT (%)	4.2 \pm 1.2	1.3–6.7	42	8.6 (0.8–55.6)	0.9–54	61	0.0058
Potassium (mEq/L)	4 \pm 0.5	2.8–5.1	54	3.7 \pm 0.4	2.9–4.6	63	0.0252
Sodium (mEq/L)	135 (126–140)	126–140	53	136 \pm 4.7	125–147	63	0.2448

Swine are probably one of the most important models for translational medicine [7], and therefore a complete and accurate knowledge of their physiology should be mandatory. This kind of knowledge would represent a big improvement when it comes to refinement of animal experiments. When using commercial hybrids for scientific purposes, it is important to acknowledge that those animals are the products of strong zootechnical manipulation that constantly requires higher breeding and production performance [18]. Moreover, very young piglets (first month of age) present high variability in many clinical and clinicopathological variables due to rapid growth, nutrition and other metabolic conditions, some which are potentially related to iron status [15, 20]. As in other species, new-born and young piglets are extremely different than adult animals regarding laboratory results [20], thus, the determination of reliable age-related reference intervals for both haematology and chemistry variables in 5- and 30-day-old piglets is warranted. It is important to acknowledge the fact that our results may not perfectly translate to every other pigs' breeds, but still represent a valid and robust general reference especially because obtained by one of the most common hybrid cross in Europe. Another important issue to address, before the discussion of the results, is the feeding protocol: P5 only received milk from the sows, while P30 were weaned at 28 days of life, therefore only ate solid feed for 2 days before blood sampling. This difference in alimentation may have contributed to some of the differences alongside with evolution of the gastro-intestinal system.

The results reported in this study showed high variability in the blood profiles among P5 and P30 animals. Unfortunately, it is hard to compare our data with the ones previously described in the literature mainly because of the poor or absent age distinction and the different types of animals used. However, our P5 and P30 animals had lower Hb, HCT, RBC, MCV and MCH values compared to animals of similar ages (days 6 and 36 from birth, respectively) [20].

In our study, P5 animals had a RBC regenerative response that was significantly reduced in P30, as further demonstrated by the results of reticulocyte indices (significantly higher Retic, %Retic, MCVr, %Macro-r and MCV delta). Similar findings have been reported previously and could represent a physiological response in the new-born pigs [15, 20]. However, a condition of iron deficiency could not be excluded in our piglets. It is well known that piglets can suffer from iron deficiency due to many causes such as immature iron metabolism, decreased iron intake or absorption and rapid growth. Iron deficiency can be associated with reduced weight gain, anaemia and even with increased mortality in these animals [22]. For these reasons, iron supplementation is highly recommended and the benefit of this treatment is well documented [18]. The

role of iron deficiency in P5 animals, although suspected based on haematological results, could not be demonstrated with the current study design. In the initial phase, iron deficiency is characterised by enhanced erythropoiesis and even a regenerative anaemia, while microcytosis and hypochromasia (reduction of MCV and MCHC) are late findings associated with iron deficiency in animals and humans [23, 24]. The P30 animals that were supplemented with parenteral iron within the first 72 h after birth had a decreased reticulocyte response compared to the new-born animals. In addition, the results of iron profile parameters, particularly TI and TSAT, supported the potential role of iron deficiency in the piglets included in the present study. Total iron and TSAT values in P5 and even P30 animals were extremely decreased compared to the adult pig values reported in the literature [25]. However, TI and TSAT values were significantly higher at 30 days after birth, compared to new-born piglets. A previous study, using a different schedule of iron treatment, reported different results with particular regard to the iron profile parameters, compared to our study [15]. In our study, the upper limit for TI in P30 animals was five times higher than the P5 upper limit, however the lower limit was similar; the same happened for TSAT. The TIBC showed a slightly different trend, with a wider interval and both lower and higher values in P30 compared to P5. The overall pattern shown by iron-related parameters indicated that circulating iron was very low in these healthy animals. For this reason iron deficiency is hard to investigate in piglets and the determination of other iron-related variables such as ferritin, which is considered the main iron storage protein, may be helpful. Further studies on non-treated animals should be performed in order to investigate and quantify the physiological erythroid response of growing pigs. However, it is possible that an enhanced erythropoiesis accompanied by a relative iron deficiency may be considered a paraphysiological condition for this type of piglet in the first month after birth.

Swine are known to have an elevated platelet count compared to other animals, with frequent platelet clumping upon blood smear examination [20]. Although the total platelet count at both experimental times was comparable to adult animal values available in the literature, PLT, volume and mass were significantly reduced in P30 pigs compared to the new-born piglets. Similar data for young pigs are lacking in veterinary medicine to the best of our knowledge. Analogous to erythropoiesis, an enhanced thrombocytopoiesis that decreases shortly after birth could be explained by the increased need for platelets due to rapid growth or even iron deficiency. Iron deficiency, in fact, is recognised as a stimulus for the bone marrow to produce and release platelets, leading to thrombocytosis in small animals and humans [26].

The P5 and P30 total WBC count results in our study were consistent with the literature: neutrophil percentage decreased from P5 to P30 while the neutrophil total number did not differ significantly. On the contrary, the lymphocyte count and percentage were significantly increased in older animals, as previously reported [20].

Many chemistry variables evaluated were significantly different between the two age groups. These differences may impact the RI definition, however, it is difficult to clarify the exact physiological significance of these changes from an observational study. Interestingly, new-born swine may have a very low concentration of albumin that was significantly higher in 30-day-old animals, while TP concentration did not differ significantly between groups. As supported by the increase in A/G in P30 piglets, albumin concentration increased with the growth of these animals and this process was associated with a progressive reduction in the globulin fraction. Similar findings are lacking in previous studies.

Creatinine and urea values were significantly higher in P30 animals compared to P5, however both values were fully comparable to the adult values available in the veterinary literature [27]. In the authors' opinion, this is the result of the fast growing rate of pigs leading to a rapid increase in muscle mass, helped by the gradual supplementation of enriched solid diet throughout the lactation period.

Another significant difference can be noticed in the ALP concentration, which was extremely higher in younger animals. The literature suggests that this finding is related to higher osteoblast activity in young, growing animals; nevertheless the exact role of ALP in swine is poorly understood, and its clinicopathological usefulness needs to be clarified in further studies [28, 29].

Age-related reference intervals for haematological and biochemical variables in wild boars have been recently published [30]. Although a similar automated haematology system (ADVIA 120) was used in that study, animals from zero to six months were referred to as piglets, and therefore a comparison of their data with our results would not be accurate or reliable. This different stratification of the population in their study design reflects changes in chemical variables as well, and their data seem to be more comparable to our P30 results.

Conclusions

In conclusion, this paper highlights the high variability in haematological and chemistry variables between new-born and 30-day-old pigs, and between these animals and adult pigs. Moreover, our study provides specific age-related reference intervals for healthy commercial hybrid piglets that can be used as physiological standards for both translational and swine medicine. Age-related reference intervals will help in the correct interpretation of experimental

results and should be considered an important step towards a more in-depth knowledge and standardisation of the swine animal model.

Additional file

Additional file 1: Haematological and Biochemical variables evaluated in the study. (DOCX 18 kb)

Acknowledgements

The authors would like to thank the personnel of the veterinary clinical pathology service, and in particular Dr Elisa Brini and Dr Marta Gruarin, for their technical assistance in the use of the ADVIA 2120 haematology system.

Funding

The study was supported by RFO 60% Ateneo di Bologna.

Availability of data and material

The datasets used and/or analysed during the current study available from the corresponding author on reasonable request.

Authors' contributions

DV drafted the manuscript, conceived and designed the study, organized the data and performed statistical analyses. FD drafted the manuscript, helped designing the study, carried out the laboratory analyses and helped organizing and interpreting the data. FB helped handling the animals and collecting blood samples, organized and interpreted the data and review the draft. FS helped acquiring the data and carrying out the laboratory and statistical analyses. AE helped collecting blood samples and organizing the data, performed and reviewed the statistical analyses. MG helped handling the animals and collecting blood samples and critically reviewed the results and the entire draft. NR coordinated the activities performed on the animals and helped drafting the manuscript. MF co-funded the study and helped conceiving and designing the study. MLB funded and conceived the study, coordinated the work team and finally approved the manuscript. All authors read and approved the manuscript.

Competing interests

The authors declare that they have no competing interests.

Consent for publication

Not applicable.

Ethics approval

Animals used in this study were already enrolled in experimental protocols approved by the Italian Ministry of Health.

Received: 17 December 2015 Accepted: 11 January 2017

Published online: 17 January 2017

References

1. Kuzmuk KN, Schook LB. Pigs as a model for biomedical Sciences. In: Rothschild MF, Ruvinsky A, editors. *The Genetics of the Pig*. 2nd ed. Wallingford: CAB International; 2011. p. 426–44.
2. Tumbleson ME, Schook LB. *Advances in Swine in Biomedical Research*. New York: Plenum Press; 1996.
3. Humphray SJ, Scott CE, Clark R, Marron B, Bender C, Camm N, et al. A high utility integrated map of the pig genome. *Genome Biol.* 2007;8:R139.
4. Forni M, Mazzola S, Ribeiro LA, Pirrone F, Zannoni A, Bernardini C, et al. Expression of endothelin-1 system in a pig model of endotoxic shock. *Regul Pept.* 2005;131:89–96.
5. Busnelli M, Froio A, Bacci ML, Giunti M, Cerrito MG, Giovannoni R, et al. Pathogenetic role of hypercholesterolemia in a novel preclinical model of vascular injury in pigs. *Atherosclerosis.* 2009;207:384–90.
6. Lavitrano M, Bacci ML, Forni M, Lazzereschi D, Di Stefano C, Fioretti D, et al. Efficient production by sperm-mediated gene transfer of human decay accelerating factor (hDAF) transgenic pigs for xenotransplantation. *Proc Natl Acad Sci U S A.* 2002;99:14230–5.

7. Swanson KS, Mazur MJ, Vashisht K, Rund LA, Beever JE, Counter CM, et al. Genomics and clinical medicine: rationale for creating and effectively evaluating animal models. *Exp Biol Med* (Maywood). 2004;229:866–75.
8. Smolenski RT, Forni M, Maccherini M, Bacci ML, Slominska EM, Wang H, et al. Reduction of hyperacute rejection and protection of metabolism and function in hearts of human decay accelerating factor (hDAF)-expressing pigs. *Cardiovasc Res*. 2007;73:143–52.
9. Hau J, Van Hoosier GL. *Handbook of Laboratory Animal Science*. Boca Raton: CRC Press; 2003.
10. Flamm EG. Neonatal animal testing paradigms and their suitability for testing infant formula. *Toxicol Mech Methods*. 2013;23:57–67.
11. Eiby YA, Wright LL, Kalanjati VP, Miller SM, Bjorkman ST, Keates HL, et al. A pig model of the preterm neonate: anthropometric and physiological characteristics. *PLoS One*. 2013;8:e68763.
12. Cook JD, Skikne BS, Baynes RD. Iron deficiency: the global perspective. *Adv Exp Med Biol*. 1994;356:219–28.
13. Clark SF. Iron deficiency anemia: diagnosis and management. *Curr Opin Gastroenterol*. 2009;52:122–8.
14. Venn JA, Davies ET. Piglet anaemia. *Vet Rec*. 1965;77:1004–5.
15. Starzyński RR, Laarakkers CM, Tjalsma H, Swinkels DW, Pieszka M, Styś A, et al. Iron supplementation in suckling piglets: how to correct iron deficiency anemia without affecting plasma hepcidin levels. *PLoS One*. 2013;8:e64022.
16. Venn JA, McCance RA, Widdowson EM. Iron metabolism in piglet anaemia. *J Comp Pathol Ther*. 1947;57:314–25.
17. Csapó J, Martin TG, Csapó-Kiss ZS, Házás Z. Protein, fats, vitamin and mineral concentrations in porcine colostrum and milk from parturition to 60 days. *Int Dairy J*. 1995;6:881–902.
18. Lipinski P, Starzyński RR, Canonne-Hergaux F, Tudek B, Oliński R, Kowalczyk P, et al. Benefits and risks of iron supplementation in anemic neonatal pigs. *Am J Pathol*. 2010;177:1233–43.
19. Egeli AK, Framstad T, Morberg H. Clinical biochemistry, haematology and body weight in piglets. *Acta Vet Scand*. 1998;39:381–93.
20. Thorn CE. Hematology of the pig. In: Weiss DJ, Wardrop KJ, editors. *Schalm's Veterinary Hematology*. 6th ed. Ames: Wiley-Blackwell; 2010. p. 843–51.
21. Kjelgaard-Hansen M, Jensen AL. Reference intervals. In: Weiss DJ, Wardrop KJ, editors. *Schalm's Veterinary Hematology*. 6th ed. Ames: Wiley-Blackwell; 2010. p. 1034–8.
22. Svoboda M, Drabek J. Iron deficiency in suckling piglets: etiology, clinical aspects and diagnosis. *Folia Vet*. 2005;49:104–11.
23. Stockham SL, Scott MA. Erythrocytes. In: *Fundamentals of Veterinary Clinical Pathology*. 2nd ed. Ames: Wiley-Blackwell; 2008. p. 107–222.
24. Weiss DJ. Iron and copper deficiencies and disorders of iron metabolism. In: Weiss DJ, Wardrop KJ, editors. *Schalm's Veterinary Hematology*. 6th ed. Ames: Wiley-Blackwell; 2010. p. 167–71.
25. Harvey JW. Iron metabolism and its disorders. In: Kaneko JJ, Harvey JW, Bruss ML, editors. *Clinical Biochemistry of Domestic Animals*. 6th ed. Philadelphia: Elsevier; 2008. p. 259–85.
26. Stockham SL, Scott MA. Platelets. In: *Fundamentals of Veterinary Clinical Pathology*. 2nd ed. Ames: Wiley-Blackwell; 2008. p. 223–58.
27. Kaneko JJ, Harvey JW, Bruss ML. Appendix VII. In: Kaneko JJ, Harvey JW, Bruss ML, editors. *Clinical Biochemistry of Domestic Animals*. 6th ed. Philadelphia: Elsevier; 2008. p. 882–8.
28. Hoffmann WE, Dorner JL. Separation of isoenzymes of canine alkaline phosphatase by cellulose acetate electrophoresis. *J Am Anim Hosp Assoc*. 1975;11:283–5.
29. Tennant BC, Center SA. Hepatic function. In: Kaneko JJ, Harvey JW, Bruss ML, editors. *Clinical Biochemistry of Domestic Animals*. 6th ed. Philadelphia: Elsevier; 2008. p. 379–412.
30. Casas-Díaz E, Closa-Sebastià F, Marco I, Lavin S, Bach-Raich E, Cuenca R. Hematologic and biochemical reference intervals for wild boar (*Sus Scrofa*) captured by cage trap. *Vet Clin Pathol*. 2015;44:215–22.

Submit your next manuscript to BioMed Central and we will help you at every step:

- We accept pre-submission inquiries
- Our selector tool helps you to find the most relevant journal
- We provide round the clock customer support
- Convenient online submission
- Thorough peer review
- Inclusion in PubMed and all major indexing services
- Maximum visibility for your research

Submit your manuscript at
www.biomedcentral.com/submit



New Techniques and Future Applications

This section shows three experiments aimed to develop and validate new techniques and future application of the piglet in the biomedical field.

The aim of the first two experiments was to develop a safe technique for both the collection of cerebrospinal fluid and injection of any compound within the intrathecal space, either by centesis of the *Cisterna magna* or lumbar spinal catheter insertion. When performing such procedures without the support of advanced imaging, operators usually rely of external anatomical landmarks acting as outer projection of the site to be injected. Again, those landmarks obviously follow the physiological body development of animals, therefore are susceptible to high variability. Both of the experiments were successful in standardizing novel approaches, seemingly safe and repeatable, in piglets. Again, the standardization of newer and safer techniques, represents an additional step toward an ethical use of biomedical animals. These two techniques, for example, represent an evolution of older surgical approaches that involved high pain, and often mortality, for piglets. Easier approaches are the key to better results and most reliable data, and should be the goal for every researcher involved in the biomedical field.

The third paper, result of more than 3 years of work, represent the vital foundation of a larger project involving piglets as preclinical models for gene therapy approaches. The aim was to create a complete and comprehensive map of CNS transduction by different serotypes of Adeno-associated Virus (AAV) upon intrathecal administration, since those viruses tend to show selective tropisms

towards different cellular populations. In the author's opinion, this experiment represents a pivotal step for gene therapy preclinical-study, helping the research community to pick the right serotype on the basis of the specific protocol.

First Paper

Access to cerebrospinal fluid (CSF) in piglets via the Cisterna magna: optimisation and description of the technique

NOTICE: this is post-print (final draft post-refereeing) author's version of a work that was accepted for publication in *Laboratory Animals*. Changes resulting from the publishing process, such as editing, corrections, structural formatting, and other quality control mechanisms may not be reflected in this document. Changes may have been made to this work since it was submitted for publication. A definitive version is published in: Romagnoli N, Ventrella D, Giunti M, Dondi F, Sorrentino NC, Fraldi A, Surace EM, Bacci ML. "Access to cerebrospinal fluid in piglets via the cisterna magna: optimization and description of the technique." *Lab Anim*. 2014 Oct;48(4):345-8. doi: 10.1177/0023677214540881.

Access to cerebrospinal fluid (CSF) in piglets via the Cisterna magna: optimisation and description of the technique

Noemi Romagnoli^{a,}, Domenico Ventrella^a, Massimo Giunti^a, Francesco Dondi^a, Nicolina C Sorrentino^b, Alessandro Fraldi^b, Enrico M Surace^b, Maria L Bacci^a*

^a Department of Veterinary Medical Sciences, University of Bologna, Italy

^b Telethon Institute of Genetics and Medicine, Napoli, Italy

**Corresponding author. Tel.: +39.051.2097550*

E-mail: noemi.romagnoli@unibo.it (N. Romagnoli).

Abstract

Cerebrospinal fluid collection is necessary for analysing its composition and can be used for the diagnosis of different diseases. The aim of the study was to develop and optimise a technique for performing a safe centesis both for the collection of cerebrospinal fluid and injection through the Cisterna Magna in piglets. The study was divided into two phases: 1) an anatomical study of 6 piglet cadavers and 2) an in vivo application of the technique in 6 anaesthetised piglets. The proposed technique

resulted in a safe puncture of the Cisterna Magna. The authors identified and confirmed the correspondence of the Cresta Occipitalis and the wings of the atlas with the external landmarks on the cadaver by means of direct radiological visualisation. The punctures were performed successfully at the first attempt in 5/6 piglets. The technique herein described provides a reproducible safe and easy route for approaching the Cisterna Magna for both cerebrospinal fluid collection, drug administration and gene delivery.

Keywords: Centesis technique, cerebrospinal fluid, cisterna magna, general anaesthesia, piglets.

Introduction

The cerebrospinal fluid (CSF) puncture technique has been described in several animal models: rats,¹ rabbits,² guinea pigs,³ primates⁴ and adult pigs;⁵ however, there are no specific studies in the literature regarding collection techniques in newborn piglets.

Moreover, the intrathecal delivery of drugs or other compounds, including viral vectors for gene therapy, into the CSF is a convenient method for targeting the central nervous system (CNS), thus overcoming the obstacle of crossing the blood brain barrier (BBB) following systemic administration and avoiding unwanted exposure of the visceral organs and involvement of the renal and hepatic metabolisms.^{4,6,7} The injection of drugs or substances in pigs has been used to experimentally reproduce human diseases^{8,9,10} and to study delivery methods for widespread gene transfer to the CNS.^{11,12}

In order to develop a specific and reliable centesis/injection technique in newborn piglets (which have size and age-dependent anatomical specificities as compared to adult subjects, a fast reproducible sampling and compound administration technique with minimal side effects is necessary.

The aim of the study was to develop and optimise a technique for performing a safe centesis both for the collection of cerebrospinal fluid and injection through the Cisterna Magna (CM) in piglets using a 22G spinal needle; the first part (phase I) of this study focused on the anatomical study of the piglets in order to approach the CM whereas the second part (phase II) was aimed at testing and validating the procedure in live anaesthetised newborn piglets.

Animals

The experiment (in vivo study) was conducted in accordance with the provisions of European Economic Community (EEC) Council Directive 86/609, adopted by the Italian Government (D.L. 27/01/1992 no. 116). The total number of animals used in the study was 12, of which 6 were Large White crossbreed female piglet cadavers and 6 were Large White crossbreed live male piglets (age range: 2-30 days; weight range: 1.2-8 kg), housed in the Department of Veterinary Medical Sciences of the University of Bologna.

Materials and Methods

The study was divided in two phases:

- Phase I: anatomical study on cadavers,
- Phase II: in vivo application of the technique

Phase I

Six Large White crossbreed female piglet cadavers, (age range: 2-30 days; weight range: 1-10 kg) were used for this phase of the experiment.

Landmarks: After hand palpation and identification of the Cresta Occipitalis, (occipital protuberance), a surgical pen was used to draw a line caudally along the spine extending from the occipital protuberance. This was done in order to identify the median spinal line. A second line was traced between the cranial margins of the wings of the right and left atlas. Using the right hand, the spinal needle (22 Gauge (G) x75 mm, Pic indolor, Artsana, Italy) was introduced along the median line to a depth of 4 mm, 5 mm posteriorly to the intersection of the two lines; the tip of the needle was directed cranio-ventrally using the cranial margin of the wings as an external landmark. The cadaver was placed in right lateral recumbency without any flexion of the head throughout the entire procedure. The centesis of the first female cadaver (8 kg) was performed using C-arm X-ray (Technix s.p.a., Italy) to evaluate the correct correspondence between the anatomical and the suggested external landmarks.

The centesis was performed using the suggested external landmarks without any radiological guidance for the remaining 5 female cadavers which were also always placed in right lateral recumbency without any flexion of the head. Small adjustments regarding the insertion site (range 4-7 mm caudally to the intersection of the two lines) and regarding the depth of the needle placement (range: 4.5-7 mm) were required according to the varying size of the cadavers. After the placement of the spinal needle in the CM, 2.5 ml of radiopaque contrast medium were injected for radiological evaluation. A radiological lateral view of the cervical spine was carried out in each animal to verify the correct distribution of the radiopaque contrast medium.

Phase II

Six male piglets (age range: 2-30 days; weight range:1.2-8 kg) were used in the in vivo study. Venous access was achieved through a lateral auricular vein.

General anaesthesia was induced through a small animal induction mask by means of the administration of an air/oxygen mixture (1:1) and 8% sevoflurane (SevoFlo, Abbott Laboratories, Abbott Park, Illinois, U.S.A.). The level of anaesthesia was continuously assessed by clinical evaluation of the respiratory pattern, heart rate, eye signs and muscle relaxation. Once stable, the piglets were orally intubated and allowed to breathe spontaneously. Following intubation, the fraction of inspired sevoflurane was reduced to 2.5-3%. Non-invasive blood pressure (oscillometric method), heart rate (BPM), electrocardiogram measurements (ECG), hemoglobin saturation (SpO₂), respiratory rate (RPM), End tidal CO₂ (EtCO₂) and rectal temperature were recorded every 5 minutes. Body temperature was maintained above

37.5°C using forced-air warming. The piglets were placed in right lateral recumbency without any flexion of the head as reported in phase I. The collection site (5x5 cm) was clipped and surgically prepared. The lines already described in phase I were drawn with a sterile surgical pen (Viscot Medical, Italy) (Fig.1) and puncture of the CM using a 75 mm 22 gauge spinal needle was performed. The CSF collected (range: 1-2.5ml) was replaced with an equal volume of radiopaque contrast medium, and a radiographic examination was performed within 5 minutes after the puncture. At the end of the procedure, the piglets were sacrificed with a bolus of Tanax (Tanax, Intervet Italia, Segrate, Milano, Italy) at a dose of 0.3 ml/kg IV.

Results

The technique described allowed the puncture of the CM to be carried out. In phase I, the authors identified and confirmed the correspondence between the Cresta Occipitalis and the wings of the atlas and the external landmarks on the first cadaver by direct radiological visualisation; the correct orientation of the needle was also tested and verified. After drawing the lines, the spinal needle was successfully placed into the CM of 4/5 animals at the first attempt. In the last case, the spinal needle was oriented too caudally, thus encountering the bone surface. The operator had to remove and reinsert the needle with a more cranial orientation in order to perform the CM puncture in the correct place.

In all the cases, the radiopaque medium confirmed the correct placement of the spinal needle. The contrast medium was identified by a sharply margined thin column in the subarachnoid space up to the seventh cervical space; it was clearly

present in the cranial cavity. The first step of phase II was the induction of general anaesthesia, which was rapidly accomplished in about 2 minutes. Intubation was challenging in the newborn animals due to the particular anatomy of the mouth and the laryngeal inlet. The clinical parameters remained stable throughout the entire procedure in all animals. In phase II of the study, the punctures were performed successfully in 5/6 piglets at the first attempt. In one subject, the operator accidentally drew a paramedian rather than a median line, thus making it impossible to carry out the puncture; it was necessary to draw a second line to obtain the correct landmark and the correct puncture of the CM. In the beginning of the collection of the CSF, the fluid showed a mild blood contamination in 5/6 animals due to the accidental puncture of the dorsal venous plexus. In every case, the radiopaque medium confirmed the correct placement of the spinal needle (Fig. 2), highlighting the ventral and dorsal contrast columns on the lateral radiograph; the spinal cord created a non-opacified band between the columns. Moreover, the cranial diffusion of the contrast medium was observed in 6/6 anaesthetised animals.

Discussion

The technique herein described provides a reproducible and easy route for approaching the CM for CSF collection, drug administration and gene delivery. The anatomical landmarks validated during phase I of the project allowed the puncture of the CM and the collection of CSF in the 6 anaesthetised piglets.

All the punctures were performed by the same experienced operator in order to minimise variables and to evaluate the “learning curve”, which was fast and

relatively problem free. The correct drawing of the reference lines (the median spinal line and the line traced between the cranial margins of the wings of the right and left atlas) was of primary importance in the procedure since any mistake, such as a misdrawn line, would have precluded achieving the correct injection into the CM. The lines were drawn with the patient in lateral recumbency; however, the results suggested that the same procedure performed in sternal recumbency would have helped in the correct positioning of the reference lines during this phase.

The anatomy of newborn piglets is substantially different since the occipital protuberance has a rounder and less inclined caudal profile as compared to adult subjects.¹³ This is the reason why, in this study, the operator decided to insert the needle more caudally along the median line and with a more cranio-ventral orientation as compared to the injection site described in the technique used for adults.^{5,14} Within the study itself, it was necessary to adjust the distance between the intersection of the lines and the insertion point of the needle in order to adapt to the different sizes of the animals. In fact, in the smaller ones, it was necessary to puncture more caudally by 1 or 2 mm. The wings of the atlas are not easily palpable, and the cartilaginous consistency of the bones makes it difficult to determine the correct positioning of the needle during its insertion since the operator strongly relies on the different consistency of tissues when puncturing the CM.

As shown by the anatomical study in neonatal patients,¹⁵ the dura contains an inner vascular plexus which is larger in the infant than in the adult. The vascular plexus in the piglet is extremely wide, making it difficult to avoid the puncturing the vessel, thus obtaining a blood-contaminated CSF while carrying out the procedure. No

clinical signs of cerebral hypertension after puncturing the vascular plexus were reported in this study; however, the blood contamination of the CFS could represent a limit when performing a cell count or even biochemical analysis.

Performing the procedure without flexing the head, allowed the piglets to breath normally, ensuring adequate ventilation. The technique here described demonstrates an easily accessible route to the CSF and widespread diffusion of the radiopaque contrast medium into distinct central nervous system (CNS) areas, allowing for both the sampling and the administration of substances in different medical and experimental procedures. The limitation of the study was the lack of follow-up of anaesthetised animals in order to evaluate the recovery and eventually any neurological complications resulting from this procedure.

In a subsequent study, the authors have verified the excellent recovery during the postoperative period in the piglets treated (unpublished data).

Acknowledgements:

This research was supported by an RFO (Ricerca Fondamentale Orientata) grant from the University of Bologna.

References

1. Consiglio AR, Lucion AB. Technique for collecting cerebrospinal fluid in the cisterna magna of non-anesthetized rats. *Brain Res Protoc* 2000; 5:109-114.
2. Kang ES, Olson G, Jabbour JT, Solomon SS, Heimberg M, Sabesin S, Griffith JS. Development of encephalopathic features similar to Reye syndrome in rabbits. *Proc Natl Acad Sci U S A* 1984; 81:6169-6173.

3. Liu CT, Guo ZM. Technique for repeated collection of cerebrospinal fluid from cisterna magna of anesthetized strain 13 guinea pigs. *Proc Soc Exp Biol Med* 1991; 197:400-403.
4. Clingerman KJ, Spray S, Flynn C, Fox HS. A technique for intracisternal collection and administration in a rhesus macaque. *Lab Anim (NY)* 2010; 39:307-311.
5. D'Angelo A, Bellino C, Miniscalco B, Capucchio MT, Biolatti C, Cagnasso A. Spinal Fluid Collection Technique from the Atlanto-Occipital Space in Pigs. *Acta Vet Brno* 2009; 78:303-305.
6. Kao JH, Chen SL, Ma HI, Law PY, Tao PL, Loh HH. Intratecal delivery of a mutant micro-opioid receptor activated by naloxone as a possible antinociceptive paradigm. *J Pharmacol Exp Ther* 2010; 334:739-745.
7. Gray SJ, Kalburgi SN, McCown TJ, Samulski RJ. Global CNS gene delivery and evasion of anti-AAV-neutralizing antibodies by intrathecal AAV administration in non-human primates. *Gene Ther* 2013; 20:450-459.
8. Storm H, Stoltenberg L, Oyasaeter S, Saugstad OD, Rognum TO, Reichelt KL. Beta-endorphin may be a mediator of apnea induced by the laryngeal chemoreflex in piglets. *Pediatr Res* 1995; 38:205-210.
9. Ko SY, Shim JW, Kim SS, Chang YS, Park WS, Shin SM, Lee MH. Effects of MK-801 (dizocilpine) on brain cell membrane function and energy metabolism in experimental *Escherichia coli* meningitis in the newborn piglet. *J Korean Med Sci* 2003; 18:236-241.
10. Xu H, Chen X, Qin Z, Gu Y, Zhou P. Effect of recombinant streptokinase on the development of chronic cerebral vasospasm after subarachnoid hemorrhage in a swine model. *Acta Neurochir (Wien)* 2011; 153:1333-1338.
11. Bevan AK, Duque S, Foust KD, Morales PR, Braun L, Schmelzer L, Chan CM, McCrate M, Chicoine LG, Coley BD, Porensky PN, Kolb SJ, Mendell JR, Burghes AHM, Kaspar BK. Systemic gene delivery in large species for targeting spinal cord, brain, and peripheral tissues for pediatric disorders. *Mol Ther* 2011; 19:1971-1980.
12. Federici T, Taub JS, Baum GR, Gray SJ, Grieger JC, Matthews KA, Handy CR, Passini MA, Salmulski RJ, Boulis NM. Robust spinal motor neuron transduction following intrathecal delivery of AAV9 in pigs. *Gene Ther* 2012; 19:852-859.
13. Barone R. *Anatomia Comparata dei Mammiferi Domestici: Vol.1° Osteologia*. Bologna: Edagricole, 2006, pp. 303-321.
14. Swindle M.M. *Swine in the laboratory: Second edition*. Boca Raton FL: CRC Press Taylor & Francis Group, 2007, pp. 283.
15. Mack J, Squier W, Eastman JT. Anatomy and development of the meninges: implications for subdural collections and CSF circulation. *Pediatr Radiol* 2009; 39:200-210.

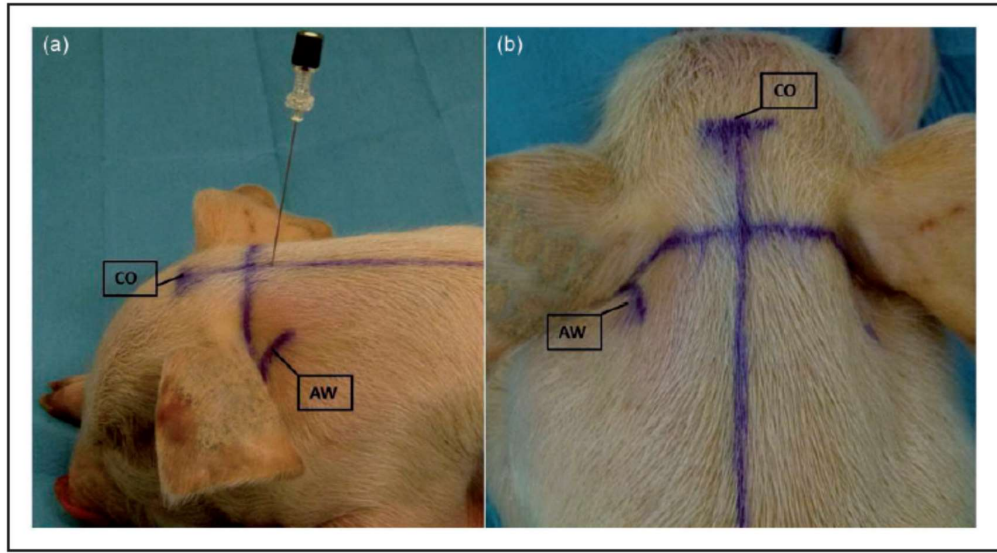


Fig 1. The external landmarks (CO: Cresta Occipitalis; AW: Atlas Wings) and the lines drawn on the piglet skin in order to identify the correct place for carrying out the centesis with the spinal needle; (a) lateral view; (b) dorsal view . The photo was obtained with the piglet in sternal recumbency (in the study the centesis was performed with the animal in lateral recumbency) in order to achieve better visualisation of the landmarks.



Fig 2. Contrast radiography of the head and cervical spine, lateral view (anaesthetised piglet): the contrast medium diffusing along the cervical tract of the spinal cord and is clearly present in the cranial cavity.

Second Paper

Transdermal spinal catheter placement in piglets: description and
validation of the technique

NOTICE: this is the pre-print (pre-refereeing) author's version of a work that was accepted for publication in the Journal of Neuroscience Methods. Changes resulting from the publishing process, such as editing, corrections, structural formatting, and other quality control mechanisms may not be reflected in this document. Changes may have been made to this work since it was submitted for publication. A definitive version is published in: Lambertini C, Ventrella D, Barone F, Sorrentino NC, Dondi F, Fraldi A, Giunti M, Surace EM, Bacci ML, Romagnoli N. "Transdermal spinal catheter placement in piglets: Description and validation of the technique." J Neurosci Methods. 2015 Nov 30;255:17-21. doi: 10.1016/j.jneumeth.2015.07.021.

Transdermal spinal catheter placement in piglets: description and validation of the technique.

Carlotta Lambertini¹°, Domenico Ventrella¹°, Francesca Barone¹, Nicolina Cristina Sorrentino², Francesco Dondi¹, Alessandro Fraldi², Massimo Giunti¹, Enrico Maria Surace², Maria Laura Bacci¹, Noemi Romagnoli¹*

¹*Department of Veterinary Medical Sciences, University of Bologna, Bologna, Italy*

²*Telethon Institute of Genetics and Medicine, Napoli, Italy*

° *equally contributed*

**Corresponding author: Dr Noemi Romagnoli, Department of Veterinary Medical Sciences, University of Bologna, via Tolara di Sopra 50, Ozzano dell'Emilia (BO)*

Email: noemi.romagnoli@unibo.it

Keywords: *Swine; Spinal catheter; Piglet; Intrathecal delivery; Translational medicine*

Abstract

Background: The swine species represent a perfect model for translational medicine due to its physiological and anatomical resemblance to humans. The development of techniques for spinal catheter insertion in swine is significantly useful, but at the moment the only technique described requires laminectomy as surgical approach.

New Method: The proposed techniques represents a transdermal approach for catheter's placement in piglets. The study was divided in: Phase I (anatomical study on 8 cadavers); and Phase II (in vivo application of the technique in 20 anaesthetized 30 days old piglets). A spinal needle was introduced between the spinous processes of L2-L3 with ventro-cranial orientation until the intrathecal space. It was then replaced with a Tuohy needle, used to introduce the catheter. Before inserting the catheter, the approximate length was measured from the insertion point to the external projection of the Cisterna Magna using the gradation markings on the device.

Results: The technique described allowed the spinal catheter placement in every piglet. In Phase I the right placement was confirmed using fluoroscopy, while in Phase II we relied on Cerebrospinal Fluid leakage from the needle. No alterations were detected both during the procedure and the following days.

Comparison with Existing Method(s): This technique is easy and requires less skilled operators when compared to the only existing method that involves a surgical approach. Moreover, being less invasive, it potentially leads to fewer complications.

Conclusions: In conclusion, the technique can be performed safely in piglets, and provides an easier and less invasive approach for spinal catheter insertion.

1. Introduction

The swine species represent a perfect model for the study of different techniques in translational medicine due to its physiological and anatomical resemblance to humans (Tumbleson & Schook, 1996; Swanson et al., 2004; Karali et al., 2011; Testa et al., 2011). The development of techniques for spinal catheter insertion in swine is significantly useful in different scientific fields, including anaesthesia and analgesia, and gene delivery (Fairbanks, 2013; Bottros & Christo, 2014)

The administration of analgesic compounds through an intrathecal catheter represents a worthwhile technique for continuous pain relief (Fairbanks, 2013). The systemic administration of analgesic drugs could lead to side systemic effects such as sedation, respiratory depression (Gutstein & Akil, 2006), bradycardia, nausea, vomiting, constipation (Lamont & Mathews, 2007). It has been proved that regional analgesic techniques are superior in terms of postoperative analgesia when compared to intravenous opioid administration, reducing these adverse effects in case of both thoracic (Behera et al., 2008) and abdominal surgery (Kainzwaldner et al., 2013).

Somatic cells gene transduction via viral vectors directly in the intrathecal space of the spinal cord is an indispensable tool in neurosciences. For example the administration of Adeno Associated Virus (AAV) vectors targeting the Central Nervous Sistem (CSN) cells is useful for gene therapy for the treatment of pediatric neurological diseases such as lysosomal storage disorders (Spampanato et al, 2011;

Bevan et al., 2011), the Spinal Muscular atrophy, the Rett syndrome, and amyotrophic lateral sclerosis (Federici et al., 2012).

The systemic administration of these vectors produces an extensive transgene expression throughout the brain and in multiple organs too (Bevan et al., 2011). However, intrathecal administration improves the direct effect on the target cells using lower vector doses than the one used for parenteral injections, reduces the peripheral expression and can minimize the risk of a systemic immune response (Bevan et al., 2011; Dayton et al., 2012). Intrathecal injection techniques by single puncture of the spinal space have already been described in laboratory animals (Bevan et al., 2011) including pigs (Romagnoli et al., 2014); but studies concerning the placement of a spinal catheter are limited to few animal models (Fairbanks, 2003; Poon et al., 2011).

To the best of the author's knowledge there is only one study describing the insertion of a spinal catheter in pigs using a surgical approach: laminectomy (Federici et al., 2012). However, there are no studies describing a less invasive insertion technique as refinement strategy for animal experimentation.

The aim of this study was to evaluate and validate the technique for spinal catheters placement in piglets using a transdermal approach.

2. Materials and Methods

The experiments were conducted in accordance with the provisions of European Economic Community (EEC) Council Directive 86/609 adopted by the Italian Government (DL 27/01/1992 No. 116).

The study was divided in two phases: Phase I (anatomical study on 8 piglet cadavers); Phase II (in vivo application of the technique in 20 anaesthetized 30 days old piglets).

2.1 Phase I

The cadaver was placed in lateral recumbency with the hind limbs flexed forward in order to widen the intervertebral spaces. The operator palpated with the non-dominant hand the last rib and detected with the index the spinous processes of the lumbar vertebrae L2 and L3 and the corresponding intervertebral space, which resulted wider than the other spaces.

A 20 G 0.9 x 70 mm spinal needle was introduced between the spinous processes of L2-L3 with ventro-cranial orientation forming an angle of 75° and as close as possible to L3 (fig. 1a). The needle was inserted through the skin and the subcutaneous tissue and then through the interspinous ligament over the epidural space up to the intrathecal space. Resistance was felt as the needle penetrated the ligament and a loss of resistance as the needle penetrated the epidural space.

The needle was then removed and substituted with a 24-gauge (G) Tuohy needle following the path previously created. It was then visualized under fluoroscopy and removed after the introduction of a 20 G catheter (fig. 1b). The injection of radiopaque contrast medium (Optiray Mallinckrodt Italia S.p.A.) through the catheter and his intrathecal spread, confirmed the right placement of the device under fluoroscopy (fig. 2).

2.2 Phase II

Piglets enrolled in this part of the study were transferred to our facility from a local breeding farm (Società Agricola Pasotti S.S., Imola, Italy) on the day of weaning (28 days post birth).

The day of the procedure anaesthesia was induced with sevoflurane (SevoFlo; Abbott Laboratories,

Chicago, IL, USA) in oxygen (1 L/min) delivered via a mask attached to a circle system and a small animal anaesthetic machine. Pigs were tracheally intubated and anaesthesia was maintained with sevoflurane in oxygen (10 ml/kg/min). Heart rate (HR), respiratory rate (RR) and End Tidal Carbon dioxide (EtCO₂) were monitored during the procedure. Venous access was achieved from an auricular vein and fluid therapy (Ringer Lactate) was administered at the rate of 10 ml/kg/h.

For the catheter insertion the piglet was positioned in lateral recumbency and the area was clipped and surgically prepared. The procedure was performed as above described. The right placement of the Tuohy needle was confirmed by the cerebrospinal fluid (CSF) leakage.

Before inserting the catheter, the approximate length was measured from the insertion point to the external projection of the Cisterna Magna using the gradation markings along the catheter as a reference and the device itself was filled with 0.2 ml of PBS. This step was crucial in order to avoid kneeling of the device into the intrathecal space and air injection. The catheter was inserted and advanced until the operator felt a resistance due to the arrival of the tip within the cranial margin of the Cisterna Magna.

At the end of the procedure, the catheter was removed and sevoflurane administration was stopped. All of the piglets recovered from anaesthesia within 15 minutes, and were strictly monitored concerning neurological alteration, for the following 6 hours to detect any complication caused by the procedure. Animals were housed in multiple stalls with heat lamps in accordance with the animal welfare and were monitored at least 5 times per day for the following week.

3. Results

The technique described allowed the spinal catheter placement in every piglet. The catheter slid in easily, proving the size of the device to be adequate for such small animals.

During phase I the authors confirmed L2-L3 intervertebral space as the widest therefore more reliable for the introduction of the needle, and the lateral recumbency as the most comfortable for the operator. At the insertion of the spinal needle, the operator felt only a mild resistance passing through the interspinous ligament and didn't felt any loss of resistance at the entrance of the epidural space as usually appreciable in vivo animals.

The technique, applied in Phase II, allowed the correct placement of the catheter in all of the animals enrolled, as confirmed by CSF leakage. Induction was smooth and rapid and recovery uneventful, minimizing any kind of stress related to the procedure itself. Anaesthesiological monitoring did not show any alterations related to the increase of pressure within the subarachnoideal space. The device was left in place for about 15 minutes, still no alterations were detected. None of the complications already described in literature such as bleeding, CSF leakage, neurological injury and

ataxia (Bottros & Christo, 2014) were observed during the recovery period and for the following days. One animal out of 20 showed a mild ataxia that disappeared without any kind of pharmacological treatment in 2 hours.

Animals were able to display all of their normal behavioural and physiological patterns within few hours from recovery, proving the procedure to be minimally invasive and painful.

4. Discussion

In the present study, we described the technique for the transdermal spinal catheter placement in piglets. The procedure was feasible in all animals both in cadavers and anesthetized animals.

Phase I helped finding the adequate technique for needles and catheter insertion. The intervertebral space was chosen as the most reliable and easy to puncture according to our experience and pediatric literature: in human medicine indeed, the intervertebral space L2-L3 is associated to a major incidence of correct catheter position in children (Kim et al., 2010). Since it is hard to verify the correct placement in cadavers due to the lack of CSF leakage and of differential tissue resistance, fluoroscopy and contrastographic examinations were pivotal to the success of the study as previously described by Federici et al. (2012). This part of the study was extremely useful to verify that the resistance encountered during the advancement of the device is imputable to its reaching the rostral area of the Cisterna Magna. In fact, further advancement can result in looping of the catheter itself (Firebanks, 2003).

During Phase II, the described technique allowed the correct catheter placement in all animals and the piglets recovered without any problem within minutes after the end of the procedure, with the exception of only one animal, which showed a mild brief ataxia. It is still important to say that the only direct confirmation to the procedure is the CSF leakage, and it is not advisable to rely on the tissue consistency, especially in neonatal animals.

Federici et al. (2012) described the insertion of the spinal catheter in pigs after laminectomy, but this kind of approach is more painful, therefore requiring higher levels of analgesia, and may lead to postoperative infections and trauma to the spinal cord. In addition, the surgical technique requires more experienced staff and more expensive equipment.

The used recumbency was the most stable and comfortable for the operator, allowing the intervertebral space to widen and, in vivo, to see the leakage of the CSF. Spinal needle, with sharp cutting point allows the operator to easily appreciate the sequential penetration of skin, adipose tissue and ligaments as it is advanced through the different tissue planes. Moreover, the clear hub allows to check the presence of blood or CSF (Read, 2013).

Thouy needles instead, have a polished and rounded inner bevel, which is useful for directing the insertion of a spinal catheter and to minimize the risk of shearing the catheter itself (Read, 2013).

Therefore, we decided to use a spinal needle first and the Thouy needle in second instance.

The epidural catheters have gradation markings along their length and they are radiopaque. These features helped us, in phase I, to verify its correct placement in the spinal space for the right length. In Phase II the gradations along the device were useful to direct it for the fitting length as previously described. A specific mark on the distal tip of the catheter assured us on the integrity of the device once removed from the piglets.

In the study we used a closed tip catheter with multiple fenestration located round the tip. In human medicine the use of multiport catheters was associated with lower incidence of inadequate analgesia (D'Angelo et al., 1997). This allowed the spreading of the contrast medium in the intrathecal space above the third lumbar vertebra up to the Cisterna Magna. While the use of open end catheter allows the diffusion of the compounds, the retraction of the device would allow the diffusion of the compound injected close to specific medulla metameres avoiding unilateral diffusion.

In conclusion, the technique can be performed safely in piglets, and provides an easier and less invasive approach for spinal catheter insertion when compared to the surgical one.

5. Acknowledgments

The study was founded by the University of Bologna-UNIBO, Ricerca Fondamentale Orientata (RFO ex 60%).

6. References

- Behera BK, Puri GD, Ghai B. Patient-controlled epidural analgesia with fentanyl and bupivacaine provides better analgesia than intravenous morphine patient-controlled analgesia for early thoracotomy pain. *J Postgrad Med* 2008;54:86-90.
- Bevan AK, Duque S, Foust KD, Morales PR, Braun L, Schmelzer L et al. Systemic gene delivery in large species for targeting spinal cord, brain, and peripheral tissues for pediatric disorders. *Mol Ther*, 2011;11:1971-80.
- Bottros MM and Christo PJ. Current perspectives of intrathecal drug delivery. *J Pain Res* 2014;7:615-26.
- D'Angelo R, Foss ML, Livesay CH. A comparison of multiport and uniport epidural catheters in laboring patients. *Anesth Analg* 1997;84:1276-79.
- Dayton RD, Wang BD, Klein RL. The advent of AAV9 expands applications for brain and spinal gene delivery. *Expert Opin Biol Ther* 2012;12:757-66.
- Fairbanks CA. Spinal delivery of analgesics in experimental models of pain and analgesia. *Adv Drug Deliv Rev* 2003;55:1007-41.
- Federici T, Taub JS, Baum GR, Gray SJ, Grieger JC, Matthews KA et al. Robust spinal Motor Neuron transduction following intrathecal delivery of AAV9 in pigs. *Gene Ther* 2012;19:852-59.
- Gutstein HB and Akil H. Opioid analgesics. In: Brunton LL, Lazo JS, Parker KL (eds) Goodman & Gilman's. The pharmacological basis of therapeutics. 11th ed. New York: McGraw-Hill 2011, pp. 547-590.
- Kainzswaldner V, Rachinger-Adam B, Mioc-Curic T, Wöhrle T, Hinske LC, Luchting B et al. Quality of postoperative pain therapy: evaluation of an established anesthesiology acute pain service. *Anaesthesist* 2013;64:453-59.
- Karali M, Manfredi A, Puppo A, Marrocco E, Gargiulo A, Della Corte M et al. MicroRNA-Restricted Transgene Expression in the Retina. *PLoS One* 2011;6(7):e22166.
- Kim YA, Kim JY, Kil HK, Kim EM, Kim MK, Kim HS. Accuracy of the epidural catheter position during the lumbar approach in infants and children: a comparison among L2-3, L3-4, and L4-5 approaches. *Korean J Anesthesiol* 2010;58:458-63.
- Lamont LA and Mathews KA. Opioids, Nonsteroidal Anti-inflammatories, and analgesic adjuvants. In: Tranquilli WJ, Thurmon JC, Grimm KA (eds) Lumb & Jones' Veterinary anesthesia and analgesia. 4th ed. Iowa: Blackwell Publishing, 2007, pp. 241-271.
- Poon YY, Chang AYW, Ko SF, Chan SHH. Catheterization of the thoracic spinal subarachnoid space in mice. *J Neurosci Methods* 2011;200:36-40.
- Read MR. Equipment for Loco-regional Anesthesia and Analgesia. In: Campoy L and Read MR (eds) Small Animal Regional Anesthesia and Analgesia. 1st ed. Iowa: Wiley-Blackwell, 2013, pp. 43-64.

Romagnoli N, Ventrella D, Giunti M, Dondi F, Sorrentino NC, Fraldi A et al. Access to cerebrospinal fluid in piglets via the cisterna magna: optimization and description of the technique. *Lab Anim* 2014;48:345-48.

Swanson KS, Mazur MJ, Vashisht K, Rund LA, Beever JE, Counter CM et al. Genomics and clinical medicine: rationale for creating and effectively evaluating animal models. *Exp Biol Med (Maywood)* 2004;229:866-75.

Spampanato C, De Leonibus E, Dama P, Gargiulo A, Fraldi A, Sorrentino NC, et al. Efficacy of a combined intracerebral and systemic gene delivery approach for the treatment of a severe lysosomal storage disorder. *Mol Ther* 2011;19:860-9.

Testa F, Surace E, Rossi S, Marrocco E, Gargiulo A, Di Iorio V, et al. Evaluation of Italian Patients with Leber Congenital Amaurosis due to AIPL1 Mutations Highlights the Potential Applicability of Gene Therapy. *Invest Ophth Vis Sci* 2011;52:5618-24.

Tumbleson ME and Schook LB. *Advances in Swine in Biomedical Research*. New York: Plenum Press, 1996.

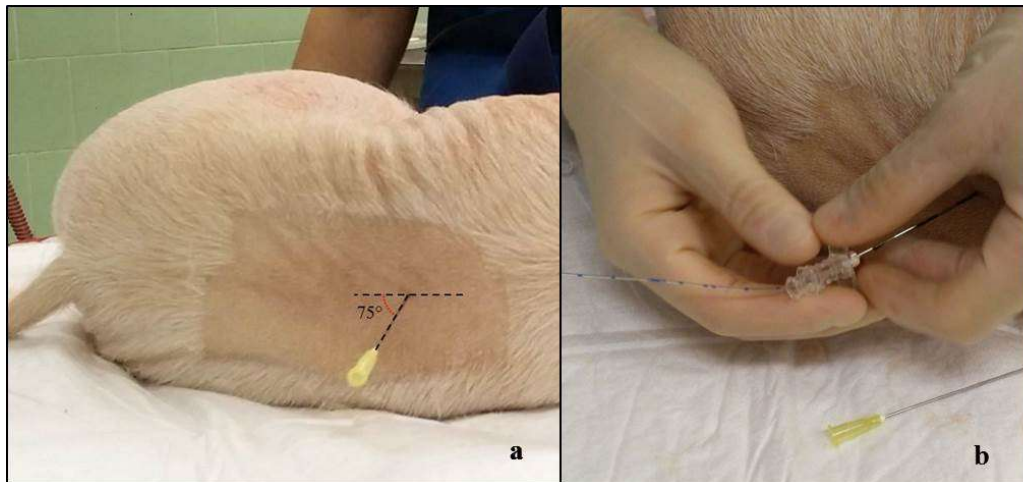


Fig 1. Steps for spinal catheter insertion (anatomical study) - With piglet in lateral recumbency a spinal needle is introduced between the spinous processes of L2-L3 with ventro-cranial orientation forming an angle of 75° with the spinal column and as close as possible to L3 (a). The spinal needle is then replaced with a Tuohy needle for spinal catheter insertion (b).

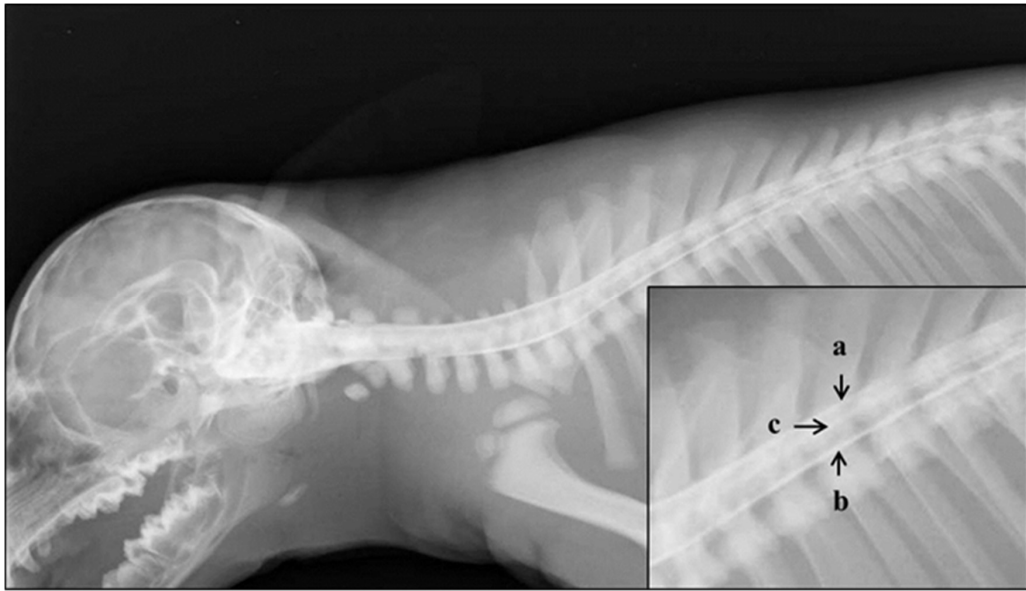


Fig 2. Fluoroscopy image of catheter placement (anatomical study)- Contrastographic evaluation in lateral recumbency . The contrast medium shows the spreading within the intrathecal space: (a) dorsal wall, (b) ventral wall, (c) catheter.

Third Paper

A Comprehensive Map of CNS Transduction by Eight
Recombinant Adeno-associated Virus Serotypes Upon
Cerebrospinal Fluid Administration in Pigs

A Comprehensive Map of CNS Transduction by Eight Recombinant Adeno-associated Virus Serotypes Upon Cerebrospinal Fluid Administration in Pigs

Nicolina Cristina Sorrentino¹, Veronica Maffia¹, Sandra Strollo¹, Vincenzo Cacace¹, Noemi Romagnoli², Anna Manfredi¹, Domenico Ventrella², Francesco Dondi², Francesca Barone², Massimo Giunti², Anne-Renee Graham³, Yan Huang³, Susan L Kalled³, Alberto Auricchio^{1,4}, Maria Laura Bacci², Enrico Maria Surace^{1,4} and Alessandro Fraldi¹

¹Telethon Institute of Genetics and Medicine (TIGEM), Naples, Italy; ²Department of Veterinary Medical Sciences (DIMEVET), University of Bologna, Bologna, Italy; ³Shire, Discovery Biology and Translational Research, Lexington, Massachusetts, USA; ⁴Medical Genetics, Department of Translational Medicine, "FEDERICO II" University, Naples, Italy

Cerebrospinal fluid administration of recombinant adeno-associated viral (rAAV) vectors has been demonstrated to be effective in delivering therapeutic genes to the central nervous system (CNS) in different disease animal models. However, a quantitative and qualitative analysis of transduction patterns of the most promising rAAV serotypes for brain targeting in large animal models is missing. Here, we characterize distribution, transduction efficiency, and cellular targeting of rAAV serotypes 1, 2, 5, 7, 9, rh.10, rh.39, and rh.43 delivered into the cisterna magna of wild-type pigs. rAAV9 showed the highest transduction efficiency and the widest distribution capability among the vectors tested. Moreover, rAAV9 robustly transduced both glia and neurons, including the motor neurons of the spinal cord. Relevant cell transduction specificity of the glia was observed after rAAV1 and rAAV7 delivery. rAAV7 also displayed a specific tropism to Purkinje cells. Evaluation of biochemical and hematological markers suggested that all rAAV serotypes tested were well tolerated. This study provides a comprehensive CNS transduction map in a useful preclinical large animal model enabling the selection of potentially clinically transferable rAAV serotypes based on disease specificity. Therefore, our data are instrumental for the clinical evaluation of these rAAV vectors in human neurodegenerative diseases.

Received 1 June 2015; accepted 22 November 2015; advance online publication 5 January 2016. doi:10.1038/mt.2015.212

INTRODUCTION

Gene transfer of recombinant adeno-associated virus (rAAVs) holds promises to treat neurological disorders.¹ Studies on different recombinant vector serotypes and modes of delivery to the

central nervous system (CNS) showed that the combination of both rAAV serotype used and delivery routes play a key role in CNS transduction properties and thus in disease phenotype rescue outcome. However, one of the major hurdles to developing an effective clinical protocol for neurological disorders is the efficiency of vectors to reach the specific cell types in disease-specific CNS subdomains.

Attempts to treat CNS defects based on parenchymal delivery of rAAV vectors demonstrated efficacious proof-of-principle studies. Nonetheless, clinical trials using this approach showed limited benefit for Batten disease, Canavan disease, aromatic L-amino acid deficiency, and Parkinson's disease.²⁻⁶ One possible explanation for this limited success, in addition to potential local inflammatory responses, is that widespread distribution within the affected brain area from the injection site was inadequate and did not target relevant cell populations. The systemic delivery of rAAVs with the ability to efficiently cross the blood-brain barrier was recently shown as an attractive means to treat diseases with widespread CNS involvement.⁷⁻¹⁰ However, the vector doses required and exposure to visceral organs may raise concerns related to manufacturing costs and safety, respectively. An alternative route to efficiently transduce the CNS is based on delivery of viral vectors directly into the cerebrospinal fluid (CSF). CSF delivery can be achieved through ventricular, lumbar, and cisternal administration. The main advantage of CSF-mediated delivery is the exposure of the virus circulating in the CSF to a large CNS surface area resulting in a broad distribution of delivered viral particles within the CNS with a relatively limited amount of vector required.¹¹ CSF-mediated delivery and spreading of molecules/virus within the CNS occurs in two steps: (i) pia mater fenestration allows access to superficial brain parenchyma (mainly composed of astroglia cells: glia limitans), which is in direct contact with the CSF. Access to deeper brain parenchyma areas is instead

V.M., S.S., V.C., and N.R. contributed equally to this work.

Correspondence: Alessandro Fraldi, Telethon Institute of Genetics and Medicine (TIGEM), Naples, Italy. E-mail: fraldi@tigem.it and Enrico Maria Surace, Telethon Institute of Genetics and Medicine (TIGEM), Naples, Italy. E-mail: surace@tigem.it

mainly mediated by perivascular CSF transport¹² and (ii) uptake by brain cells, which depends on the specific tropism of rAAV serotypes.¹³

Therefore, the CSF delivery is an attractive administration route to develop CNS gene therapy-based approaches. Interestingly, proof-of-concept studies based on CSF delivery of rAAVs have been reported for various neurological disorders affecting CNS in different animal species.^{14–17} However, to date, little is known about how CSF delivery of potentially clinically transferable rAAV serotypes impacts transgene transduction patterns in specific CNS subdomains/cell types in large preclinical animal models. This information is crucial for the future development of clinical protocols for CNS diseases based on CSF delivery of rAAV vectors. Neurological disorders often exhibit an onset/presentation that affects discrete, disease-specific structures of the brain that then spread along the entire CNS with disease progression. Therefore, in principle, a viral vector that targets the CNS substructure initially affected in disease manifestation would result in an overall therapeutic benefit, and therapy via CSF delivery may mitigate the potential for systemic toxicity.

Here, we provide a detailed side-by-side analysis of CNS region/cell transduction specificity of eight rAAV serotypes (rAAV1, 2, 5, 7, 9, rh.10, rh.39, and rh.43) selected for their potential CNS tropism from the large portfolio of rAAV serotypes available.^{13,18} This transduction pattern has been evaluated together with an assessment of safety parameters CSF injection of the viral vectors in pigs, a large animal model that is useful for preclinical studies.¹⁹ These data will provide guidance and immediate impact for the design of future translational clinical studies.

RESULTS

Pattern of GFP expression in the CNS upon intra-cisterna magna injection of rAAV1, 2, 5, 7, 9, rh.10, rh.39, and rh.43 in P30 pigs

Eight rAAV serotypes (rAAV1, 2, 5, 7, 9, rh.10, rh.39, and rh.43) carrying genes encoding for the green fluorescent protein (GFP) under the control of the CMV ubiquitous promoter were injected in the CSF at a dose of 1.5×10^{12} GC/Kg in wild-type (WT) pigs at age 30 days (P30) (**Supplementary Table S1**). CSF administration was based on an intra-cisterna magna (ICM) protocol previously described.²⁰ Age-matched WT pigs ICM injected with phosphate-buffered saline (PBS) were used as controls.

In order to evaluate the transduction capability of the different rAAV serotypes, we first analyzed the GFP expression patterns in the CNS of injected animals. Injected pigs were sacrificed 1 month postinjection, and the brains were collected and sliced in eleven 0.5-cm-thick coronal sections covering the main regions of the brain and processed either for biochemical analysis or for GFP immunostaining (**Supplementary Figure S1**). The cervical region of the spinal cord was also collected (as slice S12) and analyzed in order to evaluate the transduction of rAAV vectors in the CNS regions localized posteriorly to the injection site including the neurodegenerative relevant areas of motor neurons (**Supplementary Figure S1**).

GFP immunohistochemical (IHC) analysis was performed on frozen sections cut from selected CNS coronal slices derived from both rAAV-injected and control PBS-injected pigs. Frontal and parietal cerebral cortex (from slices S4 and S5, respectively), hippocampus (from slice S8), cerebellum (from slice S11), basal ganglia (from slice, S4 and S5), and cervical tract of the spinal

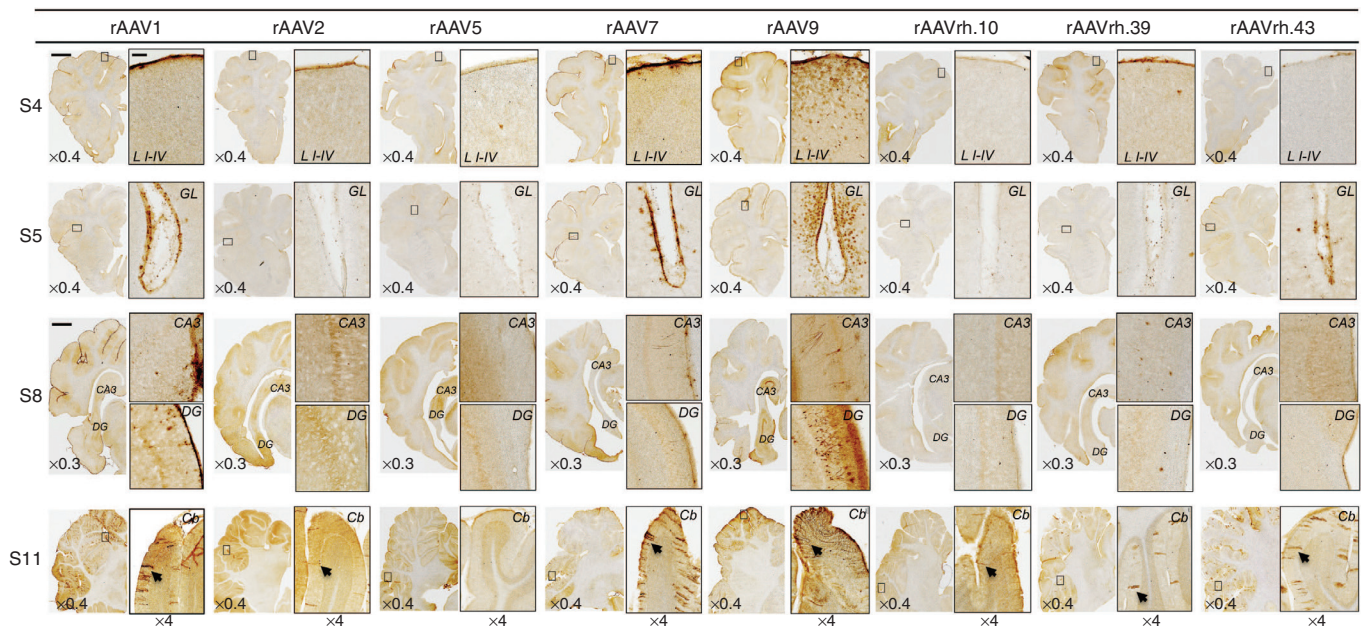


Figure 1 IHC analysis of GFP distribution pattern in main representative areas of pig brain upon ICM delivery of rAAV1, 2, 5, 7, 9, rh.10, rh.39, and rh.43. GFP expression in the brain of rAAV-injected pigs was evaluated 1 month after injection by IHC analysis in four representative 40- μ m coronal cryosections (slice S4, S5, S8, and S11). The $\times 0.3/\times 0.4$ pictures are scanned images (see Materials and Methods). Enlarged images ($\times 4$) from each slice showed transduction in layers I–IV of frontal cerebral cortex (slice S4), glia limitans (GL) of parietal cerebral cortex (slice S5), dentate gyrus (DG), and CA3 areas of hippocampus (slice S8) and cerebellum (Cb) (slice S11). Arrows indicated Purkinje cells. Bars for $\times 0.3$ and $\times 0.4$ images = 4 mm. Bar of enlarged images ($\times 4$) = 200 μ m.

cord (from slice S12) were analyzed (**Supplementary Figure S1**). The GFP signal was distributed in several CNS regions in pigs that were injected with rAAV9, as seen in **Figure 1**. In the cerebral cortex, the GFP expression was evident in the layers I–IV, particularly in the glia limitans of layer I (**Figure 1**). Cerebellum also appeared transduced in rAAV9-injected pigs, with GFP signal observed in the Purkinje cells (**Figure 1**). rAAV9 vectors penetrated into the brain parenchyma also transducing the brain stem and basal ganglia, with GFP signal present in the accumbens and putamen (**Supplementary Figure S2**). Transduction was also evident in the dentate gyrus and CA3 areas of hippocampus (**Figure 1**).

IHC analysis of rAAV1-injected pig brains showed that the first layer of the cerebral cortex was transduced with preferential localization of the GFP signal in the glia limitans (**Figure 1** and **Supplementary Figure S2**). GFP expression was also observed in the Purkinje cell layer of the cerebellum and in the hippocampus (dentate gyrus and CA3; **Figure 1**). rAAV7 showed a distribution pattern similar to that observed for rAAV1, with higher transduction of Purkinje cell layer compared with the rAAV1 serotype (**Figure 1** and **Supplementary Figure S2**). The glia limitans of the cerebral cortex and the Purkinje cells of the cerebellum appeared transduced also by the rAAV2 (**Figure 1** and **Supplementary Figure S2**). The rAAV5 showed few GFP-positive cells in the layers I–IV of the cerebral cortex (**Figure 1** and **Supplementary Figure S2**). GFP transduction was observed in the Purkinje cell layer of animals injected with rAAVrh.10, rAAVrh.39, and rAAVrh.43, while only a few GFP signal mainly localized to the layer I was detected in the cerebral cortex of these animals (**Figure 1** and **Supplementary Figure S2**). rAAVrh.39-injected pigs also displayed a few GFP signal in dentate gyrus and CA3 areas of hippocampus (**Figure 1**). IHC analysis of the cervical region of the spinal cord showed that rAAV9 was able to transduce both neurons of lamina IX and fibers in the ventral column and fibers of gracile and cuneate fasciculi in the dorsal column (**Figure 2**). Both rAAV1 and rAAV7 displayed an astroglial transduction pattern in the spinal cord; however, the GFP signal was stronger in rAAV1-injected animals compared with rAAV7-injected animals (**Figure 2**). In the spinal cord, rAAV5 and rAAVrh.43 showed a weak GFP expression, which was localized in the gray matter of the ventral horn in rAAV5-injected animals and in the glia limitans of the ventral region in rAAVrh.43-injected animals (**Figure 2**). All remaining rAAV serotypes analyzed did not exhibit any detectable GFP signal in the spinal cord (**Figure 2**).

Levels of GFP expression in CNS regions upon ICM injection of rAAV1, 2, 5, 7, 9, rh.10, rh.39, and rh.43 in P30 pigs

GFP expression levels in brain and spinal cord were quantified by western blotting experiments on 20 selected CNS areas of interest, which were dissected from coronal slices in both rAAV-injected and control PBS-injected pigs (**Supplementary Figure S1**). As seen in **Figure 3**, P30 injected pigs showed a GFP distribution pattern that overall correlated with the IHC data confirming the wide distribution of the rAAV9 serotype and underlining the specific distribution pattern of the other rAAV serotypes analyzed. However, the quantitative analysis allowed us to evaluate not only the distribution pattern of GFP but also the intensity of GFP expression in specific CNS regions of injected pigs.

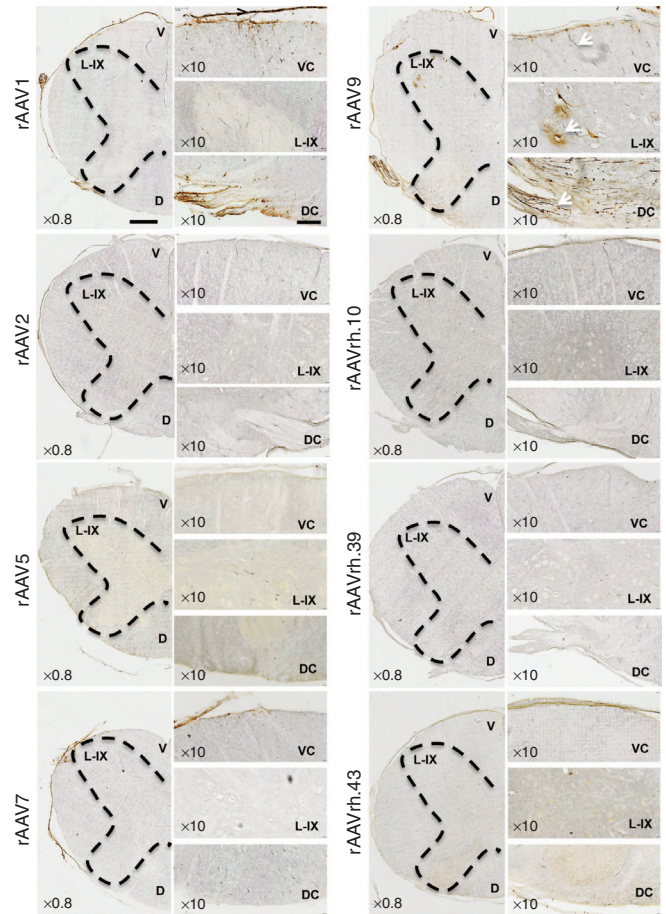


Figure 2 IHC analysis of GFP distribution pattern in spinal cord of rAAV-injected pigs. IHC GFP staining on coronal cryosections (40 μ m) of spinal cord cervical region from rAAV-injected pigs. The $\times 0.8$ pictures are scanned images (see Materials and Methods). The black dashed lines indicate the butterfly shape of gray matter of the spinal cord. Magnification images ($\times 10$) show the ventral column (VC), the lamina IX (L-IX) of the ventral horn, and the dorsal column (DC) of the spinal cord. Arrows in the panels of rAAV9-injected pigs indicate fiber transduction in the ventral columns, motor neurons transduction in the L-IX, and transduction of gracile and cuneate fasciculi fibers in the dorsal column. Ventral (V) and dorsal (D) sides of the spinal cord are shown in the $\times 0.8$ scanned images. Bar of $\times 0.80$ images = 1 mm. Bar of $\times 10$ images = 200 μ m.

Cerebral cortex. The cerebral cortex of rAAV9-injected pigs exhibited the highest intensity of GFP expression (**Figure 3**). rAAV1, rAAV5, and rAAV7 also showed relevant GFP protein levels in the cerebral cortex, with rAAV1 and rAAV7 displaying higher expression levels compared to rAAV5 (**Figure 3**).

Hippocampus. rAAV9 displayed the highest GFP expression levels in the hippocampus, followed by rAAV1, rAAV5, and rAAV7 serotypes (**Figure 3**). No detectable GFP expression was observed for all the other rAAV serotypes tested (**Figure 3**).

Midbrain and basal ganglia. The colliculi (superior and inferior) and the substantia nigra were transduced with the highest GFP expression intensity by the rAAV9 serotype (**Figure 3**). Quantitation of GFP protein levels in the substantia nigra showed higher GFP expression in rAAV5-injected animals compared to

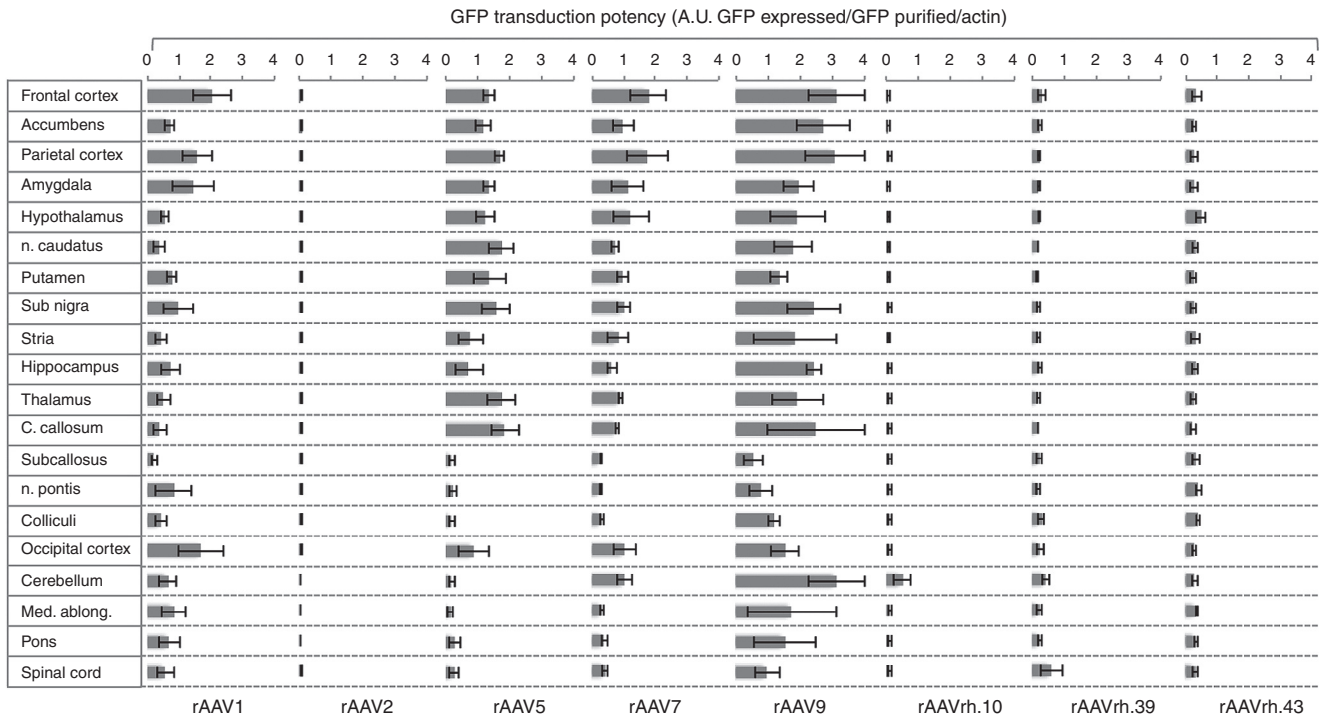


Figure 3 GFP expression levels in representative areas of the CNS of rAAV-injected pigs. Western blotting analysis with anti-GFP antibody performed on rAAV-injected pigs. Indicated areas were taken from the rostral to the caudal part of pig CNS (see Materials and Methods and **Supplementary Figure S1** for details). The GFP protein levels were quantified in dissected areas by densitometric analysis of GFP signals. For the cerebral cortex, we analyzed frontal (from slice S1 and S2), parietal (from slice S5), and occipital (from slice S8–S10) regions. Values were normalized to both actin and purified GFP protein (70 ng loaded on sodium dodecyl sulfate gels) and expressed as arbitrary units (a.u., see Materials and Methods for details). Three animals for each serotype were analyzed. Bars represent means \pm SEM from three samples (one sample for each animal).

that observed in rAAV1- and rAAV7-injected animals (**Figure 3**). Low GFP protein levels were detected in the colliculi of pigs injected with rAAV1 serotype (**Figure 3**). rAAV9 exhibited the highest intensity of GFP expression in basal ganglia region followed by rAAV5, rAAV7, and rAAV1 (**Figure 3**). All other serotypes did not show detectable GFP expression in the midbrain and basal ganglia areas (**Figure 3**).

Cerebellum. The rAAV9 and rAAV7 serotypes showed similar levels of GFP expression in the cerebellum, and these protein levels were the highest among all rAAV serotypes analyzed (**Figure 3**). Lower levels of cerebellar GFP expression were displayed by the rAAVrh.39, rAAVrh.10, and rAAV1 serotypes (**Figure 3**). The GFP expression levels were very low or undetectable in the cerebellum of rAAV2-, rAAV5-, and rAAVrh.43-injected pigs (**Figure 3**).

Spinal cord. rAAV9 displayed the highest GFP protein levels in the spinal cord, followed by rAAV1, rAAV7, and rAAVrh.39 (**Figure 3**). All other serotypes did not show detectable GFP expression in the spinal cord region (**Figure 3**).

In order to further characterize the GFP transduction pattern, we quantified delivered rAAV genomes in different CNS areas of injected pigs by quantitative polymerase chain reaction. High copy numbers of rAAV genomes were observed in the CNS regions in which strong GFP expression was observed, while negligible values of genome copy numbers were observed in the CNS regions with low/absent GFP expression, thus supporting the GFP

expression profiles obtained by both IHC and western blotting experiments (**Supplementary Figure S3**).

Cell type transduction upon ICM injection of rAAV 1, 2, 5, 7, 9, rh.10, rh.39, and rh.43 in P30 pigs

In order to precisely evaluate the specific cell types transduced by the different rAAV serotypes analyzed, we co-labeled the CNS coronal sections from rAAV-injected pigs with anti-GFP and antibodies for cell-specific markers of glial and neuronal cells.

Cerebral cortex. Analysis of parietal cerebral cortex (layers I–IV from slice S6) revealed that ~16% of cells were GFP-positive in rAAV9-injected pigs, ~2–3% of cells were GFP-positive in rAAV1-, rAAV2-, and rAAV7-injected pigs, while less than 1% of GFP-positive cells were found for all other serotypes (**Figure 4** and **Table 1**). In rAAV1-, rAAV2-, and rAAV7-injected animals GFP-expressing cells almost completely co-localized with either GFAP or S100 β astroglial markers in the layer I of cerebral cortex (GFAP and S100 β stain, respectively, fibrous and protoplasmic astrocytes), while few/no GFP-positive cells co-localizing with the microglial marker Iba1 or the neuronal marker NeuN were found, thus indicating a predominant transduction of cerebral cortical astrocytes for rAAV1-, rAAV2-, and rAAV7 serotypes (**Figure 4**). In rAAV9-injected pigs, ~26% of GFP-containing cells were GFAP-positive (mostly in the glia limitans), ~41% were S100 β -positive, ~12% were Iba1-positive, and ~25% were NeuN-positive, thus indicating the capability of this serotype to efficiently transduce both neurons and different types of glial cells in this region (**Figure 4**

Table 1 Percentage of GFP transduction

	Cerebral cortex (parietal)				Hippocampus (Dentate gyrus)				Put.	Stria	Cerebellum				Spinal cord (Ventral horn)					
	NeuN	GFAP	S100β	OLIG2	NeuN	GFAP	S100β	OLIG2			Iba1	Clb	GFAP	S100β	OLIG2	Iba1	NeuN (ChAT)	GFAP	S100β	OLIG2
rAAV1			2.1±0.4		2.5±1.1				<1	1.0±0.5			4.5±0.2							1.6±0.5
rAAV2			2.0±0.4		<1				<1	<1			4.1±2.0							<1
rAAV5			<1		<1				<1	<1			<1							<1
rAAV7			2.3±0.3		1±0.5				<1	<1			12.5±0.1							<1
rAAV9			15.9±2.0		16.3±2.0				4.4±0.6	2.0±0.1			14.6±0.1							14.0±0.5
rAAVrh.10	25.6±0.1	25.0±2.4	40.9±3.3	<1	14.8±0.1	43.2±0.4	24.6±7.1	<1	14.1±0.3	61.6±3.9	3.1±0.6	14.5±4.6	<1	14.1±0.4	66.8±2.8 (50.2±0.1)	10.5±0.4	9.5±0.6	1.5±0.6	6.6±0.5	
rAAVrh.39			1.2±0.5		<1				<1	<1			6.7±5.4						<1	
rAAVrh.43			<1		<1				<1	<1			5.1±0.8						<1	
rAAVrh.43			<1		<1				<1	<1			1.6±0.5						<1	

Values are the % of cells expressing GFP in selected brain areas. For values >10%, the relative percentage of GFP-positive cells expressing NeuN, Calbindin, GFAP, S100β, OLIG2, or Iba1 was also measured. Values are represented as mean ± SEM (N = 4).

Clb., calbindin marker; Put., putamen; Stria, stria terminalis.

and Table 1). In the cerebral cortex of pigs injected with all other rAAV serotypes, the few GFP-positive cells found mostly co-localized with astroglial markers in the layer I (Figure 4).

Hippocampus. Analysis of the dentate gyrus and CA3 areas of hippocampus in rAAV9-injected pigs revealed the presence of several GFP-expressing cells, which, as in the cerebral cortex, reflected both neuronal and astroglial cells transduction (Figure 5, Supplementary Figure S4, and Table 1). In the dentate gyrus area, GFP-positive cells co-localized with NeuN (~15%), GFAP (~43%), S100β (~45%), and Iba1 (~11%) markers (Figure 5 and Table 1). GFP-positive cells co-localizing with NeuN, GFAP, and S100β markers were also observed in the hippocampus (dentate gyrus and CA3) of rAAV1-injected pigs (Figure 5, Supplementary Figure S4, and Table 1). Few GFP-positive cells co-localizing with astroglial and neuronal markers were observed in rAAV7- and rAAVrh.39-injected pigs, while negligible GFP-positive cells were found in pigs injected with all other serotypes (Figure 5, Supplementary Figure S4, and Table 1).

Basal ganglia. In the stria terminalis and putamen areas of basal ganglia, only rAAV9-injected animals displayed detectable GFP-positive cells (Figure 6a and Table 1). Confocal images of stria terminalis showed that these GFP-expressing cells co-localized with the oligodendroglial marker OLIG2 (Figure 6a). Remarkably, analysis of this region also showed the presence of some GFP-positive signal, which, although did not co-localize with astroglial or neuronal markers, narrowed several projections, thus suggesting transduction of neuronal bodies resident in other brain regions that circuit with stria terminalis (Figure 6a).

Cerebellum. In the cerebellum, several GFP-positive cells were observed in rAAV7- and rAAV9-injected pigs (respectively ~12 and ~15%), lower numbers of GFP-expressing cells were found in rAAVrh.10, rAAVrh.39-, rAAV2-, and rAAV1-injected pigs, while few/negligible GFP-positive cells were found for all other serotypes (Figure 6b and Table 1). Co-localization analysis with Calbindin marker revealed that these values reflected an efficient transduction of Purkinje cells (Figure 6b and Table 1). GFP co-localization with either Iba1 or astroglial markers were also found in both rAAV9- and rAAV7-injected pigs (Figure 6b and Table 1).

Spinal cord. In the spinal cord, several GFP-expressing cells were observed in rAAV9-injected pigs (Figure 7 and Table 1). In the ventral horn, GFP-positive cells displayed a predominant co-localization with NeuN marker (Figure 7 and Table 1). A few GFP signal co-localizing with NeuN marker was observed in both rAAV1- and rAAV5-injected pigs, while no other serotype showed detectable GFP-positive cells in this region (Figure 7 and Table 1). The use of choline acetyltransferase (ChAT) marker revealed that NeuN-positive GFP-expressing cells were mostly motor neurons in rAAV9-injected animals (Figure 7 and Table 1). The other serotypes tested were negative for ChAT co-staining, including rAAV5, thus indicating that the NeuN-positive GFP-expressing cells in the spinal cord of rAAV5-injected pigs represent a different neuronal subtype (Figure 7 and Table 1).

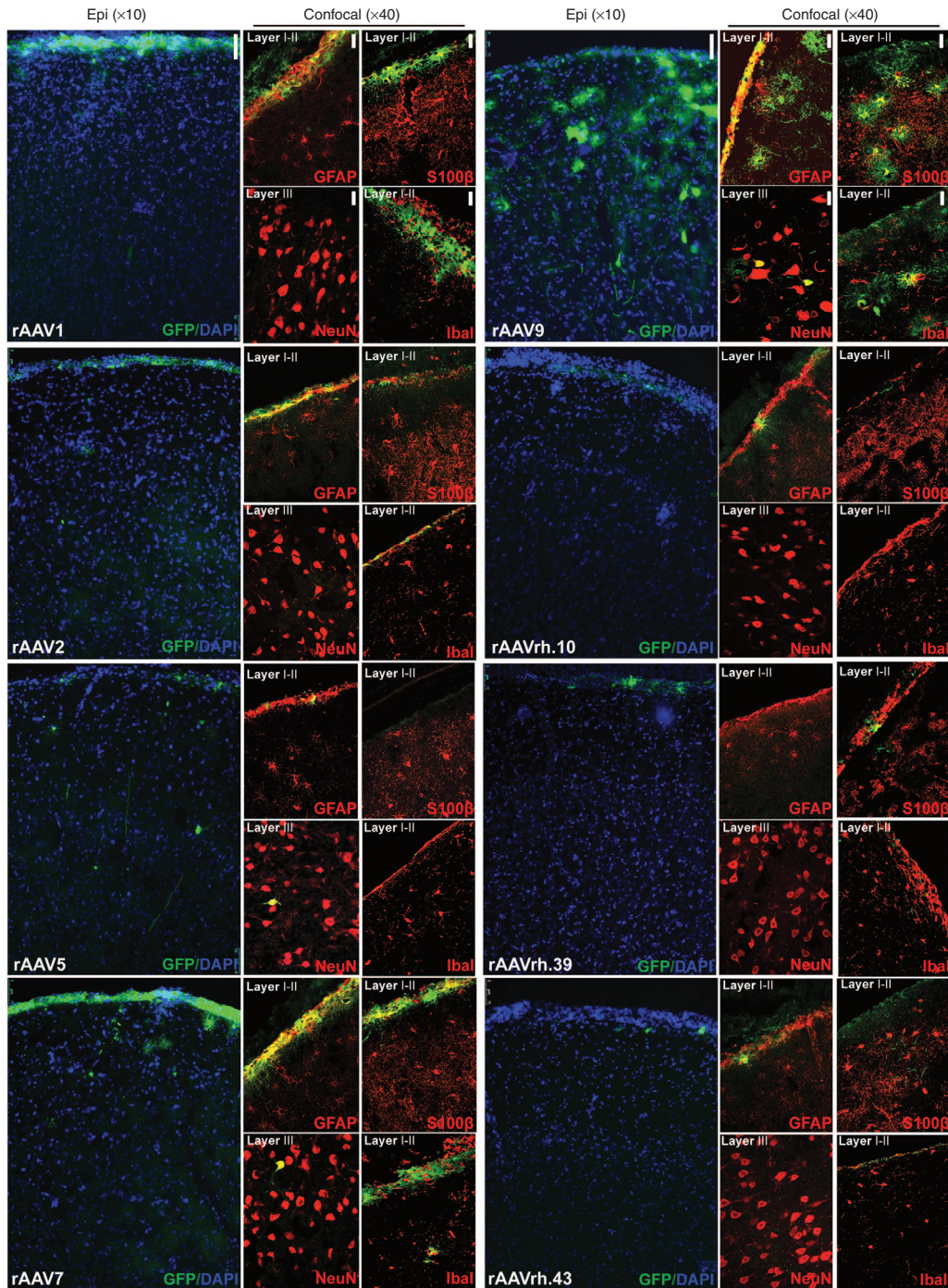


Figure 4 Cell type tropism of rAAV serotypes in the cerebral cortex of injected pigs. Epi-fluorescent images ($\times 10$) showed GFP-expressing cells co-stained with DAPI in the parietal cerebral cortex (layers I–IV from slice 6) of rAAV-injected pigs. Confocal images ($\times 40$) showed GFP co-localization with neuronal (NeuN), astroglial (GFAP, S100 β), and microglial (Iba1) markers in the same region. Bar for epifluorescent images = 75 μm . Bar for confocal images = 50 μm .

Evaluation of toxicity and immune-responses after ICM injection of rAAV 1, 2, 5, 7, 9, rh.10, rh.39, and rh.43 in P30 pigs

We then evaluated the presence of a humoral immune response in treated animals. Serum and CSF were collected and screened before and 1 month after injection in order to determine the presence of

neutralizing antibodies (NAbs) against the rAAV capsids. None of pigs analyzed showed preexisting NAbs either in serum or in CSF (**Supplementary Table S2**). At the time of sacrifice, no NAbs were observed in the serum or CSF of rAAV9-, rAAVrh39-, and rAAVrh43-injected pigs (**Supplementary Table S2**). In contrast, all animals injected with rAAV2 exhibited NAbs in both serum

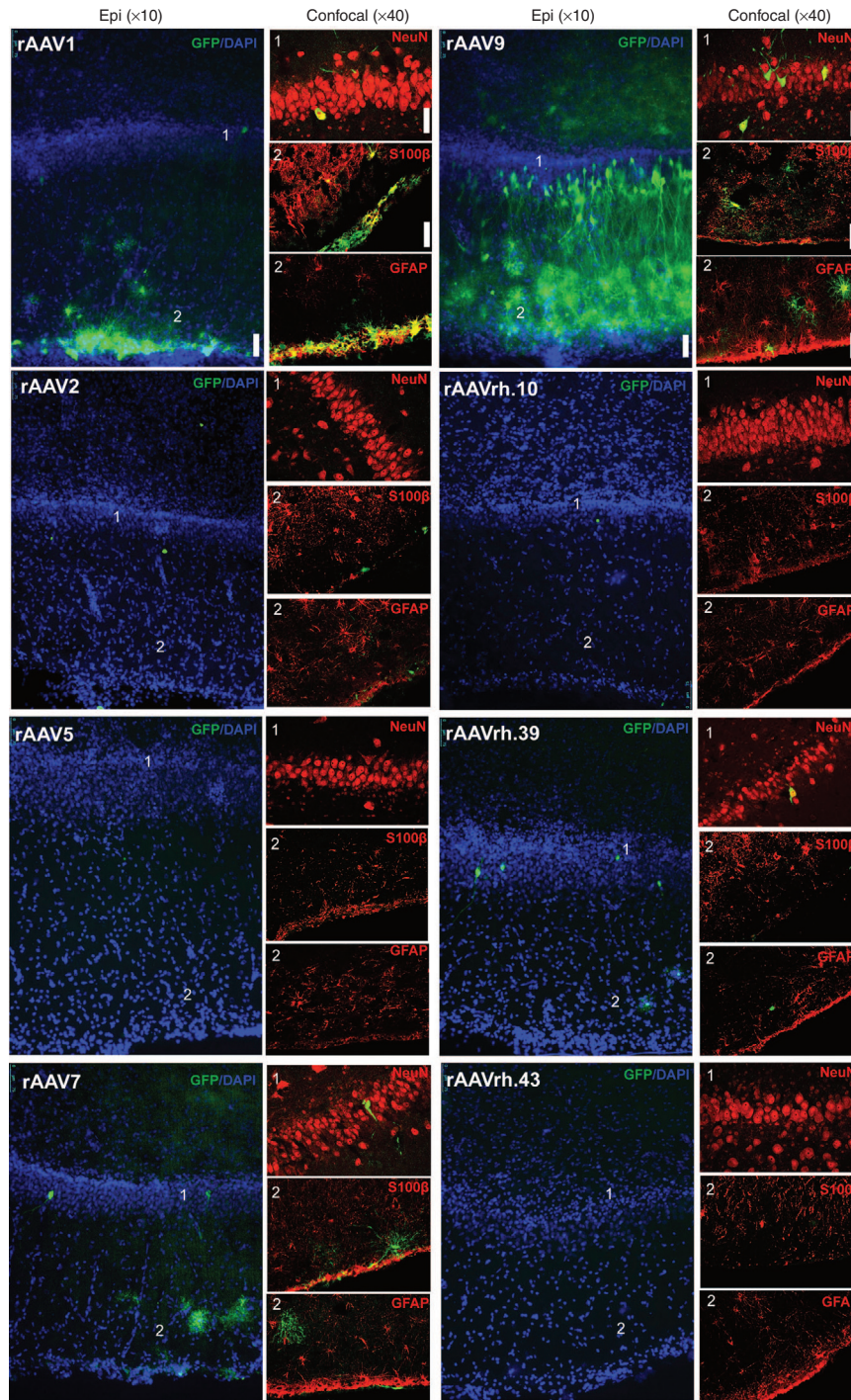


Figure 5 Cell type tropism of rAAV serotypes in the hippocampus of injected pigs. Epi-fluorescent images ($\times 10$) showed GFP-expressing cells co-stained with DAPI in the dentate gyrus of hippocampus of rAAV-injected pigs. Confocal images ($\times 40$) showed GFP co-localization with NeuN, S100 β , and GFAP markers in the same region. Bar for epifluorescent images: 75 μ m. Bar for confocal images: 50 μ m.

and CSF. Results for the remaining rAAV serotypes were variable with some, but not all, animals displaying NABs in serum and CSF (**Supplementary Table S2**).

In order to assess early safety signals, panels of biochemical and hematological markers potentially indicative of renal or hepatic damage/failure, as well as inflammation, were evaluated, and piglet weight was determined on the day of

the injection and at sacrifice to evaluate normal physiological development. No significant differences were detected between rAAV-injected animals and controls for markers tested before injection and at the end of the experimental protocol (**Supplementary Table S3**). The change in the variables that were observed in pigs (either controls or rAAV-injected) when comparing pre- and post-injection time is easily related to

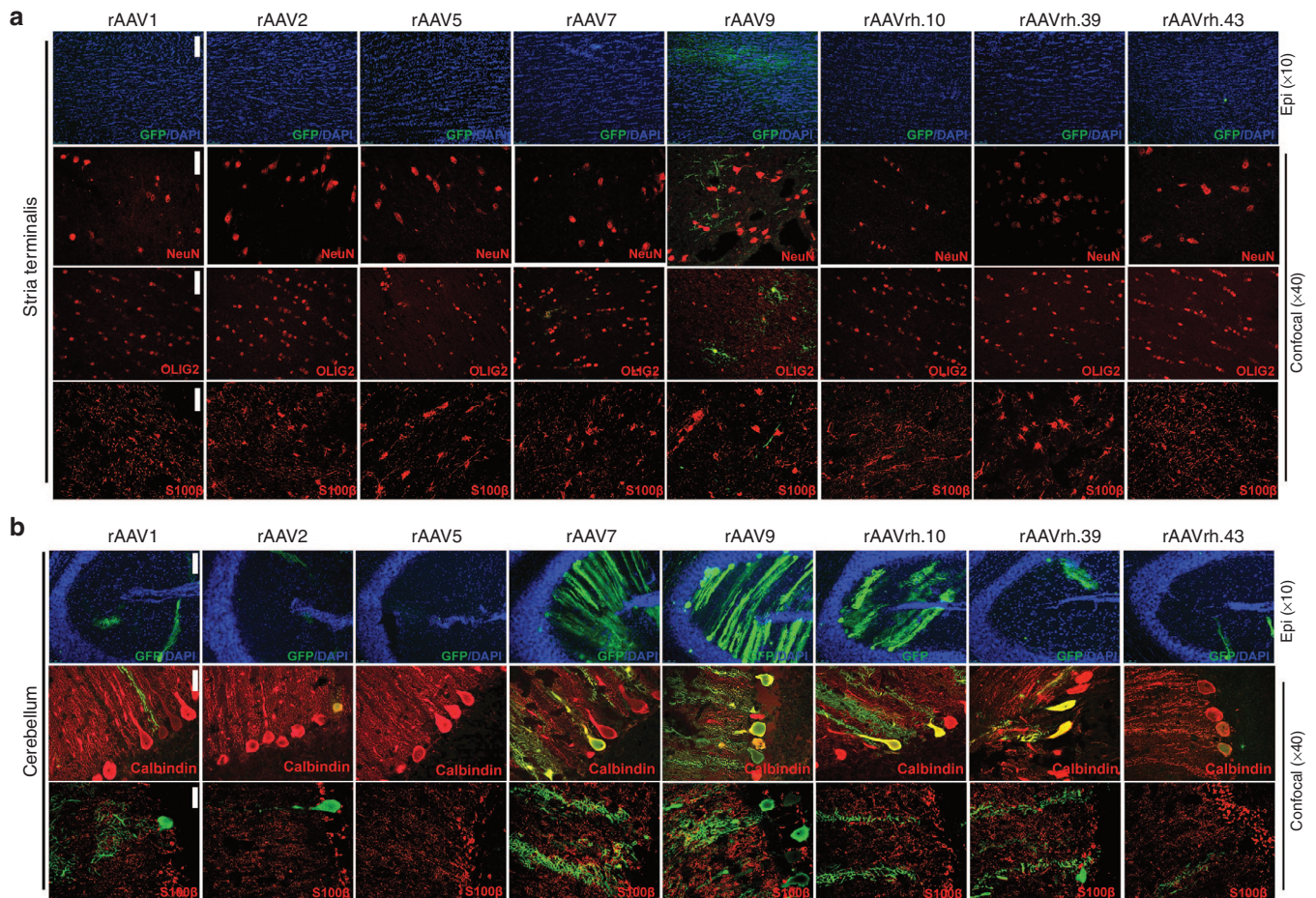


Figure 6 Cell type tropism of rAAV serotypes in the stria terminalis and cerebellum of injected pigs. Epi-fluorescent images ($\times 10$) showed GFP-expressing cells co-stained with DAPI in the (a) stria terminalis and in the (b) cerebellum of rAAV-injected pigs. Confocal images ($\times 40$) showed GFP co-localization with NeuN, OLIG2, and S100 β markers in the (a) stria terminalis and with (b) Calbindin and S100 β in the cerebellum of rAAV-injected pigs. Bar for epifluorescent images = 75 μ m. Bar for confocal images = 50 μ m.

the physiological developmental stages of the pig.²¹ Moreover, weight increase in rAAV-injected pigs was about 75%, similar to that observed in control PBS-injected pigs (**Supplementary Table S1**). No differences in behavioral patterns were observed between rAAV- and PBS-injected pigs. None of the animals showed pain-related postures or signs. A small number of animals (six pigs injected with rAAV5 and rAAV9) exhibited a very mild ataxia that resolved within 12 hours post-injection. In the following days, they were able to eat, drink, and interact normally, without any signs of stress.

Overall, these data suggest that the ICM procedure and rAAV administration were safe and well tolerated over a 1-month period without a significant impact on a number of key physiological parameters.

DISCUSSION

In this study, we generated a comprehensive and detailed CNS transduction map for eight recombinant rAAV viral vector serotypes administered via CSF delivery in a large animal model, *Sus scrofa*. We evaluated the transduction efficiency in 20 regions covering the entire brain from the prefrontal to the occipital region, including the spinal cord. This analysis encompassed the

quantification of rAAV-delivered GFP protein levels and the characterization of both the CNS distribution and cellular-specific transduction profile for each of the serotypes tested (summarized in **Supplementary Table S4**). Importantly, since CSF-mediated transport provides CSF-circulating molecules access to both superficial and deeper regions of the brain parenchyma,¹² the observed CNS distribution of rAAV vectors reflected the intrinsic capability of rAAV serotypes to transduce specific brain regions when taken up by different cells (*i.e.*, tropism).

Overall, our data showed a significant differential tropism of the rAAV serotypes tested, as illustrated by the GFP expression patterns observed. Moreover, the present study provides important information on both regional and cellular specificity of the transduction patterns that suggest potential therapeutic advantages/disadvantages when considering rAAV-based treatments for both cell-autonomous and non-cell-autonomous CNS disorders. Injection of rAAV9 resulted in the widest GFP expression along the entire CNS, showing efficient and widespread transduction of neurons and glial cells of different layers of cerebral cortex, basal ganglia, midbrain, and brain stem areas including motor neurons of the spinal cord. These data are consistent with the CNS transduction pattern of rAAV9 described by us and other

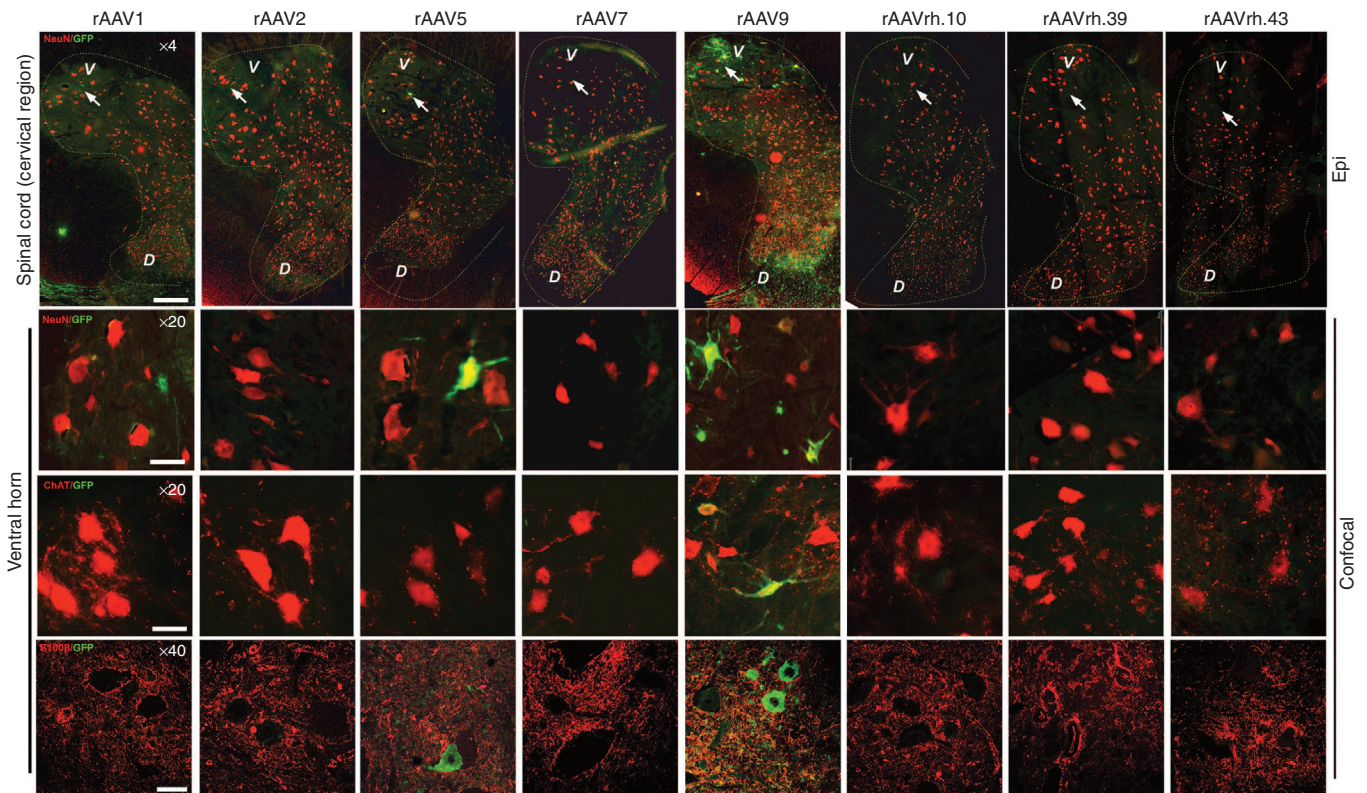


Figure 7 Cell type tropism of rAAV serotypes in the spinal cord of injected pigs. Epi-fluorescent scanned images ($\times 4$) showed GFP-expressing cells co-stained with NeuN in the spinal cord (cervical region) of rAAV-injected pigs. Confocal images ($\times 20$ and $\times 40$) showed GFP co-localization with either NeuN or ChAT (marker of motor neurons) in the ventral horn of the spinal cord (cervical region). Arrows in epi-fluorescent $\times 4$ images indicate the lamina IX area containing the motor neurons. D, dorsal horn; V, ventral horn. Bar for $\times 4$ images = $400\ \mu\text{m}$. Bar for $\times 20$ images = $100\ \mu\text{m}$. Bar for $\times 40$ images = $150\ \mu\text{m}$.

groups.^{14–16,22–24} In contrast to the wide-transduction spectrum of rAAV9, the other rAAV serotypes tested displayed more prominent cell-specific transduction profiles. In particular, rAAV1 and rAAV7 efficiently transduce the glia limitans, with rAAV7 also showing a specific Purkinje cell tropism. rAAVrh.10 also displayed a tropism to Purkinje cells, as previously reported in rats.¹⁷ Transduction of microglial cells was observed for several rAAV serotypes tested including rAAV1, rAAV2, rAAV7, and rAAV9.

An important aspect of translational studies is the demonstration of safety. While the experiments herein described were not designed to fully investigate the potential for treatment-related toxicities, an effort was made to look for early safety signals. Beside transient ataxia post-surgery in some animals, no overt signs of distress were observed. Moreover, consistent with previous studies,²⁵ we did not observe preexisting NABs against any of the rAAV capsids tested while NABs were present only for some serotypes (rAAV1, rAAV2, rAAV5, rAAV7, and rAAVrh.10) in a few injected animals (**Supplementary Table S2**). Nevertheless, it has been described that low levels of circulating NABs do not interfere with CNS gene transfer after CSF delivery.^{14,15,26} Recently, Samaranch *et al.*²⁷ described antigen-presenting cell-mediated neuroinflammation against non-self protein (GFP). In the present study, we did not evaluate the presence of such an inflammatory response; however, its potential toxicity could be overcome by the use of a self-protein as reported.²⁷ Moreover, although we observed a lack of immunotoxicity at 1 month after injection, we do not

exclude that tardive immune responses (*e.g.*, cell-mediated) might be present in treated animals after long-term analysis (>8 weeks).

The data described herein demonstrate the value of rAAV delivery via CSF as a mode to efficiently transduce the CNS, compare, contrast, and map the tropism, transduction efficiency, and cell specificity of eight rAAV serotypes in a large animal model. Therefore, although translating these results to human should take into account potential differences in the tropism features of the AAV vectors tested, our work provides a guide to investigators to better match rAAV serotypes with the needs of specific neurodegenerative diseases that could be potentially treated with a gene-therapy approach.

MATERIALS AND METHODS

Viral vectors. rAAV vectors were produced by the TIGEM rAAV Vector Core by triple-plasmid transfection of HEK293 cells and were purified by two rounds of CsCl_2 gradient centrifugation.²⁸ Viral vector titers (genome copies/ml) were determined by real-time PCR quantification using TaqMan (Applied Biosystems, Foster City, CA) and dot-blot analysis.²⁸

The final titer of each preparation was calculated as the average between the PCR quantification and dot-blot results.

Animals, rAAV administration, and tissue collection. The study was conducted in accordance with the provisions of European Economic Community Council Directive 86/609 adopted by the Italian Government (DL 27/01/1992 No. 116) under the local approval of the Ethical Committee of the University of Bologna and under the approval of Italian Ministry of Health.

All animal studies have been approved by the authors.

The animals enrolled were WT large White × Duroc hybrids, and the sex ratio between females and castrated males was ~1:1.

These animals were transferred to our facility on the day of weaning (28th day after birth) and housed in multiple stalls with infrared heating lamps. They were strictly monitored in order to rule out any pathology that may have affected the entire experiment.

AVV administration. All of the activities performed on the day of the injection have been thoroughly described by Romagnoli *et al.*²⁰ In brief, animal received an i.m. bolus of tiletamine-zolazepam (5 mg/kg) 10 minutes before induction; general anesthesia was achieved using sevoflurane with an induction mask. After orotracheal intubation and stabilization, venous access for fluid therapy was achieved from an auricular vein. Blood samples (6 ml) were collected through the femoral artery.

The dorsal area of the neck was trimmed and surgically prepared, and the puncture of the cisterna magna was performed as previously described.²⁰ One ml of CSF was collected before the injection in order to analyze it as a preinjection physiological standard. The dose of 1.5×10^{12} GC/Kg of viral vector in the volume range from 0.5 to 2.8 ml was injected slowly to avoid a sudden increase in intracranial pressure. Piglets were then placed in Trendelenburg position for 2 minutes in order to help the injected compound to spread toward the more rostral parts of the CNS. Animals were then monitored until complete recovery.

During the following days, all animals were strictly monitored in order to rule out any possible side effect of the procedure and to evaluate any changes in behavior and consequentially in welfare.

Sacrifice and tissue collection. Procedures for anesthesia, venous access, and blood sampling were exactly the same as performed on the day of the injection. CSF samples were collected by puncturing the lumbar spinal space rather than the cisterna magna. Percutaneous cystocentesis was performed to obtain sterile urine samples (3 ml). Animals were then sacrificed with a single bolus (0.3 ml/kg) of Tanax and total body perfusion with Dulbecco's phosphate-buffered saline was started. After median sternotomy, the right atrium was opened and the left ventricle was infused with 500 ml of warm Dulbecco's phosphate-buffered saline (+38 °C) and 1,000 ml of cold Dulbecco's phosphate-buffered saline (+4 °C); blood ejected from the right atrium was drained using a surgical aspirator.

As far as CNS samples, collected tissues were the whole brain and cervical region of spinal cord. Dissection was performed using the technique described by Wischnitzer²⁹ modified by Prof. C. Bombardi. Blood samples were collected using a vacuum system, and tubes with K₂ethylenediaminetetraacetic acid anticoagulant, citrate, and clot activator were used. Samples were processed within 1 hour from collection and analyzed or stored at -80 °C until analysis.

All animals had a complete blood work (ADVIA 2120, Siemens Healthcare Diagnostics, Tarrytown, NY) including complete blood count with hematocrit value, hemoglobin concentration, erythrocyte indices, platelet count, white blood cell with differential white blood cell counts and blood smear examination, and a chemistry profile including aspartate transaminase, alanine transaminase, creatinine, urea, total protein, albumin, albumin to globulin ratio. All chemistry analyses were carried out on an automated chemistry analyser (Olympus AU 400, Beckman Coulter/Olympus, Brea, CA).

Evaluation of AAV vector copy number in the CNS. Genomic DNA was extracted from five selected regions of CNS using a DNeasy Blood and Tissue Extraction kit (Qiagen, Valencia, CA). We selected CNS regions, which were efficiently transduced at least by three viral vectors. DNA concentration was determined by using a Nanodrop. Real-time PCR was performed on 100 ng of genomic DNA using a LightCycler SYBR green I system (Roche, Almere, The Netherlands). For the amplification, the EGFP fwd (5' AGC AGC ACG ACT TCT TCA ACT CC 3') and EGFP rev (5' CCA TGA TAT AGA CGT TGT GG 3') were used. Amplification was run on a LightCycler 96 device

(Roche) with standard cycles. A standard curve was generated, using the corresponding AAV vector plasmid pAAV2.1CMV-EGFP.

GFP immunoblotting. To quantify the GFP protein, 20 main regions covering the entire CNS of injected pigs were dissected and then snap-frozen in liquid nitrogen (see **Supplementary Figure S1**). Approximately 70 mg of each dissected region were homogenized with TissueLyser using 10 volumes (700 µl) of 3× Flag lysis buffer (50 mmol/l Tris-HCl pH8, 200 mmol/l NaCl, 1% Triton X100, 1 mmol/l ethylenediaminetetraacetic acid, and 50 mmol/l 4-(2-hydroxyethyl)-1-piperazineethanesulfonic acid) and a protease inhibitor cocktail (Sigma-Aldrich, St Louis, MO). The lysates were incubated in ice for 1 hour and cleared by centrifugation. Protein concentration was determined using the Bio-Rad colorimetric assay (Bio-Rad, Hercules, CA). Thirty micrograms of homogenate protein were separated on a 12% sodium dodecyl sulfate polyacrylamide gel electrophoresis, transferred to polyvinylidene difluoride membrane at 30 V over night. As control, 70 ng of purified GFP was loaded on sodium dodecyl sulfate gels. Anti-GFP rabbit polyclonal (1:1,000, NB600-308; Novus BIO, Littleton, CO) and anti-β-actin mouse monoclonal antibodies (1:2,000, A5441, Sigma-Aldrich) were, respectively, used for the detection of GFP and actin proteins. The membranes were incubated with secondary antirabbit and antimouse antibodies (1:5,000, CALBIOCHEM, San Diego, CA), and protein bands were visualized using VVP-ChemiDoc-It (Life Science Software, Hopkinton, MA). Relative band intensity was quantified by densitometric analysis using ImageJ software (National Institutes of Health, Bethesda, MD).

The intensity of bands corresponding to the GFP expressed in brain lysates was quantified by densitometric analysis. Each of these values was divided for both the value resulting from densitometric quantitation of the band corresponding to the purified GFP (which was loaded on the same sodium dodecyl sulfate gel in which the brain samples were loaded) and the value resulting from densitometric quantitation of actin. The resulting ratio was expressed as arbitrary units (a.u.)

Immunolabeling. IHC staining of GFP was performed on 40 µm floating cryosections derived from brain and spinal cord of injected pigs.

Sections were washed in PBS/Triton X-100 0.1% (wash buffer), incubated for 30 minutes at room temperature in 1% hydrogen peroxidase diluted in PBS 1× and incubated overnight at 4 °C in primary antibody solution: PBS 1×/ Triton X-100 0.1%, 2% horse serum, rabbit anti-GFP (1:1,500, NB600-308; Novus BIO). Anti-GFP was detected with MACH4 Universal HRP-Polymer Biotin-Free Detection Polymer Detection Kit (BIOCARE Medical, Concord, CA). After 1 hour, we washed three times the sections and developed the signal with diaminobenzidine (Vectorstain Kit; Vector Laboratories, Burlingame, CA). Sections were then mounted with CV Ultra Mounting Media (Leica, Wetzlar, Germany).

To identify the cell types, we performed immunofluorescence experiments on 30-µm cryosections. Samples were blocked in TBS1X-Triton 0.3% and Donkey Serum 5% for 1 hour at room temperature and incubated with anti-GFP either rabbit polyclonal (1:1,000, NB600-308; Novus BIO) or chicken polyclonal 9 (1:800, AB13970; Abcam, Cambridge, UK), anti-S100β mouse monoclonal (1:800, AB66028; Abcam), anti-IBA1 rabbit polyclonal (1:500, 234003; Synaptic System, Gottingen, Germany), anti-NeuN mouse monoclonal (1:400, MAB377; Millipore), anti-GFAP mouse monoclonal (1:200, MAB3402; Millipore, Amsterdam, the Netherlands), anti-Olig2 mouse monoclonal (1:200, MABN50; Millipore), and anti-CHAT goat polyclonal (1:100, AB144P; Millipore) to, respectively, identify GFP protein, neurons, astrocytes, oligodendrocytes, and motor neurons. After overnight incubation with primary antibody, sections were washed in PBS 1× and incubated with Alexa Fluor 488-conjugated donkey antirabbit (1:500; Invitrogen, Carlsbad, CA), Alexa Fluor 594-conjugated donkey anti-mouse (1:500; Invitrogen), and Alexa Fluor 594-conjugated donkey anti-goat (1:500; Invitrogen). Rinsed sections were mounted with VECTASHIELD mounting medium with 4',6-diamidino-2-phenylindole, dihydrochloride (DAPI) (Vinci-Biochem, Florence, Italy) and analyzed by either epi-fluorescent and confocal microscopy.

GFP quantitation (% of GFP-positive cells) in immunofluorescence experiments. We quantified the GFP immunofluorescence signal in the CNS of injected pigs in five main CNS regions (parietal cerebral cortex from slice S6, dentate gyrus of hippocampus from slice S8, putamen from slice S5, cerebellum from slice S11, and lamina IX of the cervical tract of spinal cord (slice S12)). One square millimeter area of four different sections (30 μ m) stained with DAPI and co-labeled with GFP, and the specific cell type markers (NeuN, Calbindin, ChAT, GFAP, S100 β , Iba1, or OLIG2) were scanned in z-stack using Zeiss LSM 710 microscope equipped with a Zeiss confocal-scanning laser using a 40 \times objective (Zeiss, Oberkochen, Germany). The exposure time used to acquire all images was identical. The co-localization analysis was performed by the microscope ZEISS 2008 program. Total number of DAPI- and GFP-positive signals were counted using the cell-counter program (ImageJ software) with a fixed threshold. Total GFP cell counts present in the 1 mm² area analyzed were then expressed as percentage of total cells (DAPI positive) expressing the GFP (%GFP-positive cells). For CNS regions in which the %GFP-positive cells was >10%, NeuN-, Calbindin-, ChAT-, GFAP-, S100 β -, Iba1-, or OLIG2-positive cells were also counted and expressed as percentage of GFP-positive cells expressing the specific cell type marker.

Microscopy. 3,3'-Diaminobenzidine-processed brain and spinal cord sections were digitized using a Scan-Scope slide scanner (Leica scn400). Virtual slides were viewed using Leica digital image hub, and images were generated using the same software. Immunofluorescence images of the entire cervical region of the spinal cord were digitized using a Scan-Scope slide scanner (Leica scn400). Fluorescence images at \times 10 magnification were visualized by epi-fluorescence microscope. Confocal microscopy was performed with a Zeiss LSM 710 confocal microscope equipped with a Zeiss confocal-scanning laser using 40 \times objective.

Neutralizing antibody assay. The presence of NAb to rAAV capsid was assessed, on serum and CSF collected at the day of injection and 1 month after injection, as previously described.³⁰

Data analysis. Biochemical and hematological results among groups were compared using nonparametric statistics (Mann-Whitney *U*-test, Kruskal-Wallis ANOVA, and Friedman test for paired data). Data are expressed as mean \pm 1 SEM ($n = 3$). A *P* value of <0.05 was considered to be statistically significant.

SUPPLEMENTARY MATERIAL

Figure S1. Scheme of pig brain and spinal cord dissection.

Figure S2. IHC analysis of GFP distribution pattern in basal ganglia of pig brain upon ICM delivery of rAAV1, 2, 5, 7, 9, rh.10, rh.39, and rh.43.

Figure S3. Distribution of rAAV vector genomes following ICM injection in pig.

Figure S4. Cell type tropism of rAAV serotypes in the CA3 area of the hippocampus of injected pigs.

Table S1. Summary of injections in P30 pigs.

Table S2. Neutralizing anti-AAV antibody levels.

Table S3. Biochemical and hematological parameters.

Table S4. Summary of GFP transduction.

ACKNOWLEDGMENTS

The authors thank Graciana Diez-Roux, Shipeng Yuan, and Vivian Choi for critical reading of the manuscript. Edoardo Nusco and Rossella Venditti for technical help. We acknowledge the rAAV vector core (TIGEM) for rAAV production and neutralizing antibody assay, the Advanced Microscopy and Imaging core (TIGEM), Donatella Montanaro and the Pathology core (CEINGE) for IHC image scanning. Shire funded this work as part of a project within Discovery Biology and Translational Research.

A.-R.G., Y.H., and S.L.K. are employees and stockholders of Shire. The other authors declare that they have no conflict of interest.

REFERENCES

- Simonato, M, Bennett, J, Boulis, NM, Castro, MG, Fink, DJ, Goins, WF *et al.* (2013). Progress in gene therapy for neurological disorders. *Nat Rev Neurol* **9**: 277–291.
- Worgall, S, Sondhi, D, Hackett, NR, Kosofsky, B, Kekatpure, MV, Neyzi, N *et al.* (2008). Treatment of late infantile neuronal ceroid lipofuscinosis by CNS administration of a serotype 2 adeno-associated virus expressing CLN2 cDNA. *Hum Gene Ther* **19**: 463–474.
- Leone, P, Shera, D, McPhee, SW, Francis, JS, Kolodny, EH, Bilaniuk, LT *et al.* (2012). Long-term follow-up after gene therapy for canavan disease. *Sci Transl Med* **4**: 165ra163.
- Hwu, WL, Muramatsu, S, Tseng, SH, Tzen, KY, Lee, NC, Chien, YH *et al.* (2012). Gene therapy for aromatic L-amino acid decarboxylase deficiency. *Sci Transl Med* **4**: 134ra61.
- Marks, WJ Jr, Bartus, RT, Siffert, J, Davis, CS, Lozano, A, Boulis, N *et al.* (2010). Gene delivery of AAV2-neurturin for Parkinson's disease: a double-blind, randomised, controlled trial. *Lancet Neurol* **9**: 1164–1172.
- LeWitt, PA, Rezaei, AR, Leehey, MA, Ojemann, SG, Flaherty, AW, Eskandar, EN *et al.* (2011). AAV2-GAD gene therapy for advanced Parkinson's disease: a double-blind, sham-surgery controlled, randomised trial. *Lancet Neurol* **10**: 309–319.
- Foust, KD, Nurre, E, Montgomery, CL, Hernandez, A, Chan, CM and Kaspar, BK (2009). Intravascular AAV9 preferentially targets neonatal neurons and adult astrocytes. *Nat Biotechnol* **27**: 59–65.
- Yang, B, Li, S, Wang, H, Guo, Y, Gessler, DJ, Cao, C *et al.* (2014). Global CNS transduction of adult mice by intravenously delivered rAAVrh.8 and rAAVrh.10 and nonhuman primates by rAAVrh.10. *Mol Ther* **22**: 1299–1309.
- Duncan, FJ, Naughton, BJ, Zaraspe, K, Murrey, DA, Meadows, AS, Clark, KR *et al.* (2015). Broad functional correction of molecular impairments by systemic delivery of scAAVrh74-hSCGSH gene delivery in MPS IIIA mice. *Mol Ther* **23**: 638–647.
- Chen, YH, Chang, M and Davidson, BL (2009). Molecular signatures of disease brain endothelia provide new sites for CNS-directed enzyme therapy. *Nat Med* **15**: 1215–1218.
- Lehtinen, MK, Björnsson, CS, Dymecki, SM, Gilbertson, RJ, Holtzman, DM and Monuki, ES (2013). The choroid plexus and cerebrospinal fluid: emerging roles in development, disease, and therapy. *J Neurosci* **33**: 17553–17559.
- Iliff, JJ, Wang, M, Liao, Y, Plogg, BA, Peng, W, Gundersen, GA *et al.* (2012). A paravascular pathway facilitates CSF flow through the brain parenchyma and the clearance of interstitial solutes, including amyloid β . *Sci Transl Med* **4**: 147ra111.
- Murliharan, G, Samulski, RJ and Asokan, A (2014). Biology of adeno-associated viral vectors in the central nervous system. *Front Mol Neurosci* **7**: 76.
- Hinderer, C, Bell, P, Gurda, BL, Wang, Q, Louboutin, JP, Zhu, Y *et al.* (2014). Intrathecal gene therapy corrects CNS pathology in a feline model of mucopolysaccharidosis I. *Mol Ther* **22**: 2018–2027.
- Haurigot, V, Marcó, S, Ribera, A, Garcia, M, Ruzo, A, Villacampa, P *et al.* (2013). Whole body correction of mucopolysaccharidosis IIIA by intracerebrospinal fluid gene therapy. *J Clin Invest* (epub ahead of print).
- Samaranch, L, Salegio, EA, San Sebastian, W, Kells, AP, Bringas, JR, Forsayeth, J *et al.* (2013). Strong cortical and spinal cord transduction after AAV7 and AAV9 delivery into the cerebrospinal fluid of nonhuman primates. *Hum Gene Ther* **24**: 526–532.
- Hordeaux, J, Dubreil, L, Deniaud, J, Iacobelli, F, Moreau, S, Ledevin, M *et al.* (2015). Efficient central nervous system AAVrh10-mediated intrathecal gene transfer in adult and neonate rats. *Gene Ther* **22**: 316–324.
- Weinberg, MS, Samulski, RJ and McCown, TJ (2013). Adeno-associated virus (AAV) gene therapy for neurological disease. *Neuropharmacology* **69**: 82–88.
- Lind, NM, Moustgaard, A, Jelsing, J, Vajta, G, Cumming, P and Hansen, AK (2007). The use of pigs in neuroscience: modeling brain disorders. *Neurosci Biobehav Rev* **31**: 728–751.
- Romagnoli, N, Ventrella, D, Giunti, M, Dondi, F, Sorrentino, NC, Fraldi, A *et al.* (2014). Access to cerebrospinal fluid in piglets via the cisterna magna: optimization and description of the technique. *Lab Anim* **48**: 345–348.
- Egeli, AK, Framstad, T and Morberg, H (1998). Clinical biochemistry, haematology and body weight in piglets. *Acta Vet Scand* **39**: 381–393.
- Spanpanato, C, De Leonibus, E, Dama, P, Gargiulo, A, Fraldi, A, Sorrentino, NC *et al.* (2011). Efficacy of a combined intracerebral and systemic gene delivery approach for the treatment of a severe lysosomal storage disorder. *Mol Ther* **19**: 860–869.
- Gray, SJ, Nagabhushan Kalburgi, S, McCown, TJ and Jude Samulski, R (2013). Global CNS gene delivery and evasion of anti-AAV-neutralizing antibodies by intrathecal AAV administration in non-human primates. *Gene Ther* **20**: 450–459.
- Federici, T, Taub, JS, Baum, GR, Gray, SJ, Grieger, JC, Matthews, KA *et al.* (2012). Robust spinal motor neuron transduction following intrathecal delivery of AAV9 in pigs. *Gene Ther* **19**: 852–859.
- Calcedo, R and Wilson, JM (2013). Humoral Immune Response to AAV. *Front Immunol* **4**: 341.
- Passini, MA, Bu, J, Richards, AM, Treleaven, CM, Sullivan, JA, O'Riordan, CR *et al.* (2014). Translational fidelity of intrathecal delivery of self-complementary AAV9-survival motor neuron 1 for spinal muscular atrophy. *Hum Gene Ther* **25**: 619–630.
- Samaranch, L, San Sebastian, W, Kells, AP, Salegio, EA, Heller, G, Bringas, JR *et al.* (2014). AAV9-mediated expression of a non-self protein in nonhuman primate central nervous system triggers widespread neuroinflammation driven by antigen-presenting cell transduction. *Mol Ther* **22**: 329–337.
- Doria, M, Ferrara, A and Auricchio, A (2013). AAV2/8 vectors purified from culture medium with a simple and rapid protocol transduce murine liver, muscle, and retina efficiently. *Hum Gene Ther Methods* **24**: 392–398.
- Wischnitzer, S (1972). *Atlas and Dissection Guide for Comparative Anatomy*. 2nd edn. W H Freeman and Company: San Francisco.
- Mussolino, C, della Corte, M, Rossi, S, Viola, F, Di Vicino, U, Marrocco, E *et al.* (2011). AAV-mediated photoreceptor transduction of the pig cone-enriched retina. *Gene Ther* **18**: 637–645.

**A comprehensive map of CNS transduction by eight recombinant
adeno-associated virus serotypes upon cerebrospinal fluid
administration in pigs**

Nicolina Cristina Sorrentino¹, Veronica Maffia^{1,*}, Sandra Strollo^{1,*}, Vincenzo Cacace^{1,*},
Noemi Romagnoli^{2,*}, Anna Manfredi¹, Domenico Ventrella², Francesco Dondi²,
Franscesca Barone², Massimo Giunti², Anne-Renee Graham³, Yan Huang³, Susan L.
Kalled³, Alberto Auricchio¹, Maria Laura Bacci², Enrico Maria Surace^{1,#} and Alessandro
Fraldi^{1,#}

¹ Telethon Institute of Genetics and Medicine (TIGEM), Naples, Italy

² University of Bologna, Department of Veterinary Medical Sciences (DIMEVET),
Bologna, Italy

³ Shire, Discovery Biology and Translational Research, Lexington, MA, USA

* Equally contribution

Corresponding author

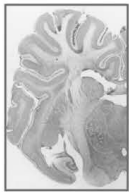
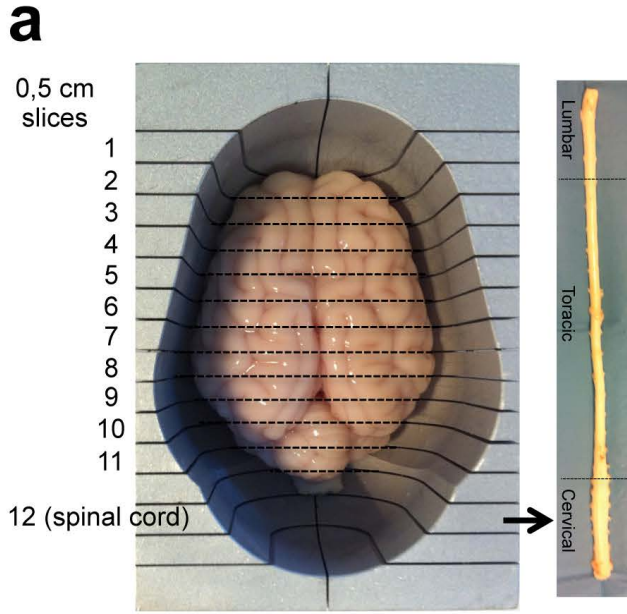
Supplementary Materials:

-Supplementary Figures

-Supplementary Figure Legends

-Supplementary Tables

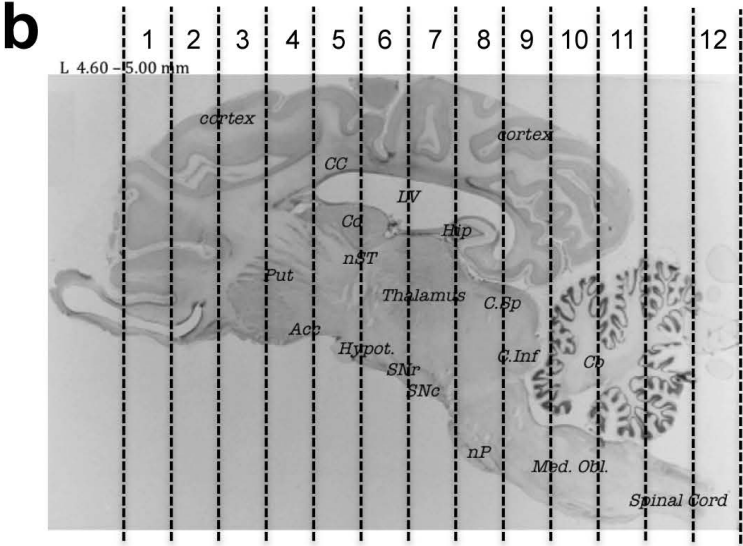
SUPPLEMENTARY FIGURE S1



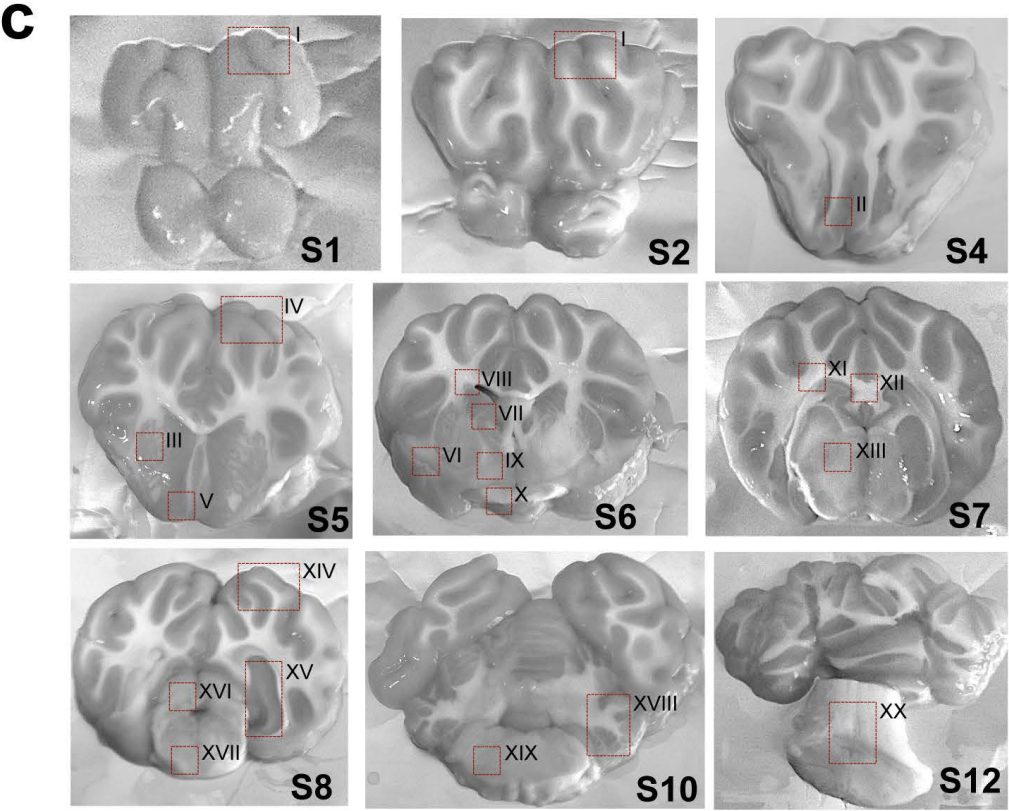
Cut of coronal sections & IHC/IF



Dissection of areas of interest & WB



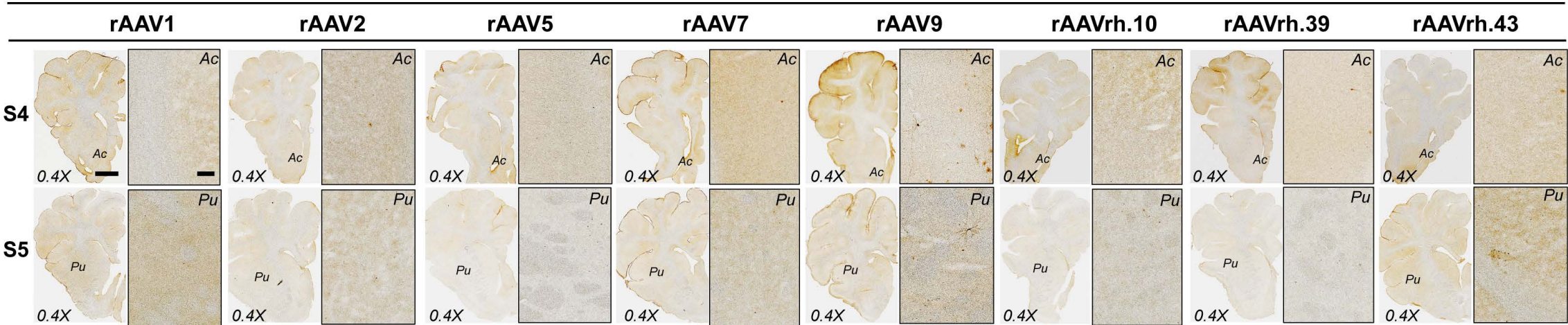
SLICES	AREAS OF INTEREST
Slices 1-3	Frontal cortex (ctx)
Slice 4	Frontal cortex, nucleus accumbens (Acc), putamen (Put)
Slice 5	Parietal cortex, amygdala, hypothalamus (Hypot), nucleus caudatus (Cd).
Slice 6	Parietal cortex, substantia nigra (SN), stria terminalis (ST).
Slice 7	Parietal cortex, hippocampus (Hip.), corpus callosum (CC), thalamus.
Slice 8	Occipital cortex, hippocampus (Hip), nuclei pontis (nP).
Slice 9	Occipital cortex, colliculus superior (CS), colliculus inferior (CInf)
Slice 10	Occipital cortex, cerebellum (Cb)
Slice 11	Medulla ablongata
Slice 12	Spinal cord (cervical region)



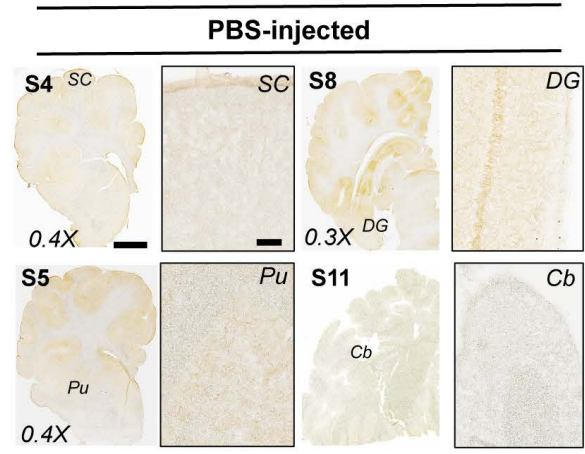
- I. Frontal cortex
- II. Accumbens
- III. Putamen
- IV. Parietal cortex
- V. Hypothalamus
- VI. Amygdala
- VII. N. caudatus
- VIII. Subcallosus
- IX. Sub. nigra
- X. N. pontis
- XI. Stria
- XII. C. callosum
- XIII. Thalamus
- XIV. Occipital cortex
- XV. Hippocampus
- XVI. Colliculi
- XVII. Pons
- XVIII. Cerebellum
- XIX. Med. ablong.
- XX. Spinal cord

SUPPLEMENTARY FIGURE S2

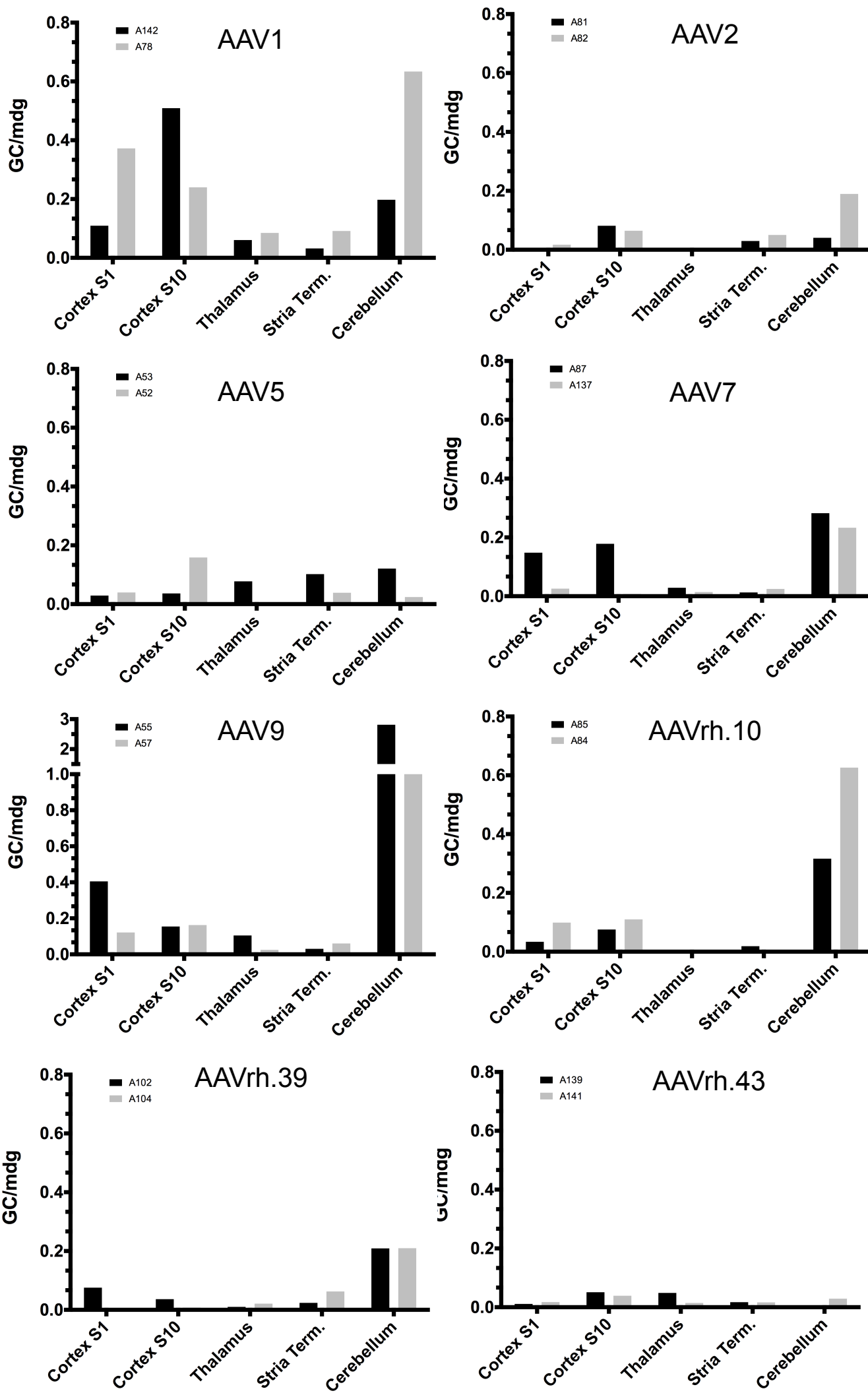
a



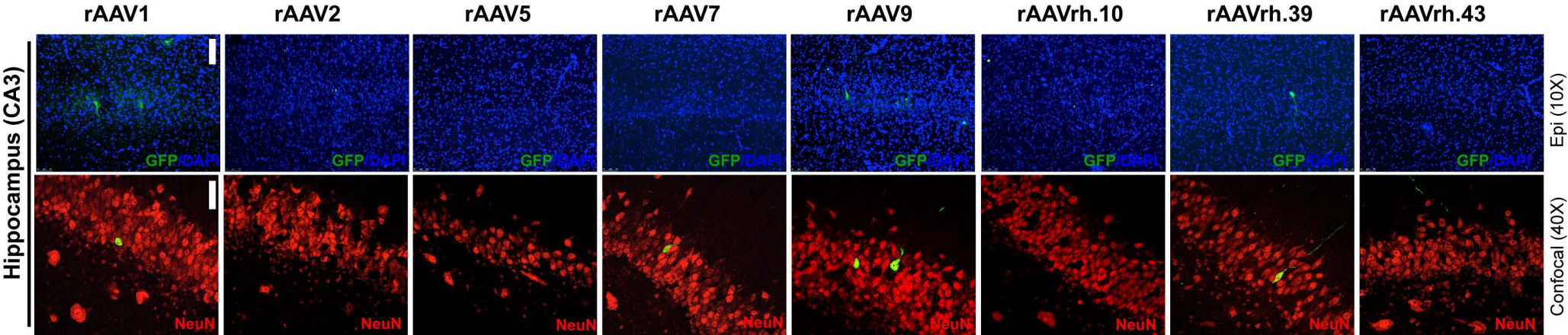
b



SUPPLEMENTARY FIGURE S3



SUPPLEMENTARY FIGURE S4



Supplementary Figure Legends

Supplementary Figure S1: Scheme of pig brain and spinal cord dissection. (a) Pig brain and spinal cord cervical region were divided in 12 coronal slices (0,5 cm) from the rostral to the caudal part to the central nervous system (CNS). Different areas were dissected from one half of each slice for biochemical analysis (western blot). The other half of each slice was used for histological analysis. (b) Sagittal representation of sliced pig brain (adapted figure derived from³¹) in which the main areas of interest are shown. In the table are listed the main areas of interest associated with each of the twelve coronal slices. (c) The CNS areas dissected for western blot analysis were shown.

Supplementary Figure S2: IHC analysis of GFP distribution pattern in basal ganglia of pig brain upon ICM delivery of rAAV1, 2, 5, 7, 9, rh.10, rh.39, and rh.43.

(a) IHC GFP expression in the brain of rAAV-injected pigs in basal ganglia (Putamen and accumbens) are shown in the enlarged (4X) images taken from the 40 µm coronal cryosections (slice S4 and S5). (b) IHC GFP in different CNS areas of control PBS-injected pigs is also shown.

Pu: Putamen; Ac:Accumbens; SC: frontal superficial cerebral cortex (layers I-III); DG: Dentate gyrus of hippocampus; Cb: Cerebellum.

Scale bar for 0,4X images: 4mm. Scale bar of 4X images: 200 µm.

Supplementary Figure S3: Distribution of rAAV vector genomes following ICM injection in pig.

Five different regions of pig brain were isolated from two animals for each serotype injected. The number of viral genome within each region was analyzed by using a LightCycler SYBR green I system. The abundance of vector genomes is showed as copies per diploid cell.

GC: genome copies; mdg: molecules of diploid genome.

Supplementary Figure S4. Cell type tropism of rAAV serotypes in the CA3 area of the hippocampus of injected pigs. Epi-fluorescent images (10X) showed GFP expressing cells co-stained with DAPI in the CA3 area of the hippocampus of rAAV-injected pigs. Confocal images (40X) showed GFP co-localization with NeuN marker in the same area.

Scale bar for epifluorescent images: 75 μm . Scale bar for confocal images: 50 μm .

Supplementary Table S1. Summary of injections in P30 pigs

	Subjects	Weight BI (Kg)	Weight PI (Kg)	Dose (E+12 GC/Kg)	Volume (mL)
rAAV1	A78	7.3	10.7	1.5	0.95
	A79	3.6	5.8	1.5	0.5
	A142	9.5	13.5	1.5	1.3
rAAV2	A81	6.5	10.8	1.5	2.2
	A82	6.4	13	1.5	2.2
	A83	4.9	8.3	1.5	1.8
rAAV5	A52	8.9	14	1.5	2.8
	A53	7.3	13.2	1.5	2.4
	A54	6.2	10.7	1.5	2
rAAV7	A87	3.7	6.5	1.5	1.5
	A137	6.5	11.3	1.5	2.3
	A138	8.3	13.1	1.5	2.9
rAAV9	A55	6.1	11	1.5	2
	A56	7	12	1.5	2.3
	A57	5.7	11.3	1.5	2.2
rAAV rh.10	A84	4.8	7.3	1.5	1.7
	A85	5.3	10.5	1.5	1.8
	A88	6.9	11.4	1.5	2.3
rAAV rh.39	A102	7.8	14.1	1.5	2.5
	A103	9	13.9	1.5	3
	A104	8.3	12.8	1.5	2.7
rAAV rh.43	A139	7.3	13.3	1.5	2.3
	A141	7.9	13	1.5	2.5
	A143	7.8	11.1	1.5	2.5
CTRL	A86	8.5	12	-	2
	A89	6.2	10.6	-	2
	A133	9	12.1	-	2

Abbreviations: GC, genome copies; CTRL, Control-PBS injected pigs.
BI: before injection; PI: post injection.

Supplementary Table S2. Neutralizing anti-AAV antibody levels

AAV vector	Subject	Serum Anti-AAV		CSF Anti-AAV	
		Pre inj.	1 month Post inj.	Pre inj.	1 month Post Inj.
<i>rAAV1</i>	#A78	-	+	-	+
	#A79	-	-	-	-
	#A135	-	-	-	-
<i>rAAV2</i>	#A81	-	+	-	+
	#A82	-	+	-	+
	#A83	-	+	-	+
<i>rAAV5</i>	#A52	-	-	-	+
	#A53	-	+	-	+
	#A54	-	+	-	+
<i>rAAV7</i>	#A87	-	-	-	-
	#A137	-	+	-	-
	#A138	-	+	-	-
<i>rAAV9</i>	#A55	-	-	-	-
	#A56	-	-	-	-
	#A57	-	-	-	-
<i>rAAVrh.10</i>	#A84	-	-	-	-
	#A85	-	+	-	-
	#A88	-	-	-	-
<i>rAAVrh.39</i>	#A102	-	-	-	-
	#A103	-	-	-	-
	#A104	-	-	-	-
<i>rAAVrh.43</i>	#A139	-	-	-	-
	#A141	-	-	-	-
	#A143	-	-	-	-

Abbreviations: CSF, cerebrospinal fluid; AAV, Adeno-Associated Viral vector; inj., injection.
 “-“ Indicates undetectable Nab response. “+” indicates the presence of anti-AAV neutralizing antibodies in the sample

Supplementary Table S3. Biochemical and hematological parameters

Target	Variable unit	Control group		rAAV1		rAAV2		rAAV5		rAAV7		rAAV9		rAAVrh.10		rAAVrh.39		rAAVrh.43	
		Pre	Post																
Renal Damage	Creatinine mg/dL	1.06 ±0.08	0.99 ±0.04	0.99 ±0.14	0.93 ±0.08	0.96 ±0.07	0.95 ±0.06	1.11 ±0.14	1.00 ±0.05	0.92 ±0.07	0.82 ±0.02	1.09 ±0.08	0.99 ±0.06	0.91 ±0.03	0.82 ±0.08	0.99 ±0.03	0.88 ±0.07	1.11 ±0.04	0.89 ±0.03
	Urea mg/dL	11.63 ±2.31	20.24 ±4.56	10.30 ±3.40	19.19 ±2.95	12.81 ±3.18	15.11 ±2.26	7.53 ±2.18	10.22 ±1.09	13.28 ±6.21	13.01 ±0.94	10.73 ±5.17	18.28 ±2.73	17.40 ±5.62	18.74 ±2.58	13.40 ±2.63	16.80 ±4.26	8.57 ±2.77	17.64 ±3.06
Liver Damage	AST U/L	27.67 ±3.17	43.60 ±7.54	30.75 ±3.47	45.00 ±4.63	47.20 ±6.16	50.00 ±7.78	41.00 ±9.99	40.25 ±7.09	33.33 ±9.40	48.50 ±6.50	34.75 ±2.95	43.00 ±3.69	46.00 ±4.80	46.75 ±4.31	60.50 ±7.01	52.00 ±9.11	31.67 ±3.84	51.07 ±9.95
	ALT U/L	39.50 ±5.68	52.80 ±9.26	41.50 ±8.29	49.33 ±7.40	36.80 ±3.61	49.40 ±8.28	45.50 ±2.50	40.50 ±8.10	39.33 ±5.61	62.50 ±4.50	35.00 ±1.08	47.43 ±4.91	49.00 ±6.77	53.50 ±0.65	50.75 ±6.56	50.25 ±9.88	36.00 ±1.53	58.10 ±6.00
Inflammation Acute Phase Response	Albumin g/dL	3.01 ±0.17	2.35 ±0.28	2.61 ±0.21	2.10 ±0.19	2.33 ±0.22	2.04 ±0.26	2.98 ±0.44	2.08 ±0.10	2.59 ±0.65	2.06 ±0.52	2.96 ±0.09	2.50 ±0.13	2.08 ±0.37	1.75 ±0.26	2.80 ±0.18	2.49 ±0.35	2.80 ±0.07	1.80 ±0.45
	Albumin/globulin Ratio	1.75 ±0.14	0.99 ±0.20	1.58 ±0.18	0.95 ±0.17	1.50 ±0.21	0.85 ±0.18	2.27 ±0.48	1.18 ±0.13	1.74 ±0.64	0.85 ±0.26	1.70 ±0.08	1.14 ±0.10	0.90 ±0.30	0.66 ±0.13	1.18 ±0.17	0.94 ±0.25	1.90 ±0.05	0.68 ±0.12
	Total Protein g/dL	4.77 ±0.17	4.88 ±0.13	4.29 ±0.24	4.51 ±0.10	3.95 ±0.16	4.72 ±0.31	4.31 ±0.35	3.90 ±0.16	4.49 ±0.35	4.52 ±0.39	4.73 ±0.12	4.78 ±0.20	4.67 ±0.10	4.50 ±0.18	5.39 ±0.48	5.89 ±0.70	4.28 ±0.09	4.88 ±0.19
	WBC x 10 ³ /μL	10.41 ±0.34	17.27 ±1.91	9.28 ±0.71	17.27 ±2.65	11.33 ±0.76	18.69 ±2.01	12.20 ±2.72	18.29 ±2.18	11.72 ±2.35	18.17 ±3.59	8.64 ±1.47	15.2 ±1.72	18.53 ±8.53	19.51 ±2.15	16.38 ±2.60	17.48 ±2.49	10.60 ±1.54	17.57 ±3.14
	Hb g/dL	8.80 ±0.39	8.98 ±0.34	8.97 ±0.42	8.85 ±0.46	9.70 ±0.79	8.54 ±0.76	9.80 ±0.50	9.56 ±0.52	8.67 ±0.74	7.37 ±1.02	11.77 ±0.94	10.50 ±0.50	10.10 ±0.81	8.00 ±0.91	10.18 ±1.30	10.28 ±0.97	8.90 ±0.38	9.33 ±0.33
Inflammation Immunodeficiency	Lymphocytes x 10 ³ /μL	5.31 ±0.64	9.14 ±1.42	5.33 ±0.57	9.13 ±0.86	6.33 ±1.04	9.81 ±0.88	7.90 ±3.53	9.43 ±0.90	5.41 ±0.74	7.37 ±1.62	4.17 ±0.85	7.33 ±0.87	12.00 ±5.75	8.93 ±0.99	6.20 ±1.37	8.31 ±0.84	5.94 ±1.19	9.03 ±1.45
	Monocytes x 10 ³ /μL	0.38 ±0.07	0.74 ±0.13	0.43 ±0.07	0.74 ±0.09	0.45 ±0.05	0.79 ±0.31	0.67 ±0.29	0.83 ±0.12	0.36± 0.09	0.74 ±0.20	0.43± 0.03	0.67 ±0.11	1.18 ±0.82	0.73 ±0.14	0.59 ±0.21	0.63 ±0.14	0.51 ±0.07	0.92 ±0.21
	Neutrophils x 10 ³ /μL	4.44 ±0.76	6.72 ±0.63	3.24 ±0.21	6.77 ±1.90	4.28 ±0.48	7.33 ±1.24	3.38 ±1.05	7.43 ±1.69	5.81 ±1.91	9.29 ±3.23	3.73 ±1.02	6.71 ±1.10	4.78 ±1.73	9.12 ±1.51	9.31 ±1.10	7.80 ±1.55	3.85 ±0.48	7.09 ±2.13
	Eosinophils x 10 ³ /μL	0.13± 0.08	0.44 ±0.01	0.09 ±0.01	0.32 ±0.07	0.07 ±0.01	0.50 ±0.23	0.09 ±0.05	0.28 ±0.03	0.05 ±0.01	0.64 ±0.26	0.20 ±0.13	0.30 ±0.04	0.06 ±0.02	0.52 ±0.17	0.08 ±0.01	0.56 ±0.26	0.15 ±0.05	0.34 ±0.11

Pre- and post-injection biochemical and hematological markers. Data are reported as mean ± standard error (SEM). Abbreviations: AST, aspartate aminotransferase; ALT, alanine aminotransferase; WBC, white blood cells; Hb, hemoglobin.

Supplementary Table S4. Summary of GFP transduction

Brain areas	WB _{n=3}								IF/IHC _{n=2}							
	rAAV1	rAAV2	rAAV5	rAAV7	rAAV9	rAAV rh.10	rAAV rh.39	rAAV rh.43	rAAV1	rAAV2	rAAV5	rAAV7	rAAV9	rAAV rh.10	rAAV rh.39	rAAV rh.43
Cortex	++	n.d.	+	++	++++	n.d.	n.d.	n.d.	++	++	½ +	++	++++	½ +	n.d.	+
Putamen	+	n.d.	+	+	+	n.d.	n.d.	n.d.	n.d.	n.d.	n.d.	n.d.	++	n.d.	n.d.	n.d.
N.caudatus	n.d.	n.d.	++	½ +	++	n.d.	n.d.	n.d.	½ + _{n=2}	n.d.	n.d.	n.d.	+	n.d.	n.d.	n.d.
Accumbens	½ +	n.d.	+	½ +	+++	n.d.	n.d.	n.d.	½ +	n.d.	n.d.	n.d.	++	n.d.	n.d.	n.d.
Corpus callosum	n.d.	n.d.	+	½ +	++	n.d.	n.d.	n.d.	+	n.d.	+	n.d.	+	n.d.	n.d.	n.d.
Thalamus	½ +	n.d.	+	½ +	++	n.d.	n.d.	n.d.	n.d.	n.d.	½ +	n.d.	+	n.d.	n.d.	n.d.
Hypothalamus	½ +	n.d.	+	+	++	n.d.	n.d.	½ +	n.d.	n.d.	½ +	n.d.	½ +	n.d.	n.d.	n.d.
Stria terminalis	½ +	n.d.	+	½ +	++	n.d.	n.d.	n.d.	n.d.	n.d.	n.d.	½ +	+	n.d.	n.d.	n.d.
Sub. Nigra	½ +	n.d.	+	½ +	++	n.d.	n.d.	n.d.	n.d.	n.d.	½ +	n.d.	+	n.d.	n.d.	n.d.
Hippocampus	+	n.d.	+	½ +	++	n.d.	n.d.	n.d.	+	n.d.	½ +	½ +	++	n.d.	n.d.	n.d.
N. Pontis	½ +	n.d.	n.d.	n.d.	+	n.d.	n.d.	n.d.	½ +	n.d.	½ +	½ +	++	n.d.	n.d.	n.d.
Colliculi	½ +	n.d.	n.d.	n.d.	+	n.d.	n.d.	½ +	n.d.	n.d.	n.d.	n.d.	n.d.	n.d.	n.d.	n.d.
Cerebellum	+	n.d.	n.d.	++	+++	+	½ +	n.d.	+	½ +	½ +	+++	++++	½ +	+	½ +
Medulla	½ +	n.d.	n.d.	n.d.	+	n.d.	n.d.	n.d.	n.d.	n.d.	n.d.	n.d.	++	n.d.	n.d.	n.d.
Ablongata	½ +	n.d.	n.d.	n.d.	+	n.d.	n.d.	n.d.	n.d.	n.d.	n.d.	n.d.	++	n.d.	n.d.	n.d.
Spinal cord	+	n.d.	n.d.	½ +	++	n.d.	+	n.d.	++	n.d.	½ +	+	+++	n.d.	½ +	½ +

Abbreviations: AAV, adeno-associated virus; WB, western blotting; IHC, immunohistochemistry; IF, immunofluorescence; n, the number of animals analyzed Scoring: maximum GFP signal detected was scored with +++++; minimum GFP signal detected was scored with ½+; n.d. not detected.

Conclusions

In the author's opinion, this PhD thesis represents an additional step toward the standardization of the physiological piglet model, thus its refinement and reduction.

The quali-quantitative studies performed on both cerebrospinal fluid and blood, thanks to the extensive statistical analyses and the high number of sampled population, provide with important reference intervals that will allow better understanding of a variety of metabolic processes. For example, the differences in cerebrospinal fluid composition found between the animals at 5, 30 and 50 days of life, can give new interesting insights regarding the timing of maturation of the blood-brain barrier and the Central Nervous System in general. This will help researchers in better translating preclinical studies to humans.

Technical experiments, aimed to find easier and relatively pain free procedures for the animal model itself, are often considered to have less impact when it comes to biomedical animal and translational medicine in general. It has to be acknowledged though that operators' skills often are a limiting factor for the feasibility of experimental protocols within a certain facility, and that easier techniques are the best way to break down these walls. Moreover, when leading to lower mortality and higher welfare of the enrolled animals, those techniques are extremely valuable and necessary, allowing for better results and higher ethical standards.

All of the above statements are completely coherent with the last experiment aimed to create a comprehensive map of CNS transduction upon intrathecal administration of adeno-associated viral vector in the piglet and to evaluate their

potential toxicity. Indeed, the obtained result will help choosing the right serotype depending on the targeted cell population, thus avoiding preliminary studies and higher number of animals.

In conclusion, studies aimed to acquire a deeper knowledge of the piglet and its applications will always be needed to fulfill all of the ethical and scientific requirement of the biomedical field.

Additional research fields and studies performed during the PhD

Throughout the last 3 years, as a PhD candidate within the Department of Veterinary Medical Sciences of the University of Bologna, I had the chance to study and work on a variety of different fields alongside the one here discussed, always under the guidance of prof. Maria Laura Bacci. These include the physiology of the reproduction, mainly focusing on the male gametes, and the anesthesia and analgesia of both pets and other experimental mammals, and led to the publication of other papers:

- Romagnoli N, Zambelli D, Cunto M, Lambertini C, Ventrella D, Baron Toaldo M. *Non-invasive evaluation of the haemodynamic effects of high-dose medetomidine in healthy cats for semen collection.* J Feline Med Surg. 2016 Apr;18(4):337-43. doi: 10.1177/1098612X15583345
- Barone F, Ventrella D, Zannoni A, Forni M, Bacci ML. *Can Microfiltered Seminal Plasma Preserve the Morphofunctional Characteristics of Porcine Spermatozoa in the Absence of Antibiotics? A Preliminary Study.* Reprod Domest Anim. 2016 Aug;51(4):604-10. doi: 10.1111/rda.12699.
- Romagnoli N, Buonacucina A, Lambertini C, Ventrella D, Peli A. *Constant-Rate Infusion of Dexmedetomidine to Manage Thiopental Anesthesia during Intracranial Surgery in Cynomolgus Macaques (Macaca fascicularis).* J Am Assoc Lab Anim Sci. 2016 Nov;55(6):801-804.
- Bryszewska MA, Laghi L, Zannoni A, Gianotti A, Barone F, Taneyo Saa DL, Bacci ML, Ventrella D, Forni M. *Bioavailability of Microencapsulated Iron from Fortified Bread Assessed Using Piglet Model.* Nutrients. 2017 Mar 13;9(3). pii: E272. doi: 10.3390/nu9030272.

References

1. Erxleben, JCP (1777). *Systema regni animalis per classes, ordines, genera, species, varietates: cum synonymia et historia animalium* (1777), Impensis Weygandianis, Lipsiae :, 764pp.
2. McCrackin, MA and Swindle, MM. Biology, Handling, Husbandry, and Anatomy. In: Swindle, MM and Smith, AC (eds.). *Swine Lab*.
3. Groenen, MAM, Archibald, AL, Uenishi, H, Tuggle, CK, Takeuchi, Y, Rothschild, MF, *et al.* (2012). Analyses of pig genomes provide insight into porcine demography and evolution. *Nature* **491**: 393–398.
4. Ganderup, N-C (2016). Use of Swine in Biomedical Research. In: Swindle, MM and Smith, AC (eds.). *Swine Lab.*, CRC Press: pp 523–537.
5. Köhn, F (2011). History and development of miniature, micro- and minipigs. In: McAnulty, PA, Dayan, AD, Ganderup, N-C and Hastings, KL (eds.). *Minipig Biomed. Res.*: pp 3–16.
6. <<http://www.thepigsite.com/info/swinebreeds.php>> The Different Breeds of Pig. *Pig Site* .
7. Blasco, A, Bidanel, JP and Haley, CS (1995). Genetics and Neonatal Survival. In: Varley, MA (ed.). *Neonatal Pig Dev. Surviv.*, CAB International.
8. Fisher, TF. Miniature swine in biomedical research: Applications and husbandry considerations. *Lab. Anim.* **22**: 47–50.
9. Swindle, MM, Smith, AC, Laber-Laird, K and Dungan, L (1994). Swine in Biomedical Research: Management and Models. *ILAR J.* **36**: 1–5.
10. Le Dividich, J and Noblet, J (1983). Thermoregulation and energy metabolism in the neonatal pig. *Ann. Rech. Veterinaires Ann. Vet. Res.* **14**: 375–381.
11. Vaughn, SE (2012). Review of the Third Edition of the Guide for the Care and Use of Agricultural Animals in Research and Teaching. *J. Am. Assoc. Lab. Anim. Sci. JAALAS* **51**: 298–300.
12. Varley, MA (1995). Introduction. In: Varley, MA (ed.). *Neonatal Pig Dev. Surviv.*, CAB International.
13. Council Directive 2008/120/ECat <<http://eur-lex.europa.eu/legal-content/EN/TXT/HTML/?uri=CELEX:32008L0120&qid=1489161560235&from=en>>.
14. Venn, J a. J, Mccance, RA and Widdowson, EM (1947). Iron metabolism in piglet anaemia. *J. Comp. Pathol. Ther.* **57**: 314–325.
15. Szabo, P and Bilkei, G (2002). Iron deficiency in outdoor pig production. *J. Vet. Med. A Physiol. Pathol. Clin. Med.* **49**: 390–391.

16. Starzyński, RR, Laarakkers, CMM, Tjalsma, H, Swinkels, DW, Pieszka, M, Styś, A, *et al.* (2013). Iron supplementation in suckling piglets: how to correct iron deficiency anemia without affecting plasma hepcidin levels. *PLoS One* **8**: e64022.
17. Lipinski, P, Starzyński, RR, Canonne-Hergaux, F, Tudek, B, Oliński, R, Kowalczyk, P, *et al.* (2010). Benefits and risks of iron supplementation in anemic neonatal pigs. *Am. J. Pathol.* **177**: 1233–1243.
18. Gaskins, HR and Kelley, KW (1995). Immunology and Neonatal Mortality. In: Varley, MA (ed.). *Neonatal Pig Dev. Surviv.*, CAB International: pp 39–56.
19. Devillers, N, Le Dividich, J and Prunier, A (2011). Influence of colostrum intake on piglet survival and immunity. *Anim. Int. J. Anim. Biosci.* **5**: 1605–1612.
20. Ogawa, S, Tsukahara, T, Imaoka, T, Nakanishi, N, Ushida, K and Inoue, R (2016). The effect of colostrum ingestion during the first 24 hours of life on early postnatal development of piglet immune systems. *Anim. Sci. J. Nihon Chikusan Gakkaiho* **87**: 1511–1515.
21. Lalles, J.P., Bosi, P., Smidt, H. and Stokes, C.R. (2007). Weaning - a challenge to gut physiologists. *Livest. Sci.* **108**: 82–93.
22. Bombà, L, Minuti, A, Moisés, SJ, Trevisi, E, Eufemi, E, Lizier, M, *et al.* (2014). Gut response induced by weaning in piglet features marked changes in immune and inflammatory response. *Funct. Integr. Genomics* **14**: 657–671.
23. Pluske, JR, Hampson, DJ and Williams, IH (1997). Factors influencing the structure and function of the small intestine in the weaned pig: a review. *Livest. Prod. Sci.* **51**: 215–236.
24. Baekbo, P, Kristensen, CS and Larsen, LE (2012). Porcine circovirus diseases: a review of PMWS. *Transbound. Emerg. Dis.* **59 Suppl 1**: 60–67.
25. Sanchez, RE, Nauwynck, HJ, McNeilly, F, Allan, GM and Pensaert, MB (2001). Porcine circovirus 2 infection in swine fetuses inoculated at different stages of gestation. *Vet. Microbiol.* **83**: 169–176.
26. Kim, J, Chung, H-K and Chae, C (2003). Association of porcine circovirus 2 with porcine respiratory disease complex. *Vet. J. Lond. Engl. 1997* **166**: 251–256.
27. Baró, J, Segalés, J and Martínez, J (2015). Porcine circovirus type 2 (PCV2) enteric disease: an independent condition or part of the systemic disease? *Vet. Microbiol.* **176**: 83–87.
28. Phaneuf, LR, Ceccarelli, A, Laing, JR, Moloo, B and Turner, PV (2007). Porcine dermatitis and nephropathy syndrome associated with porcine circovirus 2 infection in a Yorkshire pig. *J. Am. Assoc. Lab. Anim. Sci. JAALAS* **46**: 68–72.

29. Nagy, B and Fekete, PZ (2005). Enterotoxigenic *Escherichia coli* in veterinary medicine. *Int. J. Med. Microbiol. IJMM* **295**: 443–454.
30. Fairbrother, JM, Nadeau, E and Gyles, CL (2005). *Escherichia coli* in postweaning diarrhea in pigs: an update on bacterial types, pathogenesis, and prevention strategies. *Anim. Health Res. Rev.* **6**: 17–39.
31. Heo, JM, Opapeju, FO, Pluske, JR, Kim, JC, Hampson, DJ and Nyachoti, CM (2013). Gastrointestinal health and function in weaned pigs: a review of feeding strategies to control post-weaning diarrhoea without using in-feed antimicrobial compounds. *J. Anim. Physiol. Anim. Nutr.* **97**: 207–237.
32. Amezcua, R, Friendship, RM, Dewey, CE, Gyles, C and Fairbrother, JM (2002). Presentation of postweaning *Escherichia coli* diarrhea in southern Ontario, prevalence of hemolytic *E. coli* serogroups involved, and their antimicrobial resistance patterns. *Can. J. Vet. Res. Rev. Can. Rech. Veterinaire* **66**: 73–78.
33. Do, DN, Ostersen, T, Strathe, AB, Mark, T, Jensen, J and Kadarmideen, HN (2014). Genome-wide association and systems genetic analyses of residual feed intake, daily feed consumption, backfat and weight gain in pigs. *BMC Genet.* **15**: 27.
34. Jiao, S, Maltecca, C, Gray, KA and Cassady, JP (2014). Feed intake, average daily gain, feed efficiency, and real-time ultrasound traits in Duroc pigs: II. Genomewide association. *J. Anim. Sci.* **92**: 2846–2860.
35. Growth Rate - The Pig Siteat <<http://www.thepigsite.com/stockstds/17/growth-rate/>>.
36. Growth_Curve.jpg (imagine JPEG, 960 × 720 pixel)
<https://upload.wikimedia.org/wikipedia/commons/0/0b/Growth_Curve.jpg>.
37. Pond, WG and Mersmann, HJ (2001). General Characteristics. In: Pond, WG and Mersmann, HJ (eds.). *Biol. Domest. Pig*, Ithaca.
38. Raudsepp, T and Chowdhary, BP (2011). Cytogenetics and Chromosome Maps. In: Rothschild, MF and Ruvinsky, A (eds.). *Genet. Pig*, CAB International: pp 134–178.
39. Speicher, MR and Carter, NP (2005). The new cytogenetics: blurring the boundaries with molecular biology. *Nat. Rev. Genet.* **6**: 782–792.
40. Gustavsson, I, Hageltorn, M, Johansson, C and Zech, L (1972). Identification of the pig chromosomes by the quinacrine mustard fluorescence technique. *Exp. Cell Res.* **70**: 471–474.
41. Gustavsson, I (1988). Standard karyotype of the domestic pig. Committee for the Standardized Karyotype of the Domestic Pig. *Hereditas* **109**: 151–157.

42. Faraut, T, de Givry, S, Hitte, C, Lahbib-Mansais, Y, Morisson, M, Milan, D, *et al.* (2009). Contribution of radiation hybrids to genome mapping in domestic animals. *Cytogenet. Genome Res.* **126**: 21–33.
43. Rogatcheva, MB, Chen, K, Larkin, DM, Meyers, SN, Marron, BM, He, W, *et al.* (2008). Piggy-BACing the human genome I: constructing a porcine BAC physical map through comparative genomics. *Anim. Biotechnol.* **19**: 28–42.
44. Rubes, J, Pinton, A, Bonnet-Garnier, A, Fillon, V, Musilova, P, Michalova, K, *et al.* (2009). Fluorescence in situ hybridization applied to domestic animal cytogenetics. *Cytogenet. Genome Res.* **126**: 34–48.
45. Schook, LB, Beever, JE, Rogers, J, Humphray, S, Archibald, A, Chardon, P, *et al.* (2005). Swine Genome Sequencing Consortium (SGSC): a strategic roadmap for sequencing the pig genome. *Comp. Funct. Genomics* **6**: 251–255.
46. Humphray, SJ, Scott, CE, Clark, R, Marron, B, Bender, C, Camm, N, *et al.* (2007). A high utility integrated map of the pig genome. *Genome Biol.* **8**: R139.
47. Archibald, AL, Bolund, L, Churcher, C, Fredholm, M, Groenen, MAM, Harlizius, B, *et al.* (2010). Pig genome sequence--analysis and publication strategy. *BMC Genomics* **11**: 438.
48. Fang, X, Mou, Y, Huang, Z, Li, Y, Han, L, Zhang, Y, *et al.* (2012). The sequence and analysis of a Chinese pig genome. *GigaScience* **1**: 16.
49. Vamathevan, JJ, Hall, MD, Hasan, S, Woollard, PM, Xu, M, Yang, Y, *et al.* (2013). Minipig and beagle animal model genomes aid species selection in pharmaceutical discovery and development. *Toxicol. Appl. Pharmacol.* **270**: 149–157.
50. Li, M, Tian, S, Jin, L, Zhou, G, Li, Y, Zhang, Y, *et al.* (2013). Genomic analyses identify distinct patterns of selection in domesticated pigs and Tibetan wild boars. *Nat. Genet.* **45**: 1431–1438.
51. Groenen, MAM (2016). A decade of pig genome sequencing: a window on pig domestication and evolution. *Genet. Sel. Evol. GSE* **48**: 23.
52. Warr, A, Robert, C, Hume, D, Archibald, AL, Deeb, N and Watson, M (2015). Identification of Low-Confidence Regions in the Pig Reference Genome (Sscrofa10.2). *Front. Genet.* **6**: 338.
53. Skinner, BM, Sargent, CA, Churcher, C, Hunt, T, Herrero, J, Loveland, JE, *et al.* (2016). The pig X and Y Chromosomes: structure, sequence, and evolution. *Genome Res.* **26**: 130–139.

54. Andersson, L, Archibald, AL, Bottema, CD, Brauning, R, Burgess, SC, Burt, DW, *et al.* (2015). Coordinated international action to accelerate genome-to-phenome with FAANG, the Functional Annotation of Animal Genomes project. *Genome Biol.* **16**: 57.
55. Galen (1586). *Galenī Librorrum Quarta Classis.*, Venetijs Apud Iuntas.
56. Kuzmuk, KN and Schook, LB (2011). Pigs as a model for biomedical sciences.pdf. In: Rothschild, MF and Ruvinsky, A (eds.). *Genet. Pig*, CAB International: pp 426–444.
57. Dolezalova, D, Hruska-Plochan, M, Bjarkam, CR, Sørensen, JCH, Cunningham, M, Weingarten, D, *et al.* (2014). Pig models of neurodegenerative disorders: Utilization in cell replacement-based preclinical safety and efficacy studies. *J. Comp. Neurol.* **522**: 2784–2801.
58. Bernard, C (1865). *An Introduction to the Study of Experimental Medicine.*
59. Nomura, T, Katsuki, M, Yokoyama, M and Tajima, Y (1987). Future perspectives in the development of new animal models. *Prog. Clin. Biol. Res.* **229**: 337–353.
60. Denton, PW, Sjøgaard, OS and Tolstrup, M (2016). Using animal models to overcome temporal, spatial and combinatorial challenges in HIV persistence research. *J. Transl. Med.* **14**: 44.
61. Itoh, Y (2016). Translational research on influenza virus infection using a nonhuman primate model. *Pathol. Int.* doi:10.1111/pin.12385.
62. Leiter, EH, Beamer, WG, Shultz, LD, Barker, JE and Lane, PW (1987). Mouse models of genetic diseases. *Birth Defects Orig. Artic. Ser.* **23**: 221–257.
63. Erickson, RP (1988). Creating animal models of genetic disease. *Am. J. Hum. Genet.* **43**: 582–586.
64. Jaenisch, R and Mintz, B (1974). Simian virus 40 DNA sequences in DNA of healthy adult mice derived from preimplantation blastocysts injected with viral DNA. *Proc. Natl. Acad. Sci. U. S. A.* **71**: 1250–1254.
65. Hammer, RE, Pursel, VG, Rexroad, CE, Wall, RJ, Bolt, DJ, Ebert, KM, *et al.* (1985). Production of transgenic rabbits, sheep and pigs by microinjection. *Nature* **315**: 680–683.
66. Petters, RM, Alexander, CA, Wells, KD, Collins, EB, Sommer, JR, Blanton, MR, *et al.* (1997). Genetically engineered large animal model for studying cone photoreceptor survival and degeneration in retinitis pigmentosa. *Nat. Biotechnol.* **15**: 965–970.
67. Onishi, A, Iwamoto, M, Akita, T, Mikawa, S, Takeda, K, Awata, T, *et al.* (2000). Pig cloning by microinjection of fetal fibroblast nuclei. *Science* **289**: 1188–1190.
68. Lavitrano, M, Forni, M, Bacci, ML, Di Stefano, C, Varzi, V, Wang, H, *et al.* (2003). Sperm mediated gene transfer in pig: Selection of donor boars and optimization of DNA uptake. *Mol. Reprod. Dev.* **64**: 284–291.

69. Tu, Z, Yang, W, Yan, S, Guo, X and Li, X-J (2015). CRISPR/Cas9: a powerful genetic engineering tool for establishing large animal models of neurodegenerative diseases. *Mol. Neurodegener.* **10**: 35.
70. Luo, Y, Lin, L, Bolund, L, Jensen, TG and Sørensen, CB (2012). Genetically modified pigs for biomedical research. *J. Inherit. Metab. Dis.* **35**: 695–713.
71. Bode, G, Clausing, P, Gervais, F, Loegsted, J, Luft, J, Nogues, V, *et al.* (2010). The utility of the minipig as an animal model in regulatory toxicology. *J. Pharmacol. Toxicol. Methods* **62**: 196–220.
72. Liu, Y, Zeng, B-H, Shang, H-T, Cen, Y-Y and Wei, H (2008). Bama miniature pigs (*Sus scrofa domestica*) as a model for drug evaluation for humans: comparison of in vitro metabolism and in vivo pharmacokinetics of lovastatin. *Comp. Med.* **58**: 580–587.
73. Forster, R, Ancian, P, Fredholm, M, Simianer, H, Whitelaw, B and Steering Group of the RETHINK Project (2010). The minipig as a platform for new technologies in toxicology. *J. Pharmacol. Toxicol. Methods* **62**: 227–235.
74. Rogers, CS, Stoltz, DA, Meyerholz, DK, Ostedgaard, LS, Rokhlina, T, Taft, PJ, *et al.* (2008). Disruption of the CFTR gene produces a model of cystic fibrosis in newborn pigs. *Science* **321**: 1837–1841.
75. Wimmers, K, Murani, E and Ponsuksili, S (2010). Functional genomics and genetical genomics approaches towards elucidating networks of genes affecting meat performance in pigs. *Brief. Funct. Genomics* **9**: 251–258.
76. Flamm, EG (2013). Neonatal animal testing paradigms and their suitability for testing infant formula. *Toxicol. Mech. Methods* **23**: 57–67.
77. Odle, J, Lin, X, Jacobi, SK, Kim, SW and Stahl, CH (2014). The suckling piglet as an agrimedical model for the study of pediatric nutrition and metabolism. *Annu. Rev. Anim. Biosci.* **2**: 419–444.
78. Sangild, PT, Thymann, T, Schmidt, M, Stoll, B, Burrin, DG and Buddington, RK (2013). Invited review: the preterm pig as a model in pediatric gastroenterology. *J. Anim. Sci.* **91**: 4713–4729.
79. Vanderhaeghe, C, Dewulf, J, Jourquin, J, De Kruif, A and Maes, D (2011). Incidence and prevention of early parturition in sows. *Reprod. Domest. Anim. Zuchthyg.* **46**: 428–433.
80. Oosterloo, BC, Premkumar, M, Stoll, B, Olutoye, O, Thymann, T, Sangild, PT, *et al.* (2014). Dual purpose use of preterm piglets as a model of pediatric GI disease. *Vet. Immunol. Immunopathol.* **159**: 156–165.
81. Srinivasan, PS, Brandler, MD and D’Souza, A (2008). Necrotizing enterocolitis. *Clin. Perinatol.* **35**: 251–272, x.

82. Sangild, PT (2006). Gut responses to enteral nutrition in preterm infants and animals. *Exp. Biol. Med. Maywood NJ* **231**: 1695–1711.
83. Lennon, D, Zanganeh, T and Borum, PR (2011). Development of the piglet neonatal intensive care unit for translational research. *Lab Anim.* **40**: 253–258.
84. Bjornvad, CR, Thymann, T, Deutz, NE, Burrin, DG, Jensen, SK, Jensen, BB, *et al.* (2008). Enteral feeding induces diet-dependent mucosal dysfunction, bacterial proliferation, and necrotizing enterocolitis in preterm pigs on parenteral nutrition. *Am. J. Physiol. Gastrointest. Liver Physiol.* **295**: G1092-1103.
85. Siggers, J, Sangild, PT, Jensen, TK, Siggers, RH, Skovgaard, K, Støy, ACF, *et al.* (2011). Transition from parenteral to enteral nutrition induces immediate diet-dependent gut histological and immunological responses in preterm neonates. *Am. J. Physiol. Gastrointest. Liver Physiol.* **301**: G435-445.
86. Greer, FR (2001). Feeding the premature infant in the 20th century. *J. Nutr.* **131**: 426S–30S.
87. Lim, DW, Turner, JM and Wales, PW (2015). Emerging Piglet Models of Neonatal Short Bowel Syndrome. *JPEN J. Parenter. Enteral Nutr.* **39**: 636–643.
88. Turner, JM, Wales, PW, Nation, PN, Wizzard, P, Pendlebury, C, Sergi, C, *et al.* (2011). Novel neonatal piglet models of surgical short bowel syndrome with intestinal failure. *J. Pediatr. Gastroenterol. Nutr.* **52**: 9–16.
89. Bines, JE, Taylor, RG, Justice, F, Paris, MCJ, Sourial, M, Nagy, E, *et al.* (2002). Influence of diet complexity on intestinal adaptation following massive small bowel resection in a preclinical model. *J. Gastroenterol. Hepatol.* **17**: 1170–1179.
90. Laphorne, S, Pereira-Fantini, PM, Fouhy, F, Wilson, G, Thomas, SL, Dellios, NL, *et al.* (2013). Gut microbial diversity is reduced and is associated with colonic inflammation in a piglet model of short bowel syndrome. *Gut Microbes* **4**: 212–221.
91. Heemskerk, VH, van Heurn, LW, Farla, P, Buurman, WA, Piersma, F, ter Riet, G, *et al.* (1999). A successful short-bowel syndrome model in neonatal piglets. *J. Pediatr. Gastroenterol. Nutr.* **29**: 457–461.
92. Aunsholt, L, Thymann, T, Qvist, N, Sigalet, D, Husby, S and Sangild, PT (2015). Prematurity Reduces Functional Adaptation to Intestinal Resection in Piglets. *JPEN J. Parenter. Enteral Nutr.* **39**: 668–676.
93. Bryszewska, MA, Laghi, L, Zannoni, A, Gianotti, A, Barone, F, Taneyo Saa, DL, *et al.* (2017). Bioavailability of Microencapsulated Iron from Fortified Bread Assessed Using Piglet Model. *Nutrients* **9**: 272.

94. Myers, DD, Diaz, JA, Conte, ML and Swindle, MM (2016). Cardiothoracic and Vascular Surgery/Chronic Intravascular Catheterization. In: Swindle, MM and Smith, AC (eds.). *Swine Lab.*: pp 213–281.
95. White, FC, Roth, DM and Bloor, CM (1986). The pig as a model for myocardial ischemia and exercise. *Lab. Anim. Sci.* **36**: 351–356.
96. Unger, EF (2001). Experimental evaluation of coronary collateral development. *Cardiovasc. Res.* **49**: 497–506.
97. Dixon, JA and Spinale, FG (2009). Large animal models of heart failure: a critical link in the translation of basic science to clinical practice. *Circ. Heart Fail.* **2**: 262–271.
98. Mukherjee, R, Brinsa, TA, Dowdy, KB, Scott, AA, Baskin, JM, Deschamps, AM, *et al.* (2003). Myocardial infarct expansion and matrix metalloproteinase inhibition. *Circulation* **107**: 618–625.
99. Hassan, MA, Mendler, M, Maurer, M, Waitz, M, Huang, L and Hummler, HD (2015). Reliability of pulse oximetry during cardiopulmonary resuscitation in a piglet model of neonatal cardiac arrest. *Neonatology* **107**: 113–119.
100. Solevåg, AL, Dannevig, I, Šaltytė-Benth, J, Saugstad, OD and Nakstad, B (2014). Reliability of pulse oximetry in hypoxic newborn pigs. *J. Matern.-Fetal Neonatal Med. Off. J. Eur. Assoc. Perinat. Med. Fed. Asia Ocean. Perinat. Soc. Int. Soc. Perinat. Obstet.* **27**: 833–838.
101. Aroni, F, Xanthos, T, Varsami, M, Argyri, I, Alexaki, A, Stroumpoulis, K, *et al.* (2012). An experimental model of neonatal normocapnic hypoxia and resuscitation in Landrace/Large White piglets. *J. Matern.-Fetal Neonatal Med. Off. J. Eur. Assoc. Perinat. Med. Fed. Asia Ocean. Perinat. Soc. Int. Soc. Perinat. Obstet.* **25**: 1750–1754.
102. European Resuscitation Council Guidelines for Resuscitation 2015: Section 1. Executive summary | ERC Guidelines for resuscitation 2015at <<http://ercguidelines.elsevierresource.com/european-resuscitation-council-guidelines-resuscitation-2015-section-1-executive-summary/fulltext>>.
103. Kerenyi, A, Kelen, D, Faulkner, SD, Bainbridge, A, Chandrasekaran, M, Cady, EB, *et al.* (2012). Systemic effects of whole-body cooling to 35 °C, 33.5 °C, and 30 °C in a piglet model of perinatal asphyxia: implications for therapeutic hypothermia. *Pediatr. Res.* **71**: 573–582.
104. Edwards, AD, Brocklehurst, P, Gunn, AJ, Halliday, H, Juszczak, E, Levene, M, *et al.* (2010). Neurological outcomes at 18 months of age after moderate hypothermia for perinatal hypoxic ischaemic encephalopathy: synthesis and meta-analysis of trial data. *BMJ* **340**: c363.

105. Bassols, A, Costa, C, Eckersall, PD, Osada, J, Sabrià, J and Tibau, J (2014). The pig as an animal model for human pathologies: A proteomics perspective. *Proteomics Clin. Appl.* **8**: 715–731.
106. Ventrella, D, Laghi, L, Barone, F, Elmi, A, Romagnoli, N and Bacci, ML (2016). Age-Related 1H NMR Characterization of Cerebrospinal Fluid in Newborn and Young Healthy Piglets. *PLoS One* **11**: e0157623.
107. Swindle, MM (2016). Head and Neck Surgery/Central Nervous System. In: Swindle, MM and Smith, AC (eds.). *Swine Lab.*: pp 283–316.
108. Hau, J and Schapiro, SJ (2010). *Handbook of Laboratory Animal Science, Volume I, Third Edition: Essential Principles and Practices*, CRC Press, 758pp.
109. Holm, IE, Alstrup, AKO and Luo, Y (2016). Genetically modified pig models for neurodegenerative disorders. *J. Pathol.* **238**: 267–287.
110. Li, X-J and Li, S (2015). Large Animal Models of Huntington's Disease. *Curr. Top. Behav. Neurosci.* **22**: 149–160.
111. Chieppa, MN, Perota, A, Corona, C, Grindatto, A, Lagutina, I, Vallino Costassa, E, *et al.* (2014). Modeling amyotrophic lateral sclerosis in hSOD1 transgenic swine. *Neurodegener. Dis.* **13**: 246–254.
112. Prather, RS, Lorson, M, Ross, JW, Whyte, JJ and Walters, E (2013). Genetically Engineered Pig Models for Human Diseases. *Httpdxdoiorg101146annurev-Anim.-031412-103715at* <<http://www.annualreviews.org/doi/10.1146/annurev-animal-031412-103715>>.
113. Oh, HJ, Moon, J, Kim, GA, Lee, S, Paek, SH, Kim, S, *et al.* (2016). 29 POSITRON EMISSION TOMOGRAPHY IMAGING OF BRAIN METABOLISM AND DOPAMINERGIC NEURON DESTRUCTION IN PARKINSON'S DISEASE MODEL PIG. *Reprod. Fertil. Dev.* **29**: 122.
114. Choong, C-J, Baba, K and Mochizuki, H (2016). Gene therapy for neurological disorders. *Expert Opin. Biol. Ther.* **16**: 143–159.
115. Sorrentino, NC, Maffia, V, Strollo, S, Cacace, V, Romagnoli, N, Manfredi, A, *et al.* (2016). A Comprehensive Map of CNS Transduction by Eight Recombinant Adeno-associated Virus Serotypes Upon Cerebrospinal Fluid Administration in Pigs. *Mol. Ther. J. Am. Soc. Gene Ther.* **24**: 276–286.
116. Russell, WMS and Burch, RL (1959). *The principles of humane experimental technique*, Methuen, 260pp.